Russian Chemical Reviews **73** (2) 115 – 145 (2004) © 2004 Russian Academy of Sciences and Turpion Ltd

DOI 10.1070/RC2004v073n02ABEH000866

Self-assembly of nanoparticles at interfaces †

V I Roldughin

Contents

I.	Introduction	115
II.	Periodic colloid structures	116
III.	Self-assembly of nanoparticles at interfaces	120
IV.	Template methods	126
V.	Physicochemical properties of ensembles of nanoparticles	129
VI.	Conclusion	139

Abstract. Various approaches to the formation of ordered structures of colloid particles are described. The emphasis is placed on the formation of such structures by nanoparticles at interfaces. A number of processes involving the so-called self-assembly of particles are considered. Examples of the formation of ordered structures (two- and three-dimensional colloid crystals) are given. The driving forces of the self-assembly of nanoparticles and the salient features of the physicochemical properties of ordered ensembles of such nanoparticles are analysed. The bibliography includes 502 references.

I. Introduction

Studies on the properties of nanoparticles and nanoscale structures have attracted increasing interest of researchers in the last fifteen years. Extensive literature on various methods of producing nanoparticles and fabricating nanostructured materials has been published. This was accompanied by the development of experimental techniques for studying the processes occurring in nanoscale systems.

The results obtained were reviewed and summed up (see, *e.g.*, Refs 1 – 11) and the main fields of research on nanoscale systems were pointed out. The new research avenues, which are rapidly developing at present, were in the early stage of development five or six years ago. They include investigations into the self-assembly of nanoparticles at interfaces.

Interest in the self-assembly of particles is due to some reasons. First, research on such processes gives an insight into the laws governing the behaviour of nanoscale objects under different conditions. Second, self-organised ensembles of nanoparticles exhibit new (and often quite unexpected) properties. Third, if nanoparticles themselves are mainly of interest for basic research, the ensembles of nanoparticles are considered to be a kind of working element in certain devices. Fabrication of such devices implies targeted arrangement of particles on solid substrates. Because of this, investigations on the behaviour of nanoparticles at interfaces are to a great extent governed by practical demands. This opens up the possibility of creating a new generation of nanoscale devices with a multilevel architecture based on an intrinsic property of nanoparticles, namely, on their ability to spontaneously form ordered ensembles. Attempts at simulating self-organisation processes observed in real biological systems also give an impetus to research in this field.

In this review we will describe various approaches to the formation of ordered structures at interfaces. The emphasis is placed on self-assembly of colloid systems and on the methods facilitating this process. The major part of our review will be dedicated to the so-called colloid crystals that are the most interesting and promising objects. The most important properties of self-assembled structures and the conditions for their formation will also be considered.

We will not dwell on the problems concerning self-assembly of nanoscale systems in the broad sense, because this is beyond the scope of the review. We can only point to recent attempts at fabricating nanomechanical devices that are based on nanotubes and fullerenes and operate following a certain algorithm (see Ref. 12). Investigations in this field are in the early stage of development and the models and schemes proposed are to a great extent hypothetical ones despite good reproducibility in computer experiments.

We will also consider some problems concerning the formation of ordered ensembles of particles in the bulk of colloid dispersions. At the same time, the formation of disordered composite materials based on nanoparticles (in particular, using silica matrices [13 – 18]) will be left out of consideration despite the fact that in some cases this process results in the formation of quite interesting structures [14, 19] possessing unique optical and catalytic properties. This research avenue has been intensively developing and deserves detailed consideration elsewhere.

We will leave essentially untouched the problems concerning changes in the properties of the particles deposited on solid substrates. The interaction between the particles and the substrate can result in significant changes in the characteristics of the former.[20] This is due to distortion of the crystal lattice of nanoparticles,[21] which is probably responsible for, *e.g.*, the enhanced catalytic activity and the changes in the optical characteristics of nanoparticles on solid substrates.

V I Roldughin Institute of Physical Chemistry, Russian Academy of Sciences, Leninsky prosp. 31, 119991 Moscow, Russian Federation. Fax (7-095) 952 53 08. Tel. (7-095) 955 46 47.
E-mail: roldugin@phyche.ac.ru

Received 3 July 2003
Uspekhi Khimii **73** (2) 123 – 156 (2004); translated by A M Raevsky

† This is the last publication in the series of reviews concerning the main avenues of research carried out at the Institute of Physical Chemistry, Russian Academy of Sciences [see *Russ. Chem. Rev.* **73** (1) 2004].

Ordered ensembles of molecular clusters[22,23] will also be excluded from consideration. The advantage of such systems is that the corresponding 'building blocks' are of the same size. However, these systems belong to molecular crystals rather than colloid systems. Because of this, both the mechanisms of formation and the physical properties of such ordered structures are strongly different from those typical of colloids.

Yet another problem left out of consideration is self-assembly of macroscopic particles, which is similar to that of microparticles. It should only be noted that revealing self-assembly processes at microscopic level gave an impetus to studies on self-assembly of millimetre-scale particles.[24,25] To this end, such particles of various shape were specially treated (*e.g.*, different faces of cubic polyurethane particles were coated with different materials). Using particles of different geometry and different conditions for modification of their surfaces, it is possible to cause aggregation of particles to give a variety of ordered structures.

II. Periodic colloid structures

The title of this section is exactly the same as that of a book by Efremov, which was published more than three decades ago.[26] Numerous examples in this book showed that it is possible to form ensembles of particles with ordered structures (the so-called colloid crystals) in the colloid systems. These examples can be divided into two groups. The first group comprised highly ordered structures (at that time, they were observed only in natural objects, in particular, opals). The second group comprised the systems that exhibited a trend to formation of ordered structures (it included colloid dispersion prepared under laboratory conditions).

Considerable progress towards fabrication of ordered structures has been achieved since the publication of the above-mentioned book.[26] This was provided by the high level of the development of methods for the synthesis of monodisperse colloid particles, which became the subject of routine studies. Currently, search for the procedures suitable for forming colloid crystals with desired properties is carried out.[27–30] Considerable advances towards the formation of colloid crystals with perfect structure (Fig. 1) have also been achieved.

1. The interparticle interaction

Ordered ensembles of colloid particles (colloid crystals) can serve as model systems in the studies of the gas–liquid and liquid–crystal phase transitions, because they allow the processes to be visualised. The properties of the colloid structures formed in such experiments and the laws of the phase transitions in these systems are governed by the forces of the interparticle interaction. These forces are of various nature and are determined by the properties of the dispersion medium, by the state of the particle surface and by the presence of additives in the colloid system. Consider now several expressions for the potentials of the interparticle interaction, which are most often used in theoretical description of colloids. The potential of the dispersion or van der Waals interaction, which occurs in virtually all systems,[31] is given by

$$U_{\mathrm{d}}(r) = -\frac{\mathrm{A}}{12}\left\{\frac{4r^2}{(2R)^2 - 4r^2} + \frac{4r^2}{(2R)^2} + 2\ln\left[\frac{(2R)^2 - 4r^2}{(2R)^2}\right]\right\}, \qquad (1)$$

where r is the distance between the centres of the particles, A is the Hamaker constant and R is the radius of the particles.

Yet another widely used potential describes an electrostatic interparticle interaction, which is due to the overlap of ionic atmospheres that form in electrolyte solutions near the surfaces of the charged particles. Theoretical analysis usually employs a simplified model of this interaction,[31] which is described by the modified Yukava potential

$$U(r_{ij}) = \frac{Z_i Z_j e^2}{4\pi\varepsilon_0\varepsilon r_{ij}}\left(\frac{\mathrm{e}^{\kappa R_i}}{1+\kappa R_i}\right)\left(\frac{\mathrm{e}^{\kappa R_j}}{1+\kappa R_j}\right)\mathrm{e}^{-\kappa r_{ij}}, \qquad (2)$$

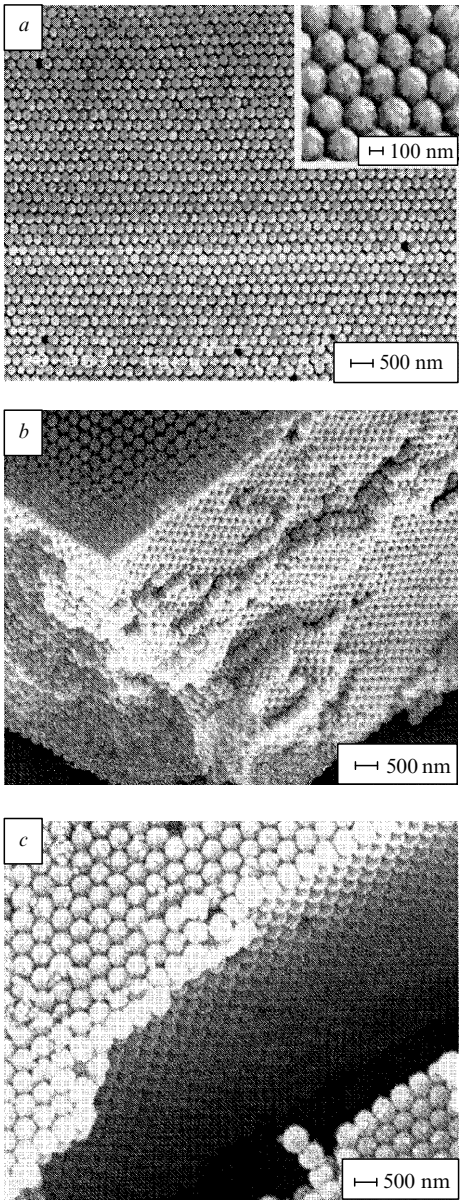


Figure 1. SEM images of three-dimensional crystalline ensembles of polystyrene beads in 12 μm-thick packs.[27]
Particle size: 220 nm for the surface of the crystal (*a*) and for the cleaved facet (*b*) and 480 nm (*c*).

where r_{ij} is the distance between the particles of the sorts i and j; Z_i and Z_j are the corresponding particle charges; e is the charge of electron; ε_0 is the electric constant; ε is the dielectric permittivity of the medium; e is the base of natural logarithm; R_i and R_j are the radii of the particles of the sorts i and j, respectively; and κ is the reciprocal Debye radius defined as follows:

$$\kappa^2 = \frac{e^2}{\varepsilon_0\varepsilon kT}\sum_i n_i z_i^2, \qquad (3)$$

where n_i is the concentration of ions of the sort i in the solution and z_i is the charge of these ions.

If particles are stabilised sterically rather than electrostatically (steric forces are due to the presence of adsorption layers of polymers or surfactants), the interparticle interaction can be quite correctly described by the repulsive potential of dense monolayers in a good solvent [32]

$$E_{st} = \frac{100R\delta_s^2}{(r-2R)\pi\sigma_{th}^3} kT \exp\left[\frac{-\pi(r-2R)}{\delta_s}\right], \quad (4)$$

where δ_s is the monolayer thickness and σ_{th} is the surface area per molecule in the monolayer.

When considering the interparticle interaction, one should take into account two potentials, *viz*., the attractive potential and the repulsive potential, which are in essence some combinations of the potentials mentioned above. Often, numerical calculations are simplified using certain model potentials, *e.g*. a rectangular potential well

$$\frac{U(r)}{kT} = \begin{cases} \infty & \text{at} \quad r < 2R \\ -\dfrac{E_0}{kT} & \text{at} \quad 2R < r < (1+\delta_w)2R \\ 0 & \text{at} \quad r > (1+\delta_w)2R, \end{cases} \quad (5)$$

where E_0 and δ_w are the depth and width of the potential well, respectively. The stick sphere potential is given by

$$\frac{U(r)}{kT} = \lim_{\Delta \to 0} \begin{cases} \infty & \text{at} \quad r < 2R \\ \ln\left(\dfrac{12\psi\Delta}{2R+\Delta}\right) & \text{at} \quad 2R < r < (1+\Delta)2R, \\ 0 & \text{at} \quad r > (1+\Delta)2R, \end{cases} \quad (6)$$

where ψ is the parameter determining the adhesive binding energy and Δ is the variable parameter. The Lennard-Jones potential (its exponents are sometimes chosen arbitrarily) has the form

$$U(r) = 4E_{LD}\left[\left(\frac{\delta_{LD}}{r}\right)^{12} - \left(\frac{\delta_{LD}}{r}\right)^{6}\right], \quad (7)$$

where E_{LD} and δ_{LD} are the energy and spatial parameters, respectively.

The potentials listed above can be used to calculate various characteristics of colloid dispersions, *viz*., the osmotic pressure, second virial coefficient, particle solubility, phase diagram, *etc*. By comparing the calculated and experimental data it is possible [33] not only evaluate the parameters of a particular potential but also determine which of them is more convenient for the description of a given colloid dispersion. If not only the thermodynamic characteristics but also the structure factor is known, one can reconstruct the pair potential of the interparticle interaction even for polydisperse colloid systems.[34]

2. Simple systems

The development of methods for the synthesis of nearly monodisperse colloid particles permitted the growth of rather large colloid crystals with a high degree of crystallinity under laboratory conditions.[35] Initially, high-quality colloid crystals were formed from electrically stabilised latex particles. The stabilisation of the particles was enhanced due to deionisation of the aqueous dispersion medium. In this medium, the interparticle interaction involves the screened Coulombic potential (2), which causes a strong repulsion between particles at long distances due to a large Debye radius. Because of this, the transition to the crystalline state occurs at a volume fraction of the particles of less than 0.01, resulting in the formation of both face-centred cubic (f.c.c.) and body-centred cubic (b.c.c.) crystals.[36, 37] Ordered structures comprised of sterically stabilised colloid particles were obtained much later.[38, 39] The steric stabilisation provided a strong repulsion between particles at short distances so the transition of the colloid dispersion from the liquid to the crystalline state occurred at a volume fraction of particles of nearly 0.5 (as a rule, the f.c.c. structure was formed). Then, more complex systems and phase transitions in them have become the focus of research activity in the field of colloid crystals.

As mentioned above, colloid systems can serve as models for studying the behaviour of atomic and molecular systems. Colloids offer some obvious advantages. In particular, their parameters, *viz*., the size, shape and potential of the interparticle interaction can be measured and varied with ease. The properties of the medium in which colloid particles are dispersed can also be controlled and measured. Because of this, a wide variety of phase states of colloid systems, namely, the gaseous, liquid-like (including glassy state) and crystalline states is observed. Even the existence of a quasi-crystal structure in the single-component colloid system was predicted.[40] Such a structure (icosahedral quasi-crystal) is typical of some binary and ternary metal alloys. It is formed at a rather high osmotic pressure in a specific concentration range.

Various models [41, 42] including those predicting the existence of the glassy state of a colloid fluid [43] were proposed to describe the phase behaviour of colloid systems. Such models are employed in the analysis of the phase transitions in colloid dispersions.[44, 45]

Under particular conditions, sterically stabilised colloid particles behave as a system of hard spheres.[39] To enhance this similarity, particles are coated with a thin adsorption layer of a polymer and then dispersed in a medium characterised by the same refractive index to weaken the van der Waals interaction. Not only the solidification transitions but also the glass transitions were observed in such systems at a volume fraction of particles of about 0.58.[39] At higher particle concentrations, no homogeneous nucleation of crystals was observed and long-range diffusion displacements of particles were suppressed (this was indicated by the shape of the fluctuation correlation function of the particle concentration).[46] Heterogeneous nucleation under the same conditions resulted in large plate-like colloid crystals. This points out that the glassy state is thermodynamically unstable and exists due to the inability of a concentrated homogeneous colloid liquid to go to the crystalline state (for this transition to occur, long-range particle diffusion must be possible). The existence of glassy colloid systems was confirmed by Speedy [47] who also showed that the equation of state of the hard-sphere fluid has singularities indicating some implicit phase transitions. These results were tested [48] and it was shown that larger (compared to those observed in Ref. 47) hard-sphere particles always crystallised at a volume fraction of 0.63 to 0.64. These values are close to the volume fraction of hard-sphere particles in a random close packing (0.644). A series of experiments with 1.03 μm poly(methyl methacrylate) particles stabilised by poly(12-hydroxystearic) acid was carried out to determine the limiting volume fraction of particles at which crystallisation of a dispersion of hard-sphere particles is possible.[49] The results obtained show that at a volume fraction of particles of 0.63 crystallisation still takes a reasonably short time; if the volume fraction of particles exceeded a value of 0.64, no crystals were formed.

Experiments with nanoparticles have opened yet another possibility of controlling the parameters of a colloid system. The nanoparticle size is comparable with the thickness of the protective shell. Experiments show that the structure of colloid crystals depends on the ratio of the chain length, L, of the ligand shell molecules to the particle radius. For saturated linear hydrocarbons, the chain length (in nanometres) is related to the number of monomeric units, n, as follows

$$L = 0.154 + 0.1265\,n. \quad (8)$$

Because of this, it is possible to obtain particles with a prescribed L/R ratio. Depending on the value of this parameter, the structures with the f.c.c. lattice (at small L/R ratios) or the b.c.c. packing of particles (at large L/R ratios) are formed. This is probably due to the fact that it is the f.c.c. lattice that is the most preferable in the case of hard spheres,[50] while the b.c.c. lattice is formed [51] if the potential of the interparticle interaction has a repulsive term (*e.g*., the Yukava potential) or some contribution that decreases in proportion to r^{-n} ($n < 6$). The mechanism of formation of ordered structures with the b.c.c. lattice from sterically stabilised nanoparticles is still to be clarified, because in this case the range of action of the repulsive potential is too short.

Korgel and Fitzmaurice [34] varied the size of gold nanoparticles stabilised by dodecanethiol or octanethiol and observed the f.c.c. – b.c.c. transition at $L/R = 0.59$ and 0.60, respectively. These values differ from that obtained for polymer micelles [52] but are close to the value determined for electrostatically stabilised colloids. [51] Calculations [34] of changes in the free energy upon the f.c.c. – b.c.c. transition were carried out assuming the Lennard-Jones potential of the interaction between nanoparticles and showed that this transition corresponds to $L/R = 0.65$ for the dodecanethiol-stabilised nanoparticles.

3. Coulombic systems

Dispersions of charged colloid particles behave as liquid metals. Such particles can be treated as ions, while the co-ions and counter-ions in solution can be considered as electrons. This is not a complete analogy because the size of colloid particles can be three orders of magnitude larger than the size of ions in liquid metals. Mixing of colloid particles of two different sizes significantly complicates the situation as compared to that in the single-component systems, because two new parameters appear, which determine the structure of the colloid dispersion, *viz*., the ratio of the particle diameters and the fraction of particles of a given sort in the mixture.

Experiments showed that if the particle diameters are close, a homogeneous crystalline solid solution is formed at any component ratio in the mixture. The solid solution is characterised by a finite shear modulus and the Bragg diffraction pattern, which is similar to that observed in the case of disordered substitutional alloys. At large differences between the particle sizes in the binary mixture, the system is either in the glassy state or in the crystalline state depending on the time interval available to reach the equilibrium state. For instance, it was found [53] that the dispersion of a mixture of polystyrene latex particles of sizes 110 and 54.5 nm is a disordered solid characterised by a finite shear modulus and non-Bragg diffraction pattern at the volume fraction of the particles of the minor fraction of greater than 5%. At the same time, the crystal structure is formed almost without no exception if the volume fraction of the minor fraction is less than 5%.

Disordered phases are also formed in dispersions of the mixtures of larger particles. For instance, the formation of a disordered phase in the system of particles of sizes 5 and 7 μm at the volume fractions of the larger particles between 10% and 90% was reported.[54] In these experiments, the disordered structure existed over a period of short observation time. If the colloid solution is allowed to stay for a rather long time, a crystal structure typical of intermetallic compounds is formed. However, the transition to crystalline state can take more than a year.[53] Four different intermetallic structures (of the $NaZn_{13}$, AlB_2, $CaCu_5$ $MgCu_2$ types) of binary mixture of spherical particles whose sizes varied from 200 to 800 nm were observed.[55, 56] The type of the crystal structure depends on the ratio of the particle diameters, on the volume fractions of different particles and on the total particle concentration. The attainment of equilibrium in such systems is a slow process and can take several years.

Thus, it does not always happen that the equilibrium in colloid systems can be achieved after passage of a reasonably short time. For this reason, conventional model experiments usually deal with metastable structures. Therefore, the glassy state of colloid dispersions rather than the formation of ordered structures similar to intermetallic compounds has been the subject of a rather large number of publications. Formally, the glassy state region of a colloid can be determined theoretically as the region corresponding to the existence of an intermetallic alloy in the equilibrium phase diagram.[57]

The thermodynamic parameters of colloid crystals can be calculated in a rather simple way. For instance, if the interparticle interaction is given by the pair potential (2), the free energy, F, of a binary system has the form

$$F = \frac{1}{2N}\sum_{i,j}\left\langle \frac{Z_i Z_j e^2}{4\pi\varepsilon_0\varepsilon r_{ij}}\left(\frac{e^{\kappa R_i}}{1+\kappa R_i}\right)\left(\frac{e^{\kappa R_j}}{1+\kappa R_j}\right)e^{-\kappa r_{ij}}\right\rangle + E_k - TS, \quad (9)$$

where $N = N_1 + N_2$ is the total number of particles in the system; the angular brackets denote the averaging over the canonical ensemble and summation is carried out over the lattice sites of the colloid crystal; E_k is the kinetic energy of the particles and the entropy, S, can be calculated using the known relationship [58]

$$S = 3k\sum_{i=1}^{2} x_i\left(1 - \ln\frac{\theta_i}{T}\right), \quad (10)$$

where $x_i = N_i/N$, $\theta_i = 2\pi\hbar\omega_i/k$ is the Einstein temperature [58] determined assuming that the particles of the first and second sorts execute oscillations at their eigenfrequencies ω_i.

The so-called dusty plasmas provide yet another group of examples of electrostatically stabilised colloid systems capable of forming ordered structures. These objects became the subject of research interest in the last decade. Dusty plasma is a sort of low-temperature plasma containing mesoscopic particles whose sizes range from a hundredth of micrometre to several tens of micrometres. Such plasmas are formed in the course of plasma etching and sputtering and in the combustion products, as well as existing near the space objects. Large plasma particles acquire a rather large charge (up to 10^5 e per particle), which is responsible for their strong, long-range repulsion. As a result, such particles form structures that are similar to those observed in liquids and solids.[59–63] In contrast to colloid systems, the mechanism of formation of ordered structures in dusty plasmas is still to be clarified. A feature of dusty plasmas is simultaneous action of the forces typical of the equilibrium systems and the forces due to the nonequilibrium state of the system. For instance, nonuniform temperature fields produce thermophoretic forces [64, 65] that are comparable in magnitude [66] with the electrical forces exerted on particles. Thermophoretic forces to a great extent govern the conditions for the formation, shape and geometry (arrangement) of the dusty plasma structures. Various models of such structures have been proposed.[67, 68] They are mainly based on the non-equilibrium state of dusty plasmas and predict realistic values of the parameters of crystals (they are close to those observed in the experiments) but sometimes include unsubstantiated admissions, which prevents the dusty plasma problem from being considered as solved. At the same time, numerical simulation of dusty plasmas is usually carried out assuming only the screened Coulombic potential of the type (2) for the interparticle interaction. Even with this limited set of the interaction parameters it is possible to predict [69] the existence of various structures in plasma.

4. Mixtures of sterically stabilised particles

Mixtures of sterically interacting colloid particles of different shape are characterised by a wide variety of the phase states and serve as well-defined models in studies of a broad spectrum of phenomena. The mixtures can be prepared in such a way that the major contribution will come from the interaction of particles considered as hard bodies (the thermodynamics of the system is governed by the entropy effects). Considerable attention is given to the systems prepared by adding various admixtures to monodisperse hard spheres. Smaller spherical particles,[70] globular non-adsorbable polymers [71] or rod-like colloid particles [72] are used as the second component. In most cases, the admixture is considered as an agent affecting the interparticle interaction. Such admixtures usually initiate attraction between particles, which is due to the presence of 'depleted layers.' The interaction following this mechanism can be explained with ease. We will consider it taking non-adsorbable polymers as an example (these are most often used for controlling the interaction between colloid particles).

Polymer molecules are separated from the surface of colloid particles by a distance of the order of the radius of gyration. The near-surface region free from the polymer molecules (more exactly, from the centres of mass of the macromolecules) is called

the depleted layer. As the colloid particles bring closer together, their depleted layers are overlapped and the volume accessible to the polymer molecules decreases. As a result, an excess external pressure is produced and applied to the particles; this is equivalent to the action of attractive forces.

The behaviour of mixtures of colloid particles and polymers (see, *e.g.*, Ref. 73) has been the subject of extensive literature concerning the corresponding theoretical models.[74] The phase diagrams constructed using the experimental data show the presence of the gas–liquid, gas–solid and liquid–solid transitions. The transition of the system to the nonequilibrium glassy state was also pointed out.[75]

The interaction due to the presence of depleted layers is typical of not only the mixtures of colloid particles and polymers but also the mixtures of colloid spherical particles of different sizes as well as the mixtures of spherical and rod-like particles. The potential of the interaction between large spherical particles dipped in a medium containing small spherical particles is given by the following approximate expression [76]

$$U(h) = -3kT\varphi\frac{R}{\sigma}\left(1-\frac{h}{\sigma}\right)^2, \tag{11}$$

where h is the distance between the surfaces of large spherical particles, φ is the volume fraction of small spherical particles, R is the radius of large spherical particles and σ is the diameter of small spherical particles. In the case of spherical particles of radius R (and rods of length L and diameter D) the depletion force potential has the form

$$U_{\mathrm{r}}(h) = -\frac{3}{2}kT\varphi\frac{L}{D}\frac{R}{D}\left(1-\frac{h}{L}\right)^3. \tag{12}$$

As can be seen, rod-like particles more efficiently 'tighten' large spheres. This was also confirmed in the experiments. The phase diagram of a mixture of spherical and rod-like colloid particles was constructed based on simple statistical considerations.[77] The results of experiments with the mixtures of 370 nm spherical silica particles and boehmite particles of length 230 nm and diameter 9 nm showed good agreement with the calculated phase diagram which included the gas–liquid, gas–solid and liquid–solid transitions. What is more, a two-step phase transition was observed. Namely, particle aggregation to give hard-sphere clusters was followed by a slower process of the formation of ordered arrangement of the clusters. In this case it is possible to draw an analogy to the phase transitions in the mixtures of hard-sphere particles of different diameters.[78] It was pointed out [77] that it was impossible to consider all the phase states of the system studied, because yet another, orientational, phase transition must be observed for the colloid dispersion of rod-like particles.[79] Calculations of thermodynamic parameters of the mixtures of spherical and rod-like particles should be carried out on the microscopic level [80] because of the key role of many body interactions. Relevant information can be found in the literature.[81,82]

Summing up, mention may be made that not only highly ordered structures but also liquid-crystalline phases can also be observed in colloid systems. The liquid-crystalline phases are formed in the dispersions of rod-like or plate-like particles as the dispersion concentrations increase. Onsager explained the transition between the isotropic and nematic phases occurring with an increase in the particle concentrations based on the entropy considerations [83] taking the phase transition in dispersions of plate-like clay particles, which was observed by Langmuir.[84] Then, analogous phase transitions were observed for many colloid systems; however, almost all experiments were carried out with rod-like particles (see, *e.g.*, Refs 85–88). New plate-like particles [gibbsite, $Al(OH)_3$, particle of thickness 20 nm and diameter 170 nm], in which the transition between the isotropic and nematic phases was observed, were obtained only recently [89] (the transition occurred even in the systems characterised by high polydisperse indices [90]). In polydisperse systems, the dispersions separated into two zones. In one zone, the isotropic phase was formed, while the nematic phase was formed in the other zone. The relative arrangement of the phases along the vertical axis (in the gravitational field) was determined by the dispersion composition. The experimental data are in qualitative agreement with the results of numerical simulation,[91] which gives the following conditions for the coexistence of the isotropic and nematic phases:

$$n_{\mathrm{i}}D^3 \cong 3.8,$$

$$n_{\mathrm{n}}D^3 \cong 3.9,$$

$$\frac{\Pi D^3}{kT} \cong 32,$$

where n_{i} and n_{n} are the particle concentrations in the isotropic and nematic phases, respectively, D is the particle diameter and Π is the osmotic pressure.

It should be noted that the matrix (dispersion medium) can also favour the formation of ordered structures (colloid and liquid crystals); here the matrix can be either a thermotropic [92] or lyotropic [93–96] liquid crystal.

5. Nonequilibrium processes

Recently, the focus of research activity in the field of colloid crystals has moved towards the investigations on the kinetics of phase transitions. In particular, the effect of the thickness of the stabilising shell on the growth rate of a colloid crystal was analysed.[97] Experiments were carried out with nearly 170 nm silica particles using various surfactants as stabilisers. This allowed the thickness of the adsorption layer to be varied from 2 to 50 nm. Colloid crystals were formed by centrifugation of dispersions. An increase in the thickness of the stabilising layer was accompanied by a dramatic increase in the rate of crystallisation. This can be explained by a decrease in the work done to form a seed crystal. The introduction of a non-adsorbable polymer into the system also led to a significant change in the rate of crystallisation. The depleted layers caused the interparticle attraction to strengthen, which favoured faster formation of colloid crystals.

Quantitative studies on the kinetics of the growth of colloid crystals were carried out taking electrostatically stabilised particles as examples.[98,99] It was found that the growth rate obeys the classical Wilson–Frenkel law

$$\upsilon^* = 1 - \exp\left(-\frac{\Delta\mu}{kT}\right), \tag{13}$$

where $\upsilon^* = \upsilon/\upsilon_\infty$ is the relative growth rate, υ_∞ is the growth rate at infinite supersaturation ($\Delta\mu = \infty$) and $\Delta\mu$ can be expressed through the chemical potential difference between the liquid and solid phases of the colloid dispersion at a given pressure p and temperature T

$$\Delta\mu = \mu_{\mathrm{f}}(p,T) - \mu_{\mathrm{s}}(p,T).$$

Theoretical estimates of the kinetic parameters of the crystal growth have been reported.[100] Calculations were carried out assuming the Yukava potential of the interparticle interaction [see Eqn (2)]. The phase coexistence curves obtained are in good agreement with the experimental data and the results of numerical simulation (see Ref. 101).

Taking into account an ordered arrangement of particles, the nonequilibrium macrocharacteristics of colloid crystals can also be calculated with ease. This was demonstrated taking calculations of the viscosity of colloid crystals as an example.[102] The viscosity was determined by numerically solving the system of hydrodynamic equations using the mapping method assuming a Newtonian fluid. Calculations were carried out for three cubic (simple, b.c.c. and f.c.c.) lattices. In this case, the viscosity is a

function of two parameters and the viscosity tensor takes the form (no summation over the repeating subscripts is performed):

$$(\eta_c)_{ijkl} = \frac{1}{2}\eta(1+\beta)\left(\delta_{ik}\delta_{jl} + \delta_{il}\delta_{jk} - \frac{2}{3}\delta_{ij}\delta_{kl}\right) + \eta(\alpha-\beta)\left(\delta_{ij}\delta_{jl}\delta_{lk} - \frac{1}{3}\delta_{ij}\delta_{kl}\right).$$

At low volume fractions, φ, of particles, the coefficients α and β can be expressed by the following series expansions

$$\alpha = \frac{5}{2}\varphi\left[1 + A_\alpha\varphi + B_\alpha\varphi^{5/3} + O(\varphi^{10/3})\right]^{-1},$$

$$\beta = \frac{5}{2}\varphi\left[1 + A_\beta\varphi + B_\beta\varphi^{5/3} + O(\varphi^{10/3})\right]^{-1}.$$

The parameters A_α , B_α and A_β, B_β are listed in Table 1.

Table 1. Parameters determining the viscosity of a colloid crystal at low particle concentrations.

$-A_\alpha$	B_α	A_β	B_β
Simple cubic lattice			
3.78699	3.42673	0.85800	−2.286
b.c.c. lattice			
0.14079	−1.07874	−1.57281	0.71916
f.c.c. lattice			
−0.23611	−0.82315	−1.50926	0.54877

At large φ values, the viscosity depends on the volume fraction of particles in another manner. The coefficients α and β can be approximated as follows:

for the simple cubic lattice

$$\alpha = \frac{3}{16}\pi\chi^{-1} + \frac{27}{80}\ln\chi^{-1} + C_\alpha + D_\alpha\chi\ln\chi^{-1} + O(\chi),$$

$$\beta = \frac{1}{4}\pi\ln\chi^{-1} + C_\beta + D_\beta\chi\ln\chi^{-1} + O(\chi);$$

for the b.c.c. lattice

$$\alpha = \frac{1}{4}\sqrt{3}\pi\ln\chi^{-1} + C_\alpha + D_\alpha\chi\ln\chi^{-1} + O(\chi),$$

$$\beta = \frac{1}{8}\sqrt{3}\pi\ln\chi^{-1} + \frac{37}{120}\sqrt{3}\pi\ln\chi^{-1} + C_\beta + D_\beta\chi\ln\chi^{-1} + O(\chi);$$

and for the f.c.c. lattice

$$\alpha = \frac{3}{32}\sqrt{2}\pi\ln\chi^{-1} + \frac{87}{160}\sqrt{2}\pi\ln\chi^{-1} + C_\alpha + D_\alpha\chi\ln\chi^{-1} + O(\chi),$$

$$\beta = \frac{3}{16}\sqrt{2}\pi\ln\chi^{-1} + \frac{47}{80}\sqrt{2}\pi\ln\chi^{-1} + C_\beta + D_\beta\chi\ln\chi^{-1} + O(\chi),$$

here

$$\chi = 1 - \left(\frac{\varphi}{\varphi_c}\right)^{1/3},$$

and φ_c is the volume fraction of particles, corresponding to the dense packing of spheres. The values of the corresponding constants are given in Table 2.

The results obtained (dependences of the viscosity on the packing density of spherical particles) are in reasonable agreement with the experimental data.

Table 2. Parameters determining the viscosity of a colloid crystal at high particle concentrations.

$-C_\alpha$	D_α	$-C_\beta$	D_β
Simple cubic lattice			
2.85	−1.3	0.604	−0.30
b.c.c. lattice			
1.83	−12.0	7.5	6.0
f.c.c. lattice			
9.54	14.0	7.4	−9.0

III. Self-assembly of nanoparticles at interfaces

1. Solid substrates

Nanoparticles possess the ability to form ordered self-assemblies both in the bulk of the dispersion [4, 103] and at interfaces.[4] Ordered layers of nanoparticles exhibit unique optical, electric, magnetic and catalytic properties.[104, 105] Recently, highly ordered colloid structures have been considered as candidates for optoelectronic devices,[106] photonic materials,[107] biosensors [108] and a new generation of memory devices. With nanoparticles it is possible to significantly shorten the time necessary for fabrication of nanoscale devices compared to, *e.g.*, electron-beam lithography (the ion-beam and X-ray lithography usually require massive equipment). Nanostructured surfaces are also required in studies of the interaction between cells and surfaces.

Depending on the character of the interparticle interaction (electrostatic, capillary, or van der Waals forces, biospecific recognition) and on the goal of a particular study, various methods of fabrication of ordered ensembles of nanoparticles are employed. It is possible to form two-dimensional and three-dimensional (3D) [24, 109, 110] ordered arrays of particles, as well as mesoporous structures and particle aggregates of specific shape. The properties of the systems obtained depend on both the characteristics of the particles (size, shape, composition) and the architecture of the ensembles (interparticle distance, structural hierarchy, *etc*.).

The simplest method of formation of ordered structures comprised of nanoparticles (see, *e.g.*, Ref. 111) is to evaporate a droplet of the nanoparticle dispersion deposited on the substrate, which causes the formation of a spatially ordered arrangement due to the capillary effects. The pioneering experiments involved fabrication of two-dimensional colloid nanocrystals by evaporating a droplet of a dispersion containing lyophobic particles, which was deposited on the substrate. This procedure was used to form the f.c.c. crystals from CdSe nanoparticles (see Ref. 111) and microscopic polystyrene particles (see Ref. 112).

The formation of a colloid crystal involves two stages.[113] First, seed crystals are formed from spheres under the action of capillary forces. Then, the solvent and spheres are supplied to the nuclei of the new phase in the course of evaporation of the liquid from the film at the peripheral area of the droplet. The formation of the colloid crystal is affected by the tilt angle of the substrate and the rate of solvent evaporation. The substrate must be tilted for nucleation to begin at the top of the droplet and for the crystal to grow on the substrate downward. Deformation of the droplet determines the limiting tilt angle for the substrate; it is related to the wetting angle hysteresis, while the capillary forces compensate the gravitational force. By changing the tilt angle it is possible to vary the parameters of the crystals grown.

Yet another important parameter is the rate of evaporation of the dispersion medium. Generally, the lower the rate of evaporation, the larger the colloid crystals that can be formed. The effect of the rate of evaporation was studied in detail.[114] Using video microscopy technique, it was shown that the particle attached to the edge of the crystal can be treated as mobile for some time, so

the freshly formed 'microcrystals' undergo rearrangements and experience reorientations on incorporating into the larger crystal. Rapid evaporation reduces the rearrangement time, thus resulting in the formation of polycrystals. The nature of the substrate also plays a significant role. For instance, the presence of hydroxyl groups on the surface of a glass substrate favours growth of larger crystals comprised of negatively charged colloid particles, because repulsion from the surface enhances their mobilities. In this case, growth of the crystals comprised of positively charged particles is strongly suppressed. Finally, an important role is played by the concentration of the dispersion medium. Knowing the droplet size, it is possible to estimate the concentration corresponding to the formation of a monolayer of particles on the substrate surface. However, in all model experiments we deal with the formation of multilayered crystals along the perimeter of the droplet. This is due to the fact that it is the peripheral area of the droplet where evaporation occurs more intensely; convective flows of the dispersion medium favour transfer of particles to that area. Therefore, fabrication of a monolayer requires that the actual particle concentration be higher than the corresponding calculated value.

Because of its simplicity, the droplet evaporation method remains quite attractive as yet.[115, 116] The technique was employed to grow colloid crystals comprised of the oxide,[117] sulfide,[118] noble metal [115, 116, 119, 120] and polymer [121] nanoparticles. Two-dimensional colloid crystals of nearly micrometre size were grown.[116] The methods developed to form ordered arrangements of the metal and semiconductor particles are also applicable to magnetic nanoparticles.[111, 122–125] In contrast to micrometre-size spheres, self-assembly of nanoparticles is governed by not only the entropy factor.[119, 126] Here, an important role is played by the particle–particle and particle–substrate interactions and by the nature of the stabiliser and binding agent molecules.[127]

The droplet evaporation method also involves self-assembly of particles on the mesoscopic level, namely, evaporation of large droplets leads to the formation of ring structures,[128, 129] which can be explained with ease [129] by analysing the hydrodynamics of the process. It should be noted that the use of more complex methods for the formation of ordered layers of nanoparticles sometimes causes [130, 131] complication of structural organisation on the mesoscopic level.

On the nanometre level, the degree of local order of the deposited nanoparticles is strongly dependent on the average particle size, because the larger particles are usually characterised by lower polydispersity [132] and are therefore more suitable for the formation of ordered structures. Such structures comprised of particles of size less than 2 nm are rare. Two-dimensional arrays of 'large' particles are characterised by orientation of the atomic lattices of nanoparticles relative to one another;[133] however, 3D-systems are usually disordered. At the same time, high-quality colloid crystals can be formed under particular conditions from particles of different size even using the classical scheme of fabrication of ordered ensembles *via* evaporation of a dispersion droplet. This was demonstrated taking alkylamine-stabilised gold nanoparticles as an example (see Ref. 134; the particle size varied from 1.8 to 8 nm). Using electron microscopy, a high degree of order of the nanoparticles in the colloid crystals was revealed, the atomic lattices of nanoparticles also being oriented in some way. Ordered structures were observed for both large and small particles organised into two- and three-dimensional arrays.

These results point out that the laws of self-assembly of particles to give ordered structures are still to be clarified. Therefore, the influence of various factors on the properties of the crystals formed from nanoparticles is studied. In particular, the effects of the temperature and initial particle concentration on the nucleation and growth of 3D-structures comprised of dodecanethiol-stabilised 5 nm silver nanoparticles were investigated.[135] Different methods of deposition of particle dispersions on the substrate were employed. In all experiments, 3D crystal structures were formed with good reproducibility. The average distance between the monolayers of spherical particles corresponded to the f.c.c. lattice or to hexagonal dense packing. Similarly to the case of monolayers, the size of the domains with ordered structure reduced as the temperature increased. This can be explained by the fact that faster evaporation of the solvent at elevated temperatures leads to shortening of the crystal growth time and the particles have no time to form ordered arrangements on large surface areas. As a consequence, fine-grained polycrystals are formed, which, by and large, corresponds to the situation with conventional crystalline substances.

However, the droplet evaporation technique has some drawbacks. There are (sometimes) irreproducible results and impossibility of fabrication of large ordered structures that are necessary in designing biosensors, biomaterials and catalysts. Large-area nanostructures are also necessary in creating functional bioactive surfaces. The nanoscale morphology of the surface strongly affects the interaction between the surface and cells and should be taken into account in the design of implants.[136]

Various methods are employed to control the nanoparticle–substrate interaction.[137–142] First of all, these are the ability of surfactant molecules to self-assemble on the substrate [143] and modification of substrates [140] by surfactant monolayers of different density to affect the structural organisation of the deposited nanoparticle layers. In some cases, substrates are covered [141, 142] with monolayers of the molecules (including dendrimer ones) containing the NH_2, CN and SH terminal groups, which are characterised by high affinity to metal particles.[141]

Particles are coated with bifunctional molecules [137–139] to bind them to the surface, which permits self-organisation of particles on the substrate surface [138] similarly to surfactant molecules. Using this method, it is possible to form rather stable structures comprised of nanoparticles. However, the procedure is of limiting use because the molecules used must form strong bonds with both the particle and the substrate.

In the early stage of studies on the self-organisation the formation of 3D colloid crystals faced some problems,[110, 144] though sometimes such objects were also formed by simply evaporating the dispersion droplets.[135] To enhance self-assembly of nanoparticles into three-dimensional crystals, electrochemical deposition of particles [145] and modification of their surfaces are employed.[144, 146, 147] Recently, it has been understood that this requires the use of special procedures that are determined by the nature of nanoparticles. For instance, two main methods employed to form ordered ensembles of gold nanoparticles are as follows. The first method involves the binding of gold nanoparticles *via* dithiol molecules, which form chemical bonds with two different particles through the terminal SH groups. By changing the alkyl chain length of dithiols, one can vary the constant of the nanoparticles' lattice.[148–153] According to the second method, ordered ensembles of nanoparticles are obtained from identically functionalised gold nanoparticles using a binding agent. Here, self-assembly of particles proceeds by the antigen–antibody reaction mechanism [154] or by the DNA binding,[155] hydrogen bonding [156] and complexation [157] mechanisms. The last-named technique is very often used to form hybrid inorgano-organic composites.[158] A comparative study of these two methods was reported.[159] Self-assembly of gold nanoparticles was performed using alkanedithiols and mercaptoaniline. In the latter case, succinyl chloride was added to the solution to control the bonds between NH_2 groups. Experiments with dithiols showed that nanoparticles on the substrate form a hexagonal lattice with a lesser degree of perfection than in the case of mercaptoaniline. This can be explained by faster aggregation of nanoparticles in the case of dithiols.

At present, a number of methods of fabrication of three-dimensional lattices have been developed. The next step is to perform targeted control of the structures of three-dimensional crystals to impart particular electrophysical and other characteristics to these objects.[160, 161] Recently, studies on the laws of formation of ordered structures in three-dimensional arrangements of polydisperse particles have begun.

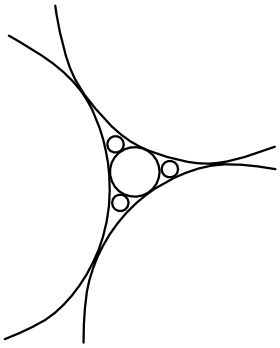


Figure 2. Ordered ensemble of polydisperse particles that form an Apollo figure.

The formation of cubic lattices in monodisperse systems of nanoparticles has been repeatedly pointed out. A bimodal ensemble of particles on the substrate can either undergo a separation into the components or form an ordered binary 'alloy'.[162, 163] Ordered structures in binary mixtures were also observed for two-dimensional systems.[164] Usually, the formation of ordered ensembles in polydisperse systems is thought to be impossible. However, numerical experiments[165] showed that the so-called Apollo figures (small particles fill the voids that form upon contact of large particles, see Fig. 2) can be formed in the systems characterised by 'hierarchical' polydispersity. Even more complex structures comprising polydisperse nanoparticles were observed in the experiments,[166] namely, the particles self-assembled into ordered structures in compliance with their sizes and the transition regions between the areas covered with particles of different sizes were smooth and defect-free. The formation of structures in ensembles of colloid spheres with controllable polydispersity was studied. The particle sizes varied between 5 and 50 nm. The ensemble of nanoparticles was prepared to provide a Gaussian particle size distribution with a polydispersity index of 30%. Particles were dispersed in an organic solvent and then a droplet of the dispersion was transferred on a solid substrate. Visual observations showed that after evaporation of the solvent the substrate surface is covered with large aggregates containing large particles in the central region and small particles in the peripheral regions. Within the aggregates, particles also form ordered arrangements (Fig. 3). The formation of such structures, which were called the 'Zenon clusters', was explained by the strength of the van der Waals interparticle interaction and by peculiarities of the fluid flow in the evaporating droplet.

A few theoretical studies on self-organisation of nanoparticles on substrates are available. Simulation[167] of particle deposition on solid substrates was carried out to study salient features of the structural organisation of nanoparticles that form upon electrochemical deposition on substrates.[29] Numerical experiments reproduced the situation corresponding to the binding of particles to the surface through bifunctional molecules and allowed the effect of polydispersity on the ordering of the particle monolayer to be studied.[168, 169] It was shown that the length of the binding agent molecule governs the particle layer morphology, which can correspond to the liquid, the hexatic phase or to two-dimensional crystal. Theoretically, the liquid–solid phase transition in two-dimensional system of hard disks has long been reported.[170] Recently, considerable attention has been given to the existence of the hexatic phase as intermediate between the liquid and crystalline phases[171] (for more detailed discussion, see below). Investigations on the effect of polydispersity on the two-dimensional phase transitions showed[169, 172, 173] that in polydisperse systems the liquid–crystal phase transition is shifted towards larger coverages and there is a limiting polydispersity value, starting from which no phase transition occurs. No hexatic phase is formed if the polydispersity index is rather high.[169]

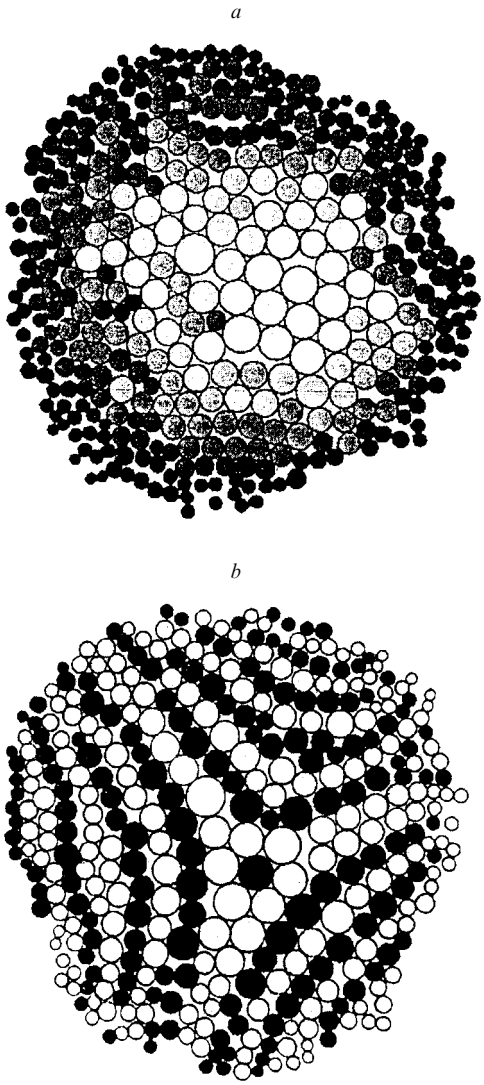


Figure 3. Ordered arrangement of polydisperse particles.[166] Experiment (*a*) and model (*b*).

Numerical experiments were also carried out to study peculiarities of the deposition of polydisperse nanoparticles on substrates in the case of random successive adsorption[174] and various packing types of particles in the monolayer at a given volume fraction of the particles.[175]

2. Non-spherical particles

The structural organisation of non-spherical particles on substrates corresponds to the cases reported in the literature[88, 176] and observed in bulk systems.[177–179] In the case of two dimensions, the phase behaviour is also governed by the maximum entropy condition. Various methods of formation of two-dimensional ordered structures comprised of non-spherical nanoparticles are developed. For instance, melt growth of silicon nanocrystals in the gap between two SiO_2 plates permits fabrication of ordered ensembles of such crystals with mutually oriented atomic lattices.[180]

It is possible to deposit rod-like cadmium selenide nanoparticles in such a way that their principal axis will be directed along the normal to the surface while the particles will be hexagonally packed in the plane of the substrate.[181] This way of packing nanoparticles imparts unusual optical properties to the crystal. Ordered ensembles of rod-like particles can also be fabricated by the droplet evaporation technique, which was demonstrated taking gold particles of length 55 nm and diameter

12 nm as an example.[182] The particle layers exhibited not only translational but also orientational symmetry. According to X-ray diffraction data, nanorods have a nearly identical crystallographic orientation at a length scale of the order of 500 nm. Namely, a total of 200 rod-like particles have the same crystallographic orientation (either [110] or [100]). This can be explained by the fact that nanorods on the {110} and {100} faces can be involved in the intercrystalline contacts.

The formation of ordered structures was attributed to the effect of capillary forces. If rod-like particles are oriented normal to the surface, the forces acting along the principal axis of the particles are greater than those acting in the transverse direction (for spherical particles, lateral capillary forces are proportional to the square of the particle radius).[183] This reason and the pressure applied to the particle monolayer [184] determined the packing of nanorods.

3. Effects of external fields

Self-assembly of particles (first of all, magnetic particles) can be favoured by the external fields. Most studies carried out in this field are concerned with the single-domain particles and their ensembles; however, data on the magnetic properties of ensembles of nanoparticles are strongly different. A possible reason for such discrepancies is the inhomogeneity of the ensembles studied. Because of this, increasing interest in the synthesis of ordered ensembles of magnetic particles has been expressed recently.[122, 123] Note that fabrication of ordered ensembles comprised of the nanoparticles that can be involved in strong interaction with external fields involves the formation of structures whose properties change under the action of external factors (the structures are usually similar to those formed by the 'inert' particles).

In contrast to the gold, silver and sulfide particles, no self-assembled three-dimensional ordered crystals comprised of magnetic cobalt particles are available as yet.[185] Usually, experiments resulted in structureless multilayered ensembles, which can be explained by magnetic interaction between nanoparticles. However, application of a magnetic field along the normal to the substrate led to the formation of two-dimensional structures [186] with hexagonally packed magnetic cobalt nanoparticles, which exhibited co-operative magnetic properties. Search for optimum methods of formation of ordered ensembles of magnetic particles is currently in progress.[187–189] The magnetic field can be used for both preliminary fractionation of nanoparticles and control of their self-assembly. For instance, evaporation of a droplet of a dispersion containing nanocrystallites of ferromagnetic or superparamagnetic cobalt on various substrates in a field of strength less than 1 T gave two-dimensional colloid crystals. An increase in the field strength up to 6 T led to the formation of three-dimensional crystals. The character of the structures obtained was independent of the size of the cobalt nanoparticles but changed with the change in the direction of the magnetic field. In some cases application of the magnetic field caused partial ordering of nanoparticles, which formed ensembles of isolated aggregates (points) or labyrinth structures.[185] The magnetic properties of the nanoparticle films differ from those of dispersions or bulk materials. This opens prospects for practical applications of the structures fabricated.

Deposition of 8 nm cobalt nanoparticles from a droplet of dispersion on the substrate (highly oriented pyrolytic graphite) at different orientations of the external magnetic field was studied.[190] If the field was directed normal to the substrate, evaporation of the dispersion medium led to the formation of a hexagonal arrangement of nanoparticles. If the field was directed along the substrate surface, aligned nanoparticle 'filaments' with nearly equidistant separation were formed. The lattice constant and the filament width depended on the magnetic field strength and decreased as the field strength increased. The 'filaments' were nearly 2 μm thick. This is close to the size of the 'points' at the sites of the hexagonal lattice formed upon deposition of nanoparticles in the field directed normal to the substrate.

A way to fabricate ordered colloid structures is to expose a colloid system to the standing electromagnetic waves created by interfering laser beams.[191] Colloid particles placed in the field of the standing electromagnetic wave can be considered as being in the potential

$$V_e(r) = -\frac{1}{2}\chi_p E^2(r),$$

where χ_p is the particle polarisability and $E(r)$ is the electromagnetic field strength at a given point. By varying the fringe pattern it is possible to change the structure formed from colloid particles. A number of nonlinear effects were observed at rather strong external electromagnetic fields. For instance, a colloid liquid compressed by an electromagnetic wave experienced a phase transition (crystallisation).[192] Often, the structures created using laser radiation are used to study the dynamics of colloid particles, *viz*., the diffraction characteristics of the probe beam are used to determine the spreading velocity of the structures, which allows the dynamic characteristics of the colloid dispersions to be determined.

Two- and three-dimensional colloid structures were also formed using the field of external mechanical forces.[193] On the glassy substrate covered with a thin layer of poly(methyl methacrylate), a system of grooves was created, which had the shape of stripes or rectangles. The plate was dipped in the colloid solution of poly(methyl methacrylate) spheres stabilised by 12-hydroxystearic acid. Then, a non-adsorbable polymer was introduced into the system. The polymer produced a pressure (by the depleted layer mechanism) to press the particles against the surface of the 'puckered' substrate. This resulted in the formation of ordered structures on the substrate. The particle size was either smaller or larger than the intergroove separation. Depending on the particle size, the structures had different symmetry (from linear to hexagonal). In the latter case, successive multilayered deposition of particles gave a f.c.c. crystal.

4. Gas–liquid interface

In the text above, we considered the main methods of fabrication of ordered arrangements of nanoparticles, namely, the droplet evaporation method and self-assembly due to modification of nanoparticles by bifunctional molecules. Both of them have some drawbacks. The first method gives poorly reproducible results, while practical implementation of the second procedure requires that particles be rather strongly bound to the substrate. In both cases, ordered structures are obtained only from the particles with specific ligand shells. The reactivity of particles, electron transfer between them, the ability of particles to participate in various physicochemical processes depend on the nature of the ligand shell. For instance the electrical conductivity of thiolate-stabilised gold nanoparticles can be substantially enhanced upon replacement of the alkanethiol ligands by bifunctional molecules (*e.g*., molecular wires). Electron transfer also depends on the character of the chemical bonds between the ligand shell and the metal core (the Au–S bond in thiolate molecules). It was established [194] that some thiolate ligands used to obtain metal nanoparticles can be replaced by other ligands, which opens up great prospects for variation of the functional properties of nanoparticles and their ensembles (surprisingly, ligands exhibit some mobility on the particle surfaces). In this connection we can say that a new research avenue, *viz*., the 'tuning' chemistry, is now in the early stage of its development. Research in this field requires the elaboration of such methods for fabrication of ordered nanoparticle layers that are almost independent of the nature of the ligand shell. The Langmuir–Blodgett method meets this condition.

Probably, it was Nagayama *et al*.[195, 196] who first employed the Langmuir–Blodgett method to this end. To form self-organised layers of polymer nanoparticles, they proposed to use the capillary forces, which are due to the meniscus between particles,

belong to attractive forces and can therefore favour self-assembly of crystals from nanoparticles.

Owing to the capillary forces, the Langmuir – Blodgett method also permits the formation of ordered particle monolayers on vertical surfaces; removal of the plate from the colloid solution and subsequent evaporation of the solvent causes the formation of ordered arrangements of particles. This method works well for the particles of size less than 400 nm, because larger particles precipitate under the action of the gravitational force faster than the solvent evaporates. However, sedimentation can be suppressed by, *e.g.*, applying a temperature gradient to the meniscus (such a gradient causes a convective motion of the fluid, which hampers sedimentation of particles).[197]

Hydrophobised nanoparticles can also be organised at the air – water interface and assembled in multilayered structures using the conventional Langmuir – Blodgett technique. Self-assembly of such particles at the interface is also possible in the absence of the ordering effect of the Langmuir surfactant monolayers, while hydrophobisation as such can be achieved in the course of particle formation in the organic medium.[198] This technique was employed in the fabrication of ordered arrangements of various metal and oxide nanoparticles [199–208] and bimetallic particles.[209] Bimetallic nanoparticles were obtained [209] immediately in the subphase and then, after special treatment, came to the surface. The Langmuir – Blodgett method can also be used for the formation of heterocolloid layers.[210, 211]

The Langmuir – Blodgett technique allows the particle size to be varied from several to several tens and even hundreds of nanometres. Nanoparticles can be stabilised using various compounds [212] and form a variety of structures on the surface of the liquid phase.[213] The hexagonal structure, which is usually formed at high monolayer pressures, remains after transfer of the monolayers to solid substrates. The degree of local order in the particles strongly depends on the stabiliser type. In the case of charged particles, the character of their packing is affected by the pH value of the solution. Under particular conditions, wire structures are formed.[214, 215] Usually, the compression isotherms of nanoparticle monolayers do not reflect structural peculiarities (see, *e.g.*, Refs 216 and 217, where both the particle size and the parameters of the stabiliser molecules were varied). At the same time, they exhibit hysteresis, the width of the hysteresis loop being dependent on the compression – expansion rate.

Practical implementation of the Langmuir – Blodgett method is complicated by the problem of fabrication of extended ordered structures. Similarly to compression of surfactant monolayers, compression of a monolayer of nanoparticles causes the formation of a domain structure, the particles being ordered only within domains. To some extent this problem can be considered solved.[218] Rather large ordered structures were fabricated due to particle aggregation caused by an increase in the system's temperature. On raising the temperature, convective flows are induced on the surface of the liquid phase and displace particles towards the growing two-dimensional crystal. Intense convection and capillary waves favour a rapid escape of defects from the growing crystal, which results in extension of the ordered structure.

Ordered structures can be transferred from the surface of the liquid phase to the solid substrate without significant distortion of two-dimensional crystal order (see above). However, the growing ensembles of nanoparticles are unstable, especially if monolayers are transferred at rather low surface pressures. This is due to weak particle – particle and particle – substrate interactions. Therefore, methods for improving the stability of nanoparticle monolayers are required. One of them is to modify the existing layers.[219] However, more efficient is the procedure for fabrication of stable monolayers from nanoparticles bound through bifunctional molecules,[220, 221] *e.g.*, dithiols (remember that these compounds are used [147] to form three-dimensional ordered structures) using the Langmuir – Blodgett method. By chemically binding nanoparticles it is possible to obtain rather stable ensembles. For instance, nanoparticles stabilised by alkanethiols (C_6 – C_{12}) can be strongly bound by arenedithiols at rather high monolayer pressures.[220, 221] To form two-dimensional structures, nanoparticles and the solid dithiol were simply placed in contact on the surface of the aqueous phase. Nanoparticle binding occurred due to the exchange reaction between dithiol and thiol that forms a protective layer on the particle surface. Transmission electron microscopy (TEM) studies showed that particles form two-dimensional layers with hexagonal packing. The interparticle distance was determined by the length of the binding agent molecule (dithiol), being virtually independent of the length of the stabiliser molecules.

If ordered arrangement of particles in the monolayer is not required, the Langmuir – Blodgett procedure is significantly simplified. At the same time, it permits fabrication of layered structures from nanoparticles [222] with the interlayer spacing, which is determined by the thickness of the ligand shell. According to data of X-ray diffraction studies, such layered structures exhibit a rather high degree of perfection.

Practical implementation of the Langmuir – Blodgett method in the case of magnetic particles faces some problems. Attempts at using this technique in experiments with iron oxide particles protected by fatty acid layers led to the formation of inhomogeneous films [223, 224] (multilayered ferroparticle films were also formed).‡ A procedure for fabrication of two-dimensional ensembles of magnetite (Fe_3O_4) and cobalt ferrite ($CoFe_2O_4$) particles stabilised by oleic acid was reported.[225] The particles were characterised by a broad size distribution. They were fractionated and fractions with narrow size distributions (particle size range 2 to 10 nm with a scatter of 10% to 20%) were isolated. Dispersions of the particles in octane or heptane were placed on the surface of water and the solvent was evaporated at 80 °C. The degree of order of the structures formed was particle size dependent, namely, larger particles (6 nm) formed ordered 'crystals' while small particles (2 nm) formed disordered structures. The size of the ordered areas reached several micrometres.

The Langmuir – Blodgett method can also be applied to non-spherical particles, which form a greater variety of ordered arrangements. The self-assembly technique was employed to obtain three-dimensional structures comprised of anisotropic $BaCrO_4$,[226] FeOOH [227] and CdSe [181] particles stabilised by oleic acid, as well as gold [182] and silver [228] nanorods. The formation of structures from rod-like $BaCrO_4$ particles of length 20 nm and diameter 5 nm was TEM monitored to follow the effect of the monolayer pressure on the organisation of particles.[229] At low pressures, 'raft'-shaped isotropic particle aggregates were observed. As the pressure increased, the 'rafts' formed the two-dimensional nematic phase, then the smectic phase and, finally, the three-dimensional nematic phase (Fig. 4). These changes in the structural organisation correspond to the Onsager scheme, according to which the ordering processes are responsible for an increase in entropy due to a decrease in the volume per particle.

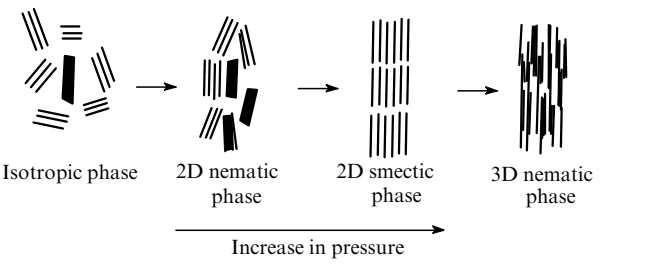


Figure 4. Structural rearrangement of the monolayer of rod-like particles upon an increase in the surface pressure.[229]

‡ Taking into account successful experiments with gold particles, these results seem to be quite unexpected.

5. Liquid – liquid interface

Self-assembly of particles can also occur at the liquid – liquid interface. It was shown that liquid-like colloid silver films can be obtained at the interface between the organic (dichloromethane) and aqueous phases.[230] However, these films are insulators.[231] More recently,[232] similar films were formed from both electrostatically and surfactant-stabilised gold nanoparticles. The formation of ordered structures nanoparticles at the liquid – liquid interface was also reported.[233]

Gold nanoparticles at the interface between the organic and aqueous phases can be immobilised by introducing aromatic molecules (*e.g.*, benzene or anthracene, which are strongly bound to the particle surfaces) into the organic phase.[232] In the case of anthracene the nanoparticle film formed at the liquid – liquid interface is a highly elastic membrane. Films can be transferred to the solid substrate by simply evaporating the contacting solvents. A detailed study on the mechanism of formation of such films showed [234] that the benzene and anthracene molecules are strongly bound to the gold particles due to the π-interaction with the gold cations present on the surface of nanoparticles and that ordered structures cover rather large surface areas.

Ordered layers of nanoparticles at an interface between two immiscible liquids can also be formed by chemical reduction immediately at the interface. For instance, interfacial reaction between an aqueous solution of cadmium carbonate and a solution of carbon disulfide in carbon tetrafluoride resulted in the formation of multilayered films comprised of cadmium sulfide nanoparticles of size from 1.8 to 3.9 nm.[235]

The thermodynamic properties of the particle monolayers were studied taking the monolayers of 2.6 μm polystyrene latex particles at the octane – aqueous surfactant solution interface.[236] In this system under particular conditions it is possible to form ordered interfacial structures, which represent hexagonally packed monolayers of particles with a polycrystalline structure. The monolayer compression isotherm exhibited no features. It was found that the pressure necessary to destroy the monolayer coincided with the interfacial tension at the interface between the above-mentioned liquids in the absence of particles. Destruction of the monolayer occurred by bending rather than transfer of particles to a certain phase. A similar phenomenon was observed [237] for the Langmuir monolayers of negatively charged latex particles of size 0.2 to 2.6 μm at the air – water and octane – water interfaces. The structure of the monolayer at the surface of water is sensitive to the electrolyte concentration. At low electrolyte concentrations, an ordered ensemble of hexagonally packed nanoparticles was formed; an increase in the concentration led to particle aggregation and the formation of disordered structures. At the octane – water interface, a hexagonal packing was formed at low surface pressures and a rhombohedral arrangement was formed at elevated pressures; the electrolyte concentration had little effect on the degree of local order of the monolayer.

6. Layer-by-layer deposition of nanoparticles

The method of layer-by-layer deposition developed [238] as an alternative to the Langmuir – Blodgett method involves successive immersion of a substrate into a dispersion of particles and into a solution of oppositely charged polymer or surfactant. To form polylayers of nanoparticles, this technique was first employed [239] in order to obtain stable ultrathin films comprised of alternating layers of the polyelectrolyte and semiconductor particles. The films appeared to be more stable than those formed using the Langmuir – Blodgett method. Yet another important advantage of the layer-by-layer deposition technique is that films can be deposited on substrates of any size and shape. However, similarly to the Langmuir – Blodgett method, the interparticle interaction is hard to control.

The layer-by-layer deposition method can be applied to obtain various structures.[240, 241] The absorption of the perfect films formed by this method increases linearly with their thickness in the visible and UV spectral regions, which means that all particle layers are characterised by the same packing density. High quality (constant period) of the films prepared by the layer-by-layer deposition is illustrated in Fig. 5, where the SAXS intensity is plotted *vs.* the angle of incidence. If nanoparticles are involved in strong electrostatic and dispersion interactions, the deposition of the polymer layer only slightly disturbs the structure of the ensemble. Immobilisation of particles makes it possible to create strongly inhomogeneous films by deposition of different polymer – particle bilayers in a specified order. By changing the order in which layers are deposited it is possible to impart particular functional properties to the films. Yet another advantage of the layer-by-layer deposition method is the possibility of formation of structures that are inhomogeneous in different directions. For instance, the preparation of gradient composite films of CdTe nanoparticles was reported.[242] The size of the films increased with their thickness. Such films are thought to be promising as elements of photodetectors, bipolar transistors and other high-speed electronic devices. They behave in an unusual manner upon injection and charge transport and can be used as light traps. Fabrication of these films using conventional methods based on molecular beam epitaxy or plasma-enhanced chemical vapour deposition requires various tricks (see, *e.g.*, Refs 243 and 244). The gradient films mentioned above [242] were prepared using four types of particles of size from 2 to 6 nm, which exhibit the luminescence bands in the 495 – 505, 530 – 545, 570 – 585 and 605 – 620 nm regions (from the red to green spectral region), thus providing a broadband luminescence spectrum. Note that the layer-by-layer deposition technique also permits fabrication of ordered layers of nanoparticles with a prescribed particle concentration gradient in the plane of the monolayer.[245]

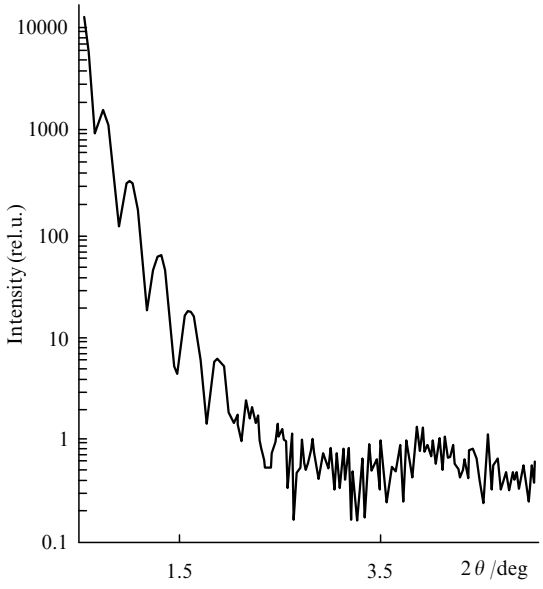


Figure 5. SAXS intensity by the polylayers of particles fabricated by layer-by-layer deposition plotted *vs.* angle of incidence.[241]

7. Biosystems and polymers

One way of development of methods for fabrication of colloid nanocrystals involves stabilisation of nanoparticles using some molecules that have binding sites. Such sites serve as specific 'pointers' of the positions to which other nanoparticles must be attached. On mixing, nanoparticles of one dispersion are linked to particles of the other dispersion through these sites. This permits the formation of a desired architecture of the colloid crystal. In this connection considerable attention is paid to aggregation of nanoparticles that are involved in biospecific interaction.[153, 154, 246 – 251] Interest in the studies of such objects is also

due to great prospects for their application in both microelectronics and biology.

The strategy of using biomolecules is based on their ability to interact with nanocrystals that have various active sites. As biomolecules are introduced into the system, the sites are recognised and a particular arrangement of nanocrystals is formed. Even replication of ensembles of nanoparticles is possible. To this end, it was proposed to use gold nanoparticles covered with adlayer of biotin (more exactly, a sulfur-containing analogue of biotin).[252] As streptavidine (this compound binds biotin) is introduced into the solution, aggregation of gold nanoparticles occurs (Fig. 6). The particles within aggregates are separated from one another by the distance equal to the bond length of the biotin and streptavidine molecules. The diffraction pattern exhibits several maxima, thus revealing some ordered arrangement of particles within aggregates.

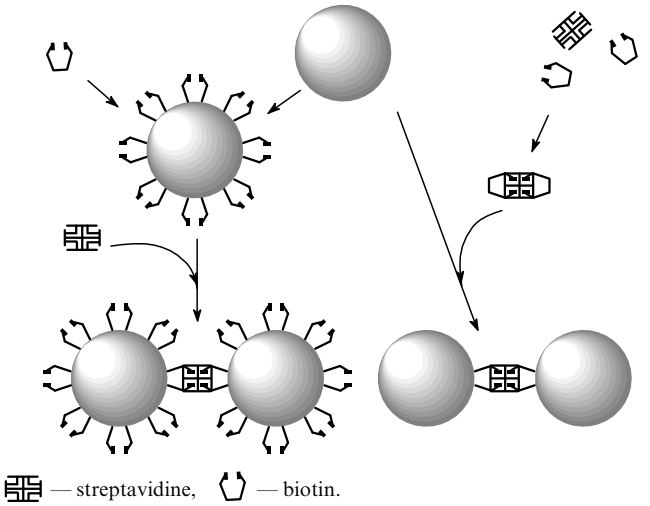


Figure 6. A scheme of aggregation of nanoparticles involving streptavidine molecules.[252]

A procedure for fabrication of gold nanoparticles stabilised by a chemisorbed monolayer of a dodecanethiol derivative and dibenzo-24-crown-8 was reported.[253] Such nanoparticles can recognise dibenzylammonium cations in solution and add them to form a pseudorotaxane shell. Therefore, introduction of bis(dibenzylammonium) into the dispersion of stabilised gold particles causes aggregation due to the assembly of the pseudorotaxane molecules. This approach was employed to study the laws of aggregation of gold and silver nanoparticles.[254]

An analogous procedure was used to obtain ordered (i) monolayers and multilayered structures on substrates and (ii) aggregates in the bulk of solution using proteins,[255] organic molecules [256–259] and polyelectrolytes.[260] Of particular interest is to use DNA molecules for binding particles, because this permits the interparticle distance, period of the particle arrangement and the aggregate compositions to be programmed by choosing a particular amino acid sequence in the DNA molecule.[246, 261–263] In this case, it is also possible to affect the optical characteristics and the melting temperatures of the particle aggregates. Studies on these effects will allow nanoparticle aggregates to be widely used as elements of biosensors. This can be exemplified by the development of a new method of DNA detection using oligonucleotide-functionalised nanoparticle probes.[246, 261, 264, 265] The method is based on the use of two different DNA-complementary oligonucleotides. As the probe meets the DNA molecule and aggregation occurs, the red dispersion turns purple. The change in the colour is due to the interaction between plasmons in the aggregated particles.[262, 266, 267]

This approach differs from other DNA hybridisation methods by enhanced selectivity, which is due to the well-defined melting point of the material fabricated from the oligonucleotide-functionalised gold nanoparticles linked through DNA molecules. The melting transitions in colloid crystals of different sizes formed on silica substrates were studied.[268] Crystals were obtained from 13 nm gold nanoparticles functionalised by various nucleotides. Structures containing different number of layers were formed. Raising the temperature caused breakdown of the adlayer structures due to the melting of nucleotides; the melting temperature depended on the number of the deposited particle layers. The temperature-dependent structure breakdown was found to be reversible; the sharpness of the transition was governed by the number of the layers deposited, while the transition region was nearly three times narrower than in the case of melting of nucleotides in the absence of particles. This narrowing is probably due to the co-operative effect.

It was proposed [269, 270] to use biosystems as substrates for fabrication of ordered colloid ensembles. For instance, latex particles were physically or chemically deposited on a giant lipid vesicle.[269] A single deposited particle deformed the surface of the vesicle and occupied the position corresponding to the highest curvature of the surface. This behaviour can be predicted with ease taking into account the energy expenditure for the deformation of the vesicle. If many particles are deposited, the interparticle interaction is determined by the attractive forces that are also related to the deformation of the vesicle. They cause particle aggregation and the formation of a quasi-two-dimensional hexagonal structure.

A procedure for fabrication of ordered structures, which involves the use of natural two-dimensional crystal order of bacteriorhodopsin molecules, was proposed.[270] This protein forms both *in vivo* and *in vitro* self-organised ordered structures that are called 'purple membranes'. Crystals of bacteriorhodopsin are used as specific templates for fabrication of ordered structures from nanoparticles.

IV. Template methods

1. Template techniques

Recently, methods of increasing the length scale of structural organisation of inorganic materials have been intensively developed. There are several ways of increasing the length scale to which the structural organisation of the assemblies fabricated is extended. One of them involves preliminary formation of 'building blocks'. This approach to fabrication of organised materials was called 'nanotectonics'.[271] Various schemes of practical implementation of the nanotectonics strategy involving biomaterials have been considered.[217] Design of such structures is to a great extent based on the principles of biomimetism (Biomimetic Materials Chemistry). Fabrication of hierarchically ordered structures is of interest for catalysis, materials science and development of resolution methods. Based on the biomimetic principles, some advances were made in creating inorganic materials with prescribed shape, molecular orientation and polymorphous crystal structure.[272] A number of methods for the synthesis of structures of a rather complex shape [273] and highly ordered hybrid ensembles [274, 275] that resemble natural hierarchical structures [276] were also developed. However, these structures are mainly of theoretical interest. More convenient for practical purposes are the 'classical' templates and first of all those based on micro- and nanospheres.

Nanosphere-based templates are used in lithography (see below) and for preparation of composite materials with ordered structure or porous metals with an ordered pore system. Porous metals are necessary for many practical purposes, *e.g.*, production of filters, catalysts, various carriers, heat transfer agents, fuel cells, electrochemical cells, thermal screens and vibration dampers. Often, porous metals with very large specific surface areas are required. Such metals can hardly be obtained by conventional

methods (sintering of powders, production of wires, foaming, *etc*.). This problem can be solved using the method of colloid templates,[277–286] which involves the formation of an ordered structure from spherical particles followed by filling of the interparticle space with the desired material (in particular, metal). The fact that usually the spherical particles contact one another allows them to be completely etched; as a result, a system of ordered spherical voids (the so-called inverted opals) is formed. This permits fabrication of materials with large specific surface areas, three-dimensional ordered pore systems and the pore sizes of several hundreds of nanometres. The pore system is an open system and possesses unique transport properties; these materials are also of considerable interest for photonics [287] (see below).

The technological procedures for fabrication of such materials are based on various methods. For instance, porous structures from Ni, Cu, Ag, Au and Pt were obtained [280] using chemical reduction, colloid crystals (silica) as templates and metal nanocrystals as catalysts. To form 'inverted' colloid crystals from gold the space between large particles was filled with gold nanoparticles.[277] Electrochemical reduction of metals was also employed. Three-dimensional porous crystals were fabricated *via* thermal decomposition of metal (Ni, Co, Fe) salts.[279] Templates are removed using various methods; the properties of the material obtained are strongly dependent on the procedure for template synthesis.

This approach was also used to form ordered structures of metal particles.[288] To this end, a non-metal (*e.g*., oxide) porous matrix was fabricated, which was filled with metal and then etched. This scheme can be used for preparation of ordered structures from not only metals and alloys but also semiconductor materials (see, *e.g*., Refs 289 and 290).

Porous membranes and ensembles of carbon nanotubes are also widely used as templates. In this case, either particles of irregular shape distributed within narrow channels or nanorods are formed.[291–293] It is also possible to obtain ensembles of rather complex composition and morphology. This approach was employed for the synthesis of polymer–cadmium sulfide composite nanowires [294] and various nanotubes [295–297] including those filled with metals [297, 298] (recently, considerable attention has been given to such objects, see review [299]).

Nanorods are most often formed using anodised porous alumina layers as templates. The pore diameter in these templates varies over a wide range (from 5 to 300 nm), the pore length exceeds 100 μm and the pores themselves are characterised by good linearity. Methods of fabrication of alumina templates have been well developed.[300, 301] Using these templates, it is possible to obtain composite materials with various nanowires [302–308] and fill almost all pores up to a depth of 100 μm (usually, only 10% to 20% of the pore space volume is filled) by employing specific procedures.[308] X-Ray studies showed that nanowires formed within the matrices have a crystal structure while their diameter is governed by the pore size. Ensembles of metal nanowires were also obtained using mesoporous silica SBA-15.[309]

Ordered ensembles of metal nanoparticles can be fabricated [310] with mesoporous silicas with an ordered pore structure, *viz*., MCM-41 (hexagonal structure) and MCM-48 (cubic structure). Silica is washed with the solution of a salt of the corresponding metal and then heat treated to form metal nanoparticles within the pore space. At elevated temperatures, the metal nanoparticles go to the outer surface of silica, thus forming an ordered lattice whose structure reproduces the two-dimensional pore structure of the silica template.

Ordered ensembles of nanoparticles can also be obtained by metal reduction in the 'micelles' of block copolymers, which can have a well-organised spatial structure. A procedure for fabrication of gold nanoparticles in laser irradiated copolymer of styrene and 4-vinylpyridine was considered.[311] The results of an experimental and theoretical study of the chemical method of preparation of lead sulfide nanoparticles in films of the same microseparated block copolymer were also reported.[312] The studies on the synthesis and properties of nanoparticles of different nature in polymer matrices were reviewed.[313]

Gel matrices of mixtures of a polyelectrolyte, surfactant [314] and organosilicon polymer [315, 316] are similar to the block copolymer matrices. They were used to obtain ordered ensembles of gold and platinum nanoparticles *via* chemical reduction. By varying the parameters of the microscopic gel network the particle size and the spatial distribution of the particles can be changed with ease.

2. Nanolithography methods

Not only the formation of colloid crystals but also fabrication of large ordered patterns from colloid ensembles is of considerable interest. Such patterns are prepared using a variety of methods, *viz*., lithography,[317] microcontact printing,[318] self-assembly involving polymers,[319] bidentate molecules,[320, 321] evaporation [322–324] or selective wetting.[325, 326] Various lithographic techniques allow one to obtain structures with prescribed geometric distribution, size and shape of the primary elements. The methods employed in the field include electron beam lithography,[327] X-ray lithography,[328] ion-beam lithography [329] and photolithography. The last-named technique is most widely used but, unfortunately, is unsuitable for the formation of structures whose elements are smaller than half the wavelength in the visible region. The region with $\lambda < 300$ nm is accessible to UV lasers [330] and holographic interferometry [331] only. The electron, ion-beam and X-ray lithographies cover the nanometre region; however, wide use of these methods is impossible as yet. The formation of ordered structures using heteroepitaxy of metals [332] and semiconductors [333] also faces some difficulties.

It was proposed [334] to use ordered arrangements of colloid particles as lithographic mask. This method was employed by many researchers. The possibilities of the technique were significantly extended.[335–338] It was shown that the use of two layers of spherical colloid nanoparticles allows the method of fabrication of nanostructures to be significantly simplified and the patterns formed to be diversified. The modified method permits fabrication of nanostructures comprised of different materials on various substrates. According to the data of atomic force microscopy studies, the type of the structure formed can be predicted with ease based on geometric considerations. This method allows the particle size to be varied with ease, thus changing the optical properties of the particles.[339]

A combined technique was also proposed.[340, 341] Patterns comprised of ordered gold nanocrystals were created with an electron beam. First, an ordered arrangement of gold particles was formed on the silicon nitride substrate by the droplet evaporation method. Then, the monolayer was exposed to an electron beam to destroy the protective ligand shell. This led to stronger binding between the particles and the substrate on the electron-beam patterned area of the substrate. The unbound particles were removed from the substrate with a solvent; as a result, the substrate was patterned in the desired manner.

Recently, the method of microcontact printing has been intensively developed. The technique involves fabrication of a pre-patterned stamp followed by transfer of the pattern (nanoparticles) to the substrate [325, 342] and permits the use of substrates of any nature.

Scanning tunnelling and atomic force microscopies are also used to obtain ordered structures. For instance, patterning was done by etching an organosilane monolayer from the substrate using a scanning tunnelling microscope (STM).[343] This was followed by nanoparticle deposition on the etched areas. A similar procedure was employed [320] to obtain ordered arrangements of gold nanoparticles with an atomic force microscope (AFM), which was used for detection of the STM-etched area and subsequent particle transfer to this area. An AFM was used to fabricate two-dimensional and three-dimensional ordered structures.[344] The technique was improved,[345] namely, deposition of 3 nm gold particles on a pre-treated surface area was followed by the formation of ordered structures using an AFM and then by

post-growth of the particles *via* immersion of the substrate in a $HAuCl_4$ solution.

Particular emphasis should be placed on the so-called dip-pen nanolitography technique,[346–349] which allows one to deposit films comprised of both organic molecules containing thiolate groups and nanoparticles on the surface of gold substrates. The method involves the spontaneous condensation of molecules or particles in the gap between the AFM tip and the substrate (Fig. 7); by scanning the surface it is possible to create the desired pattern. In the dip-pen nanolithography scheme, the microscope tip, organic molecules and substrate play the roles of 'pen,' 'ink' and 'paper,' respectively.

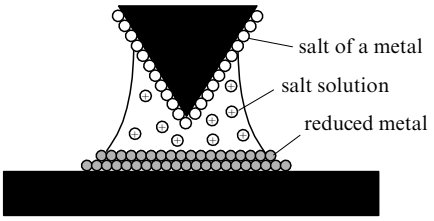


Figure 7. A scheme of dip-pen nanolithography.[349]

A method of preparation of gold 'ink' was proposed.[348, 349] This can be done using both electrochemical reduction of gold and a procedure which does not require a voltage to be applied to the microscope tip. According to the method, the microscope tip is preliminarily covered with a salt of gold and then a nanodroplet of water is placed within the gap between the salt and the silicon substrate. Dissolution of the salt as well as the metal reduction and deposition on the substrate proceed in the absence of special treatment of the system. The gold layer formed in the course of reduction was 0.4 – 1 nm thick. Details of the mechanism of gold reduction are still to be clarified; however, it was pointed out that no reduction of gold proceeds on the silica substrates. By appropriately choosing the salt – substrate pair it is possible to obtain structures from various materials.

3. Nanosphere lithography

Ordered arrangements of metal and semiconductor nanoparticles are usually fabricated by lithography techniques using planar substrates. Recently, a new trend has been towards deposition of ordered arrangements of nanoparticles on the surfaces of organised larger spherical particles. Such systems are of interest in studies on the Raman scattering and photoelectrochemical catalysis and as working elements of optical sensors. A uniform packing of nanoparticles on spherical particles can also be used for further fabrication of hollow spheres (the case where the core is somehow etched) [350] that have found application in pharmacology, catalysis, photonics and materials science.[351]

Metal particles are deposited on the surface of larger dielectric particles using various methods, *e.g.*, chemical reduction on the surface (to cover polystyrene latex particles with platinum [352] and silica particles with silver [353]), reactions with free radicals (to form silver nanoparticles on the surface of microspheres [354]) and sonochemical deposition of platinum,[355] zinc sulfide,[356] nickel [357] and cobalt.[358] An alternative approach involves activation of the surface of large particles with metal 'seeds' obtained by, *e.g.*, reduction of the corresponding precursor.[359, 360] It was employed to fabricate gold shells on silica spheres [359] and silver shells on polystyrene spheres.[360] Both these methods permit a uniform distribution of metals over the surface of spheres, though sometimes it is impossible to provide a dense packing of nanoparticles on large spheres.

The layer-by-layer deposition of nanoparticles and polymers (see, *e.g.*, Refs 361 – 363) is also employed in nanosphere lithography. Using this method, one can obtain composite films of different compositions, containing both the polymer and nanoparticles. The formation of dense layers of gold nanoparticles covered with thin silica layers on the surface of polystyrene spheres was reported.[364] To this end, layers of gold particles and poly(dialkyldimethylammonium chloride) were successively deposited on the surface of polystyrene spheres.

Ordered arrangements of 1 μm silica spheres 'capped' with gold or titanium were fabricated.[365] To this end, an ordered layer of silica particles was formed on the substrate and then covered with a photoresist layer. Then, photoresist was etched from the upper segments of the spheres, metal was deposited on the system and the remaining photoresist layer was completely etched. This led to the formation of ordered layers of metal 'capped' silica particles. The 'cap' size was varied by etching the deposited metal.

4. Functionalisation of substrates

Yet another efficient method of fabrication of ordered layers of nanoparticles involves pre-structurisation of the substrate.[366–368] Particles can be deposited using various procedures including a combination of the self-assembly on functionalised substrates with the droplet evaporation method. Other procedures include flow-induced packing of particles in the cavities with prescribed size and shape (Fig. 8); adsorption of particles on self-assembled monolayers characterised by different surface charge of different surface regions [370] and assembling of particles on the surface regions created by microcontact printing [371] or lithography.[372] A promising approach was also proposed,[373] which involves self-assembly of the charged particles on structured polyelectrolyte polylayers. In contrast to conventional self-assembly methods, this technique permits fabrication of ordered layers not only on the metal and oxide but also on the polymer surfaces. Layer-by-layer deposition of polyelectrolytes and particles allows films with unique properties to be designed.[374] In such films, the polyelec-

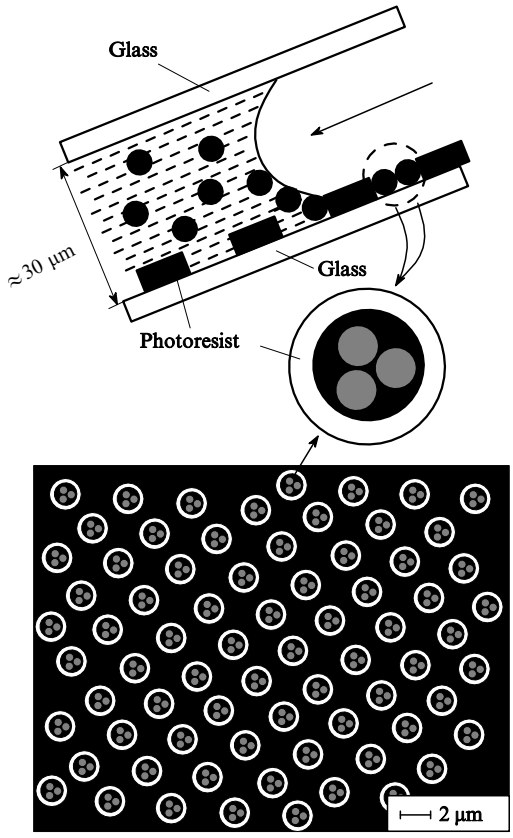


Figure 8. Deposition of nanoparticles on an ordered system of voids on substrate.[369]

trolyte polylayers can contain various functional groups [375] that provide the necessary electro-optic [376] and electroluminescent [377] properties, as well as the conducting [378] or dielectric layers and functional organic [379] and inorganic [380] particles. Polyelectrolytes permit enhancement of the adhesive binding between particles and the substrate. Patterns for polyelectrolyte deposition can be created using the microcontact printing technique;[381] therefore, the structures deposited can have arbitrary geometries.

Yet another widely used method is based on the creation of alternating hydrophilic and hydrophobic zones on the solid surface. It was employed to form ensembles of CdS nanoparticles on gold and silver substrates covered with self-assembled monolayers.[382] The methods necessary to prepare surface regions with different properties are based on the scanning probe nanolithography [383] or electron-beam patterning.[384] They are rather complicated; therefore, search for simpler procedures is currently in progress. Recently,[385] it was proposed to obtain ordered ensembles of nanoparticles as follows. First, a regular structure is formed on a silicon plate covered with the natural oxide layer from a self-assembled monolayer of siloxane containing a terminal CH_3 group by microcontact printing (see, *e.g.*, the procedure for fabrication of polydimethylsiloxane punches [386]). Then, the plate is dipped in a solution of the corresponding metal nitrate. After the plate is taken out from the solution, the droplets cover only the hydrophilic areas. The plate is then tilted so that the droplets are accumulated at the boundaries of the hydrophilic zones. After evaporation of the droplets the samples were heat treated, which resulted in the formation of nanoparticles. This method was used to fabricate ordered arrangements of cobalt, nickel and ferrite (MFe_2O_3; M = Mg, Ni) nanoparticles. The particle size and the interparticle distance were controlled by varying the solution concentration and by changing the structure of the monolayer (template), respectively.

An interesting effect, which can found practical applications, was reported.[387] The Si (100) surface covered with a natural 2 nm thick silica layer was coated with a patterned photoresist layer and the unpatterned photoresist was etched. Then, the a droplet of organic dispersion of thiol-stabilised gold particles was transferred to the substrate. It was found that narrow 'stripes' of the dispersion leak beyond the droplet at the resist – substrate interface. The 'stripe' length is at most 600 μm. Evaporation of the solvent (toluene) resulted in the formation of cluster chains of width $\approx$120 nm. The chain width remains nearly constant along the whole chain length. An analogous effect of 'escape' of nanoparticles along the boundaries of different-nature regions involving the formation of nanowires was also observed.[388]

V. Physicochemical properties of ensembles of nanoparticles

1. Electronic properties

Ordered arrangements of nanoparticles are considered as candidates for elements of electronic devices; because of this, considerable attention has been given to their electronic and optical properties.

The authors of numerous studies (see, *e.g.*, references cited in Ref. 4) observed a nonlinear current – voltage curve (the so-called Coulomb stairs) on passing electric current through individual particles. The current – voltage curves obtained in analogous experiments with self-assembled arrays of nanoparticles also have the shape of the Coulomb stairs.[138, 389, 390] For nanoparticles in organic media it is possible to draw a nearly complete analogy between the Coulomb stairs exhibited by single particles and their monolayers. For aqueous media, the current – voltage curves measured [390] on applying positive and negative potentials to the monolayer (experiments were carried out with 2 nm gold particles stabilised with alkanethiols and self-assembled into a monolayer using dithiols) are significantly different. Namely, the Coulomb stairs were observed after application of the positive potential and were not observed after the negative potential was applied. No unambiguous explanation for this effect has been given as yet.

Currently, considerable attention has been given to the studies on the laws of electron transfer within the monolayer plane. Electron transfer in the monolayered nanoparticle films involves the motion of electrons between the metal nanoparticles and overcoming of the potential barrier in the region of the stabiliser molecules (surfactant). The electron energy diagram for a composite film comprised of nanoparticles and a dielectric matrix is schematically shown in Fig. 9. Electron transfer between particles separated by an insulator proceeds by two main mechanisms, namely, by tunnelling and *via* thermally induced overcoming of the energy barrier. In weak electric fields ($eU_p < kT$, where U_p is the potential difference between the neighbouring particles), the insulator conductivity for electron transfer by the thermoionic emission mechanism is given by:

$$\sigma_e = \alpha T^2 \frac{e}{kT} \exp\left(-\frac{\phi_e}{kT}\right),$$

where α is a constant and ϕ_e is the height of the energy barrier. The barrier height is close to the work done by an electron to go from the metal particles to the matrix and includes the contribution of the image forces, which become significant in the case of small particles.

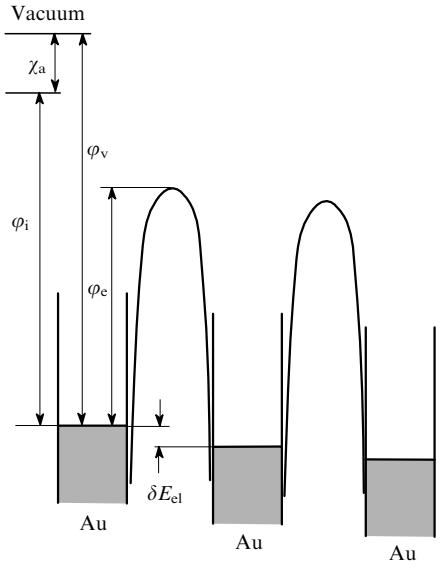


Figure 9. Electron energy diagram for a composite material of the 'nanoparticles – dielectric matrix' type;[390]
χ_a is the electron affinity towards the dielectric matrix, φ_v is the ionisation potential of the metal and φ_i is the ionisation potential of the metal in the dielectric medium.

The image forces reduce the work function by a value of the order of

$$\delta\phi = \frac{2e^2}{\varepsilon_\infty \varepsilon_0 h},$$

where ε_∞ is the high-frequency dielectric permeability of the medium and h is the interparticle distance. For gold particles, the work done to go vacuum is $\approx$5 eV and the decrease in the barrier due to the image forces at an interparticle distance of $\approx$1 nm is $\approx$2 eV. For dielectric media, the work done to go from gold decreases by up to 1 eV. Usually, the height of the energy barrier in the nanoparticle films is $\approx$2.5 eV.

The tunnelling current flowing between two metal particles is given by

$$J \propto \left(\frac{8me}{\pi^2\hbar^3 B}\right)\mathrm{sh}\left(\frac{eU_\mathrm{p}}{kT}\right)\exp(-A\phi_\mathrm{av}^{0.5})\exp\left\{-\left(\frac{\delta E_\mathrm{el}}{kT}\right)\right.$$
$$\left.\times\,[1-\exp(-B\delta E_\mathrm{el})]\right\},$$

$$B=\frac{A}{2\phi_\mathrm{av}^{0.5}},$$

$$A=\frac{4h(2m)^{0.5}}{\hbar},$$

$$\phi_\mathrm{av}=h^{-1}\int_0^h \phi_\mathrm{e}(x)x\mathrm{d}x.$$

Here, m is the mass of an electron and δE_el is the energy required to transfer an electron from one neutral particle to another,

$$\delta E_\mathrm{el}=\frac{0.5\,e^2h}{(4\pi\varepsilon\varepsilon_0 R)(R+h)}, \qquad (14)$$

where R is the particle radius.

Temperature dependences of the conductivity of two-dimensional ordered films fabricated using the Langmuir–Blodgett method from silver nanoparticles were reported.[391] Let us take them as examples. The 8 nm silver particles were stabilised by thiols with different chain length. The films were formed at different monolayer pressures. The temperature dependences of the film resistances are shown in Fig. 10. As can be seen, initially the resistance exponentially decreases with temperature. These dependences are well described by the relationship

$$R \propto \exp\frac{E_0}{kT},$$

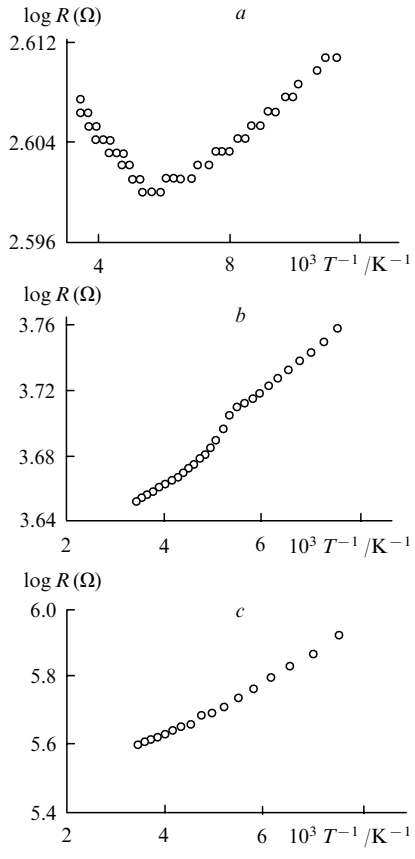


Figure 10. Temperature dependences of the resistance of the films formed by silver nanoparticles stabilised by ethanethiol (*a*), pentanethiol (*b*) and octanethiol (*c*).[391]

where E_0 is the activation energy for all the films under study. At $T \approx 200$ K, the resistance reaches its minimum value, which corresponds to the transition from the activation mechanism to the metal mechanism of conductivity. These dependences are indicative of the metal–dielectric transition in the two-dimensional monolayer. An analogous transition was detected using the tunnelling [392] and impedance spectroscopies.[393] The experimental E_0 values correspond to those calculated assuming that the energy barrier is due to Coulombic interaction between electrons and nanoparticles.

Somewhat different results were obtained in a study [394] on the electrical conductivity, photoconductivity and photoelectrochemical properties of the films comprised of dithiol-stabilised gold nanoparticles. Ordered layers were fabricated by particle deposition on substrates dipped in a colloid dispersion. At nearly the same size (6–8 nm) of particles covered with thiols of different chain lengths, the activation energy was found to lie between 5 and 25 meV, which is two or three orders of magnitude lower than the estimate (see above). Similar activation energies were obtained earlier.[147, 395] This probably indicates that the conductivity in these systems occurs by direct particle–particle contacts. Indeed, Fig. 10 shows that in the case of, *e.g.*, ethanethiol the temperature dependence of the conductivity has a complex shape and the resistance increases with raising the temperature in a certain interval. This is most probably due to the breakdown of interparticle contacts in the conductivity channels. Prolonged heating (100 °C) of the layer of particles was accompanied by a dramatic decrease in the resistance, which can be explained by thermally induced removal of the 'binding agent' from the interparticle space. The dependences of the photocurrent yield on the photon energy (Fig. 11) show that the work done to transfer electrons to the matrix is ~1 eV. Analysis of the dependences presented [the (yield)$^{0.5}$–energy dependence obeys the Fowler law for photoemission] suggested that the conductivity is of mixed character and is due to both the particle–particle contacts and the hopping mechanism. It should be noted that the mixed mechanism of

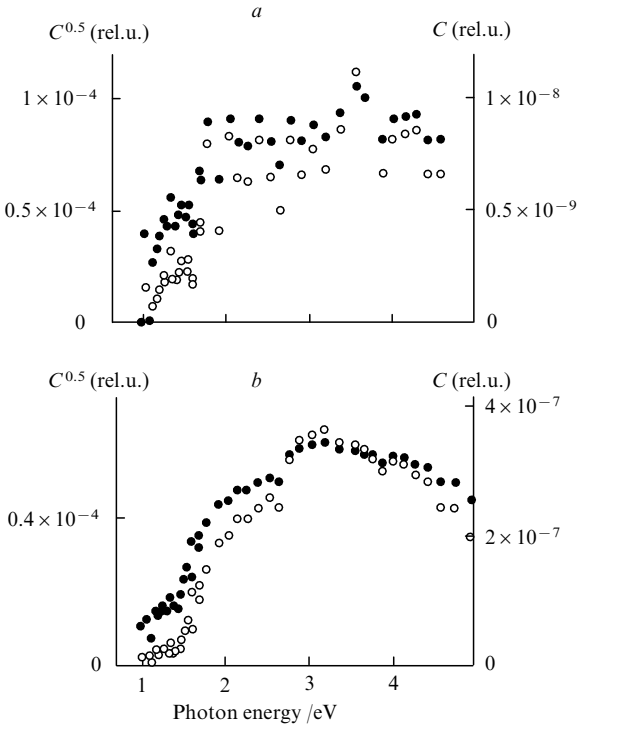


Figure 11. Photocurrent yield (C) for films comprised of silver nanoparticles stabilised by pentanethiol (*a*) and octanethiol (*b*).[391]
The right and left ordinate axes are for the open and full circles, respectively.

conductivity is typical of conventional composite materials.[396–398] The reversible metal–dielectric transition also occurs as the thickness of the ligand shell [213, 399] of nanoparticles changes.

A large number of experimental studies on various characteristics of ensembles of nanoparticles are available. At the same time, theoretical studies in this field are scarce. This is a consequence of the complexity of the systems under study (relevant solvable models can hardly be chosen). Yet another problem is that, strictly speaking, ordered ensembles are inhomogeneous structures. Structural inhomogeneity is due to the following reasons. First, nanoparticles are characterised by some size distribution. Second, it is virtually impossible to obtain a perfect structure comprised of nanoparticles. Third, different nanoparticles have different compositions because their ligand shells are also characterised by some degree of inhomogeneity. Fourth, nanoparticles execute thermal motion, thus introducing distortions in the lattice structure of the colloid crystal. Finally, electron transfer between particles can be accompanied by the electron scattering by structural inhomogeneities of the organic layer (this process can occur in different manner). In spite of this, serious efforts were made to take into account many salient features of the ensembles of nanoparticles. For instance, the following Hamiltonian was proposed to describe the electronic properties of ordered ensembles [400]

$$H_0 = \sum_{i,j}^{n} h_{ij} \sum_{\mu}^{2} \alpha_{i\mu}^{+} \alpha_{j\mu} + \frac{1}{2} I \sum (n_i - 1)^2 + \frac{1}{2} \gamma \sum_{i,j} n_i n_j, \qquad (15)$$

$$h_{ij} = \begin{cases} \alpha_i & i = j \\ \beta_{ij} & i \neq j, \end{cases}$$

where α_i is the energy level of an electron of particle i; β_{ij} is the 'transfer integral,' which is determined by the overlap of the electron orbitals of the neighbouring nanoparticles; $\alpha_{i\mu}^{+}$, $\alpha_{j\mu}$ are respectively the production and annihilation operators of electrons with the spin μ at the particle i; and n_i is the operator of the number of electrons at the particle of the type i,

$$n_i = \sum_{\mu}^{2} \alpha_{i\mu}^{+} \alpha_{i\mu} .$$

In expression (15), the second term describes the effect of Coulombic blockage and is determined by the energy required to charge a single particle

$$I = \frac{e^2}{4\pi\varepsilon_0 \varepsilon R},$$

while the last term describes the mutual polarisation of the neighbouring particles

$$\gamma = e^2 \left[2R \left(\frac{H}{2R} + \frac{e^2}{2IR} + a \right) \right]^{-1},$$

where H is the distance between the centres of the particles and a is a constant.

Calculations were carried out assuming that the constants α_i and β_{ij} fluctuate near their average values with the fluctuation amplitudes $\Delta\alpha$ and $\Delta\beta$, respectively. It was pointed out [400] that all the parameters introduced can be determined experimentally. Calculations of the electronic states of the system revealed the possibility for two types of the metal–dielectric transition (according to Anderson [401] and to Mott [402]) to occur in the system due to the fluctuations of different parameters. The Anderson transition occurs if the interaction between the neighbouring particles is rather weak and does not compensate the energy difference between the levels, which is due to fluctuations of the particles' characteristics. The Mott transition is observed when compression of the lattice of a colloid crystal causes suppression of the mutual repulsion between the electrons bearing oppositely directed spins and belonging to the same particle owing to the cooperative effects (screening), merging of the lowest occupied and upper unoccupied bands and the insulator–conductor transition. Disorder in the system also affects the Mott transition; however, this transition can be masked if the energy fluctuations due to structural inhomogeneities exceed the Coulombic interelectron repulsion energy. At small amplitudes of the energy level fluctuations, the Anderson transition occurs at much shorter interparticle distances compared to the Mott transition. These results were confirmed by the experimental data,[403] according to which at a rather long interparticle distance the ensembles behave as dielectrics due to the Anderson-type electron localisation even in the absence of the Coulombic gap.

The conducting properties of ensembles of nanoparticles can be changed by varying the layer compositions and using those particles whose state can be changed with ease under the action of external factors. In this connection mention may be made that it is possible to control the photoinduced electron transfer between the monolayers of the donor [a polypyridyl complex of Ru(II)] and acceptor [an acetylacetonate complex of Ru(III)] complexes by separating them by insulator layers [404] and that the probability of electron tunnelling in the superlattice of magnetic cobalt particles depends on the external field applied to the system, *i.e.*, on the orientation of the electron spins.[405]

2. Optical properties

Recently, increasing interest in the optical properties of nanoscale systems has been expressed.[406] This is mainly due to some prospects for the use of the near-field effects in creating devices for ultrahigh information recording density and ultrafast reading devices. In the case of three-dimensional ordered structures, of particular interest are the so-called photonic crystals (see below).

We will first consider the optical properties of two-dimensional aggregates and single-layered films comprised of metal nanoparticles. Single spherical particles are characterised by the resonance absorption band at the frequency ω_0 corresponding to the excitation of surface plasmons.[4, 406] Ellipsoidal particles are characterised by two maxima corresponding to the polarisation along and perpendicular to the principal axis. The absorption spectrum is usually calculated based on the Maxwell equations at a given dielectric constant of the external medium. The dependences of the optical and relaxation characteristics of nanoparticles on their size and shape were recently reviewed,[407] so we leave them out of our consideration.

The absorption spectra of aggregates should be calculated with inclusion of the interparticle interaction (*i.e.*, the size and shape of the aggregate formed). Pileni [408] reported the results of a detailed study of the optical and electronic properties of ordered films comprised of silver nanoparticles. Figure 12 presents the absorption spectrum of an aggregate comprising a total of nineteen hexagonally arranged nanoparticles. The characteristic feature of the spectrum is the appearance of maxima at certain ω^- and ω^+ values that meet the condition $\omega^- < \omega_0 < \omega^+$. For the s-polarised wave, there is only one maximum at $\omega = \omega^-$, while for the p-polarised wave there are two such maxima and the amplitude of the high-energy maximum increases as the angle of incidence increases. This is a consequence of the optical anisotropy of the system, namely, its polarisability is different along the normal and parallel to the surface of the substrate. This anisotropy manifests itself for the p-polarised wave, because it has components both in the surface plane and along the normal to this plane (the s-wave has only the component parallel to the surface). Experimental data obtained for silver nanoparticles [408] are in good agreement with the results of calculations.

The optical properties and electronic characteristics of the ordered films comprised of nanoparticles are determined by the classical (dipolar) and quantum (exchange) interactions between nanoparticles. The quantum interaction occurs only at distances shorter than 1 nm.[213] Because of this, the optical properties of composite materials are most often described using the Maxwell–Garnett theory as a first approximation, according to which

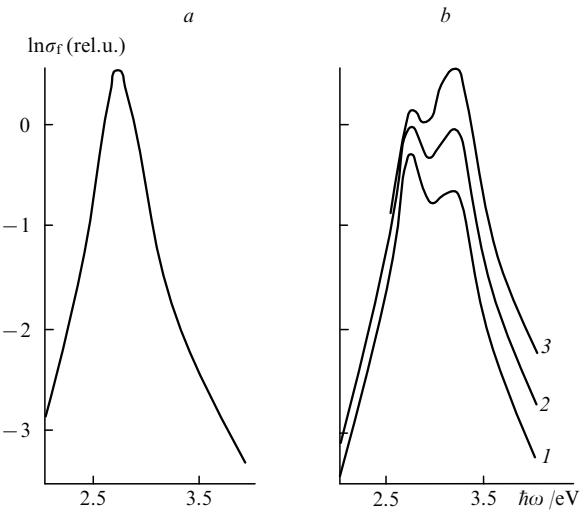


Figure 12. Absorption section by an aggregate comprised of nineteen silver nanoparticles for the s- (*a*) and p-polarised (*b*) waves.[408]
Angle of incidence /deg: 45 (*1*), 51 (*2*) and 60 (*3*).

the dielectric susceptibility of the medium is determined *via* the dielectric susceptibility of individual particles. This theory works well for dilute colloid systems. Various methods have been developed to calculate the dielectric susceptibility at a large volume fraction of particles. Here, we will present the main results of the most consistent approach.[409, 410] The frequency dependence of the nanoparticle polarisability can be obtained using the data on the dielectric response of bulk silver, on the electron relaxation time in nanoparticles and the Clausius–Mossotti formula. The dielectric susceptibility of bulk silver is given by the Drude relationship

$$\varepsilon_{\rm p} = 1 - \frac{\omega_0^2}{\omega^2 + v^2} + \frac{i\omega_0^2 v}{\omega(\omega^2 + v^2)},$$

where ω_0 is the plasmon frequency for the bulk metal and v is the collision frequency of electrons with impurities in the bulk of the metal and with the surface of nanoparticles (the width of the plasmon band),

$$v = \left(\frac{1}{l} + \frac{1}{R}\right) v_{\rm F},$$

where l is the free path length of electrons in the bulk metal, R is the particle radius and $v_{\rm F}$ is the Fermi velocity of electrons.

The Clausius–Mossotti formula for the polarisability of a metal sphere dipped in a dielectric medium with permeability $\varepsilon_{\rm m}$ has the form

$$\chi_{\rm p} = \frac{\varepsilon_{\rm p} - \varepsilon_{\rm m}}{\varepsilon_{\rm p} + 2\varepsilon_{\rm m}}.$$

The effective dielectric permeability of a two-dimensional composite medium comprised of spherical particles that are uniformly distributed over the volume of the matrix is given by

$$\varepsilon_{\rm ef} = \frac{1 + \chi_{\rm p}\varphi - (1-\varphi)^2\chi_{\rm p}^2\zeta}{1 - \chi_{\rm p}\varphi - (1-\varphi)^2\chi_{\rm p}^2\zeta}\varepsilon_{\rm m},$$

where φ is the packing density of the particles and ζ is the structure parameter, which includes three-particle correlations in the arrangement of spheres (calculated in Ref. 409). The parameter ζ depends on φ and changes from 0 (for dilute systems) to 1 (for close-packed systems). It also depends on the character of the packing of spherical particles, being much larger for random packing compared to regular one. In the former case, the parameter ζ has virtually the same value for both two-dimensional and three-dimensional systems.

Having found the dielectric permeability, it is an easy matter to calculate various optical characteristics of films, *e.g.*, the reflection coefficient $|R_{\rm s}|^2$, where

$$R_{\rm s} = \frac{r_1 + r_2 e^{-2i\delta}}{1 + r_1 r_2 e^{-2i\delta}}.$$

Here r_1 and r_2 are the Fresnel coefficients for the air–film and film–substrate interfaces,

$$\delta = \frac{2\pi}{\lambda} d n \cos\theta,$$

λ is the radiation wavelength, d is the film thickness, n is the refractive index of the films, θ is the angle of incidence of radiation.

The dependence of the reflection coefficient on the interparticle distance is shown in Fig. 13. As can be seen, the calculated and experimental data are in good agreement at rather long interparticle distances, being substantially different at short distances. Good correspondence between the theory and experiment holds up to $H/2R \approx 1.25$. This is due to the fact that the dielectric–metal transition occurs in the monolayer at $H/2R \approx 1.15$, which is not included in the model considered above. As the system approaches the transition point, rather large clusters are formed, which are characterised by the metal conductivity. For this reason, the differences between the theory and experiment increase. The metal–dielectric transition is also

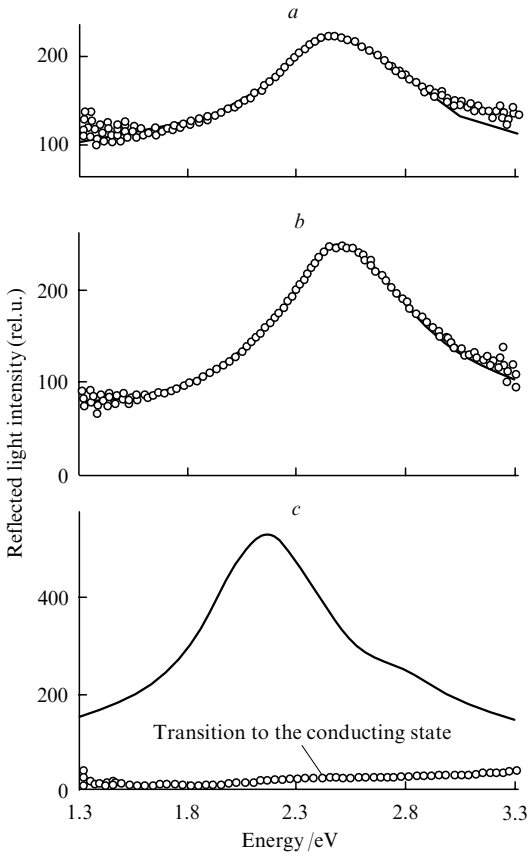


Figure 13. Reflected light intensity plotted *vs.* photon energy for different interparticle distances.[399]
Experimental data (open circles) and results of calculations (solid lines). The 'interparticle distance-to-particle-size' ratio ($H/2R$) is 1.60 (*a*), 1.38 (*b*) and 1.17 (*c*).

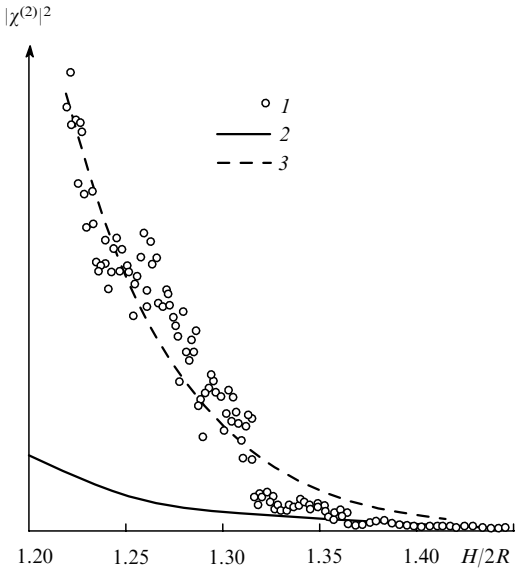


Figure 14. Second optical harmonic intensity as a function of the relative interparticle distance.[399]
Experiment (*1*) and results of calculations using the classical model (*2*) and exponential approximation (*3*).

clearly detected in measuring the intensity of the second optical harmonic (Fig. 14), namely, marked deviations of the calculated values from the experimental data are observed on approaching the point of the metal–dielectric transition.

A study on photon emission from a monolayer of particles under the action of a voltage applied to the tip of an STM also led to quite unexpected results.[408] Experiments were carried out with ordered layers of 4 nm silver nanoparticles separated by a distance of 2 nm on the Au(111) surface. First, the motion of particles across the surface was observed. Second, surprisingly, photon emission from the monolayer was inhomogeneous, that is, dark zones were observed near certain particles (the darkest zones corresponded to the vertices of the particles). The intensity of emission from the particle vertices was ten times lower than from the other sites. Experiments showed that highly mobile particles are bad photons emitters (*i.e.*, quenching of the emission is due to the motion of particles). The measurements were carried out in the d.c. regime, which is manily due to the resonant tunnelling of electrons. Non-resonant electron transfer and, correspondingly, photon emission are of the fluctuation nature. The photon emission is related to the relaxation of plasmons that are excited in the case of non-resonant electron transfer (non-resonant tunnelling).[411] Therefore, photon emission is affected by many factors. Electron relaxation can occur *via* the excitation of a plasmon, production of a photon or interaction with the surface phonons. For small particles, electron transfer to the particle occurs in the ballistic regime.[412] Because of this, electron relaxation is possible only *via* the electron–plasmon or electron–phonon interaction. The latter interaction is known to play an important role in the relaxation processes in the particles whose size is less than the free path length of an electron. It is assumed that the phonon excitation of highly mobile particles is facilitated as compared to the immobilised particles. Probably, the excitation of collective phonons also occurs. This effect, along with the well-known effect[4,413] of change in the transmission and reflection of light upon electrochemical injection of charges into the film, opens up new possibilities in controlling the electronic properties of nanofilms. In the latter case, changes in the electronic properties of the films can be explained by the change in the electron density in certain particles for which the relative changes in the electron density much exceed the corresponding value for the bulk material.

It should be noted that the interaction of electromagnetic waves with two-dimensional arrangements of particles are still poorly studied. At the same time, their understanding is necessary for not only the description of the optical properties of films but also creation of a new generation of memory devices. At the nanometre scale and femtosecond times, the electromagnetic energy is transferred by plasmons. For this reason, revealing the localisation effects of electromagnetic waves is of great practical interest. Delocalised modes govern energy transfer in the whole system, while the localised modes allow the energy to be concentrated within small regions of the system. A study[414] was reported on the properties of the eigenmodes in a two-dimensional composite containing randomly distributed metal inclusions that covered half the surface area. According to calculations, localisation of the surface plasmons in the whole spectral region is impossible. The localisation radius is distributed over the whole admissible range of sizes, from the smallest size to the size of the entire system. A typical eigenmode is simultaneously localised and delocalised, that is, there are small areas with intense field, which are distributed over a large surface area and are coherent. This propertiy of the surface plasmons makes them a promising object for data storage and transmission applications for ultrafast computations. The localisation areas can serve as energy reservoirs, while their long-range coherence allows information to be rapidly transmitted over long distances.

Currently, a new research avenue in the optics of nanofilms deposited on substrates is in prospect. It was shown[415] that the $Au@SiO_2$ particles (gold particles covered with silica layer) are suitable for fabrication of plasmon waveguides whose size is of the order of the particle size. Numerical experiments[416] showed that nanoparticles organised in linear chains are capable of transferring the energy localised in the regions with the characteristic size much smaller than the optical diffraction limit. The most important requirement is that the particles be separated by a layer, which must be sufficiently thin for the interaction between the plasmon modes in nanoparticles to occur in the near field.[417] According to numerical simulation, the signal propagation velocity in this plasmon waveguide is one tenth of the speed of light. The waveguide geometry admits the presence of acute angles.

From the aforesaid it follows that the optical properties of nanoparticle films are still far from being completely studied; therefore, they have been the subject of intensive research. The dependences of the optical characteristics of films on the properties of the substrate[418] and the dispersion medium were studied in detail.[419] Ellipsometry can also be used to study the properties of films.[420] Enhancement of the plasmon resonance upon reflection of light from bilayered films (from the substrate side)[421] and the luminescent characteristics of quantum dots upon their self-assembly into ordered structures were reported;[422–424] self-organised structures do possess not only the electroluminescence properties[425] but also enhance the laser effect.[426,427]

The surface plasmon resonance is used to study the interaction between various materials and thin metal films.[428] This method has found its main application in biochemical systems, especially in studies of proteins and DNA molecules. It involves studies on the shift of the plasmon resonance caused by the change in the refractive index of the medium contacting the metal. Such a change is observed upon variation of the interaction between macromolecules and solvents; it also manifests itself as a change in the angular dependence of the coefficient of reflection of electromagnetic radiation from metal films. The well-known effect of change in the scattering coefficient in the case of interaction between biomolecules and nanoparticles[265,266] can be considerably enhanced[429] by depositing nanoparticles on the surface of metal films. Experiments showed that the coefficient of reflection of laser radiation from a gold film significantly changes after deposition of gold nanoparticles of size 30–60 nm on the surface of the film (Fig. 15). The magnitude of the change depends on the particle size and is nearly proportional to the particle concentration on the surface. This effect permits significant improvement

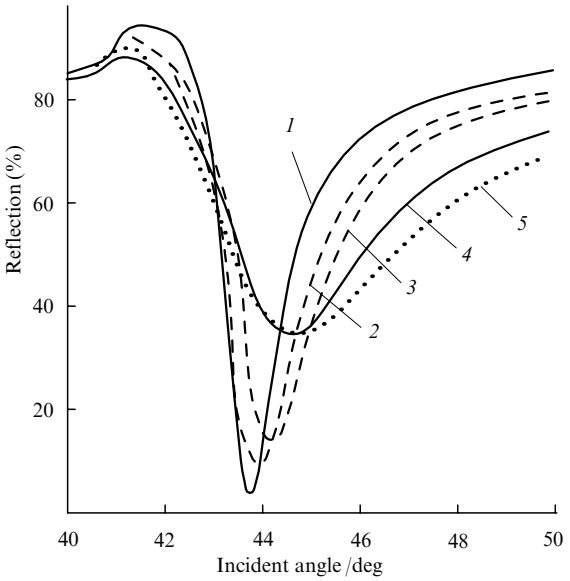


Figure 15. Reflected intensity *vs.* incident angle in the presence of gold particles of different size on the substrate.[429]
Pure gold plate (*1*); particle size /nm: 30 (*2*), 35 (*3*), 45 (*4*), 59 (*5*); particles 1.3×10^9 cm^{-2}.

of the sensitivity of detection of biomolecules using gold nanoparticles. The nature of the effect of the particles deposited on the surface is obvious: these particles make the surface rough, which causes broadening of the resonance peak.

Yet another biochemical application of single-layered films comprised of metal nanoparticles involves the use of the effect of surface enhanced Raman scattering (SERS), which is intrinsic in some metal nanoparticles. In the case of SERS, the section of scattering by the molecules adsorbed on rough metal surfaces increases by several orders of magnitude.[430] It is assumed that the nature of the SERS effect is related to both localisation of the surface plasmons and to the charge-transfer induced increase in the molecular polarisability near the metal surface.[431] In most cases, the former effect predominates; therefore, considerable attention has been given to the formation of various rough surfaces (in most cases, using colloid particles). The shape of the particle strongly influences the magnitude of the effect,[432] while the particles on the substrate should not be necessarily ordered.[433]

Numerous studies on the molecule – photon – surface interaction have been carried out since the discovery of the SERS effect; however, the mechanism of this effect is still to be clarified. It was established [434–436] that only a small fraction of particles is SERS active and that the active particles enhance the Raman scattering by 14 – 15 orders of magnitude. It was also found that the nanoparticle size is related to the exciting radiation wavelength corresponding to the SERS maximum.[434] For instance, 90 nm (140 nm) silver particles are most efficiently excited at 514 nm (570 nm). For 63 nm gold particles, the maximum enhancement is observed at an exciting radiation wavelength of 647 nm. This indicates that by sizing nanoparticles it is possible to obtain nanostructured materials with enhanced optical characteristics. Indeed, pre-fractionation of particles permits significant enhancement of the SERS effect.[437] To this end, films comprised of fractionated nanoparticles (particle size ranged from 30 to 100 nm) were obtained. Experiments confirmed that the use of certain fractions causes enhancement of the SERS effect by several orders of magnitude. The magnitude of the effect is also strongly influenced by the interaction between nanoparticles within the film.

Figure 16 presents the dependence of the SERS intensity on the degree of coverage of the substrate surface by nanoparticles for rhodamine 6G. As can be seen, the SERS intensity remains

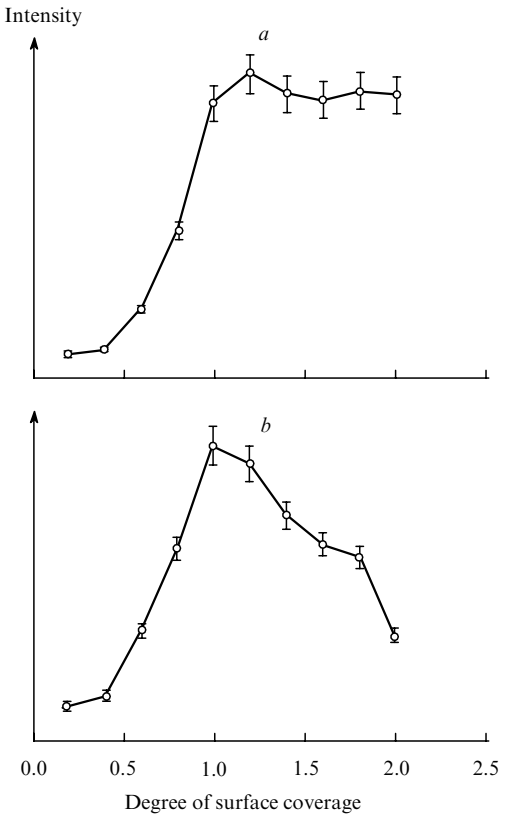


Figure 16. Absolute (*a*) and normalised (*b*) SARS intensities plotted *vs.* the degree of coverage of the substrate surface by nanoparticles.[437]

virtually unchanged as the coverage increases from 0 to 0.5, then markedly increases as the coverage approaches a unity and then remains constant. The presence of a plateau indicates that the three-dimensional ensemble of particles behaves as a two-dimensional film. Introduction of salt into the system causes a twofold increase in the intensity of the SERS signal.[437] The laws established permit the use of nanogranulated metal films as sensors in detecting biomolecules.

Consider now the optical characteristics of three-dimensional ordered colloid structures. Such structures are characterised by unusual colour gamma, being in many cases responsible for the unique protective colour of animals due to the formation of microstructures comprised of colloid particles on the surface of their bodies. Diffraction of light by such structures provides the appearance of a colour gamma which is different from that formed in the case of light absorption by dyes. Recently, studies on the optical properties of three-dimensional colloid structures have become of great importance, because colloid crystals are used as sensors,[438] tunable diffraction gratings,[439] narrow-band filters [440] and photonic crystals.[441–445] Photonic crystals serve as the basis for design of pigments and creation of a new generation of optical devices.[446–449]

The use of three-dimensional colloid crystals opens up new prospects for nanophotonics (because of this, such crystals are called photonic crystals). Nanophotonics is a new branch of optics, which describes the propagation, scattering and interaction of electromagnetic waves on the nanometre length scale. Research in this field is concerned with the interaction between the electromagnetic waves and matter at the length scales shorter than the wavelength of electromagnetic radiation, and, in particular, localised photochemical reactions. At present, nanophotonics has stimulated the elaboration of a number of novel technologies. Namely, a new type of laser and a number of optical systems and physicochemical methods were developed.[450] Colloid crystals allowed localisation of light to be performed experimentally and

have found application in laser physics and laser chemistry.[446, 447, 451–454] Recently, it has been shown that photonic crystals with band-shaped optical structure and thoroughly chosen parameters permit localisation of light, which is multiply scattered by nanoparticles.

Photonic crystals are three-dimensional structures with a periodic arrangement of particles (different phases). The refractive index of such a system is a periodic function with a period of the order of the optical wavelength. The propagation of light in photonic crystals is similar to the motion of electrons in a conventional crystal lattice. The refractive index difference between the particles and the matrix and the ordered arrangement of particles cause a strong scattering of electromagnetic waves with particular wavelengths. The Bragg diffraction occurs, which is characterised by forbiddenness for waves with particular wavelengths to propagate through the photonic crystal. Figure 17 presents the dependence of the transmission of a 12 μm-thick colloid crystal formed by polystyrene latex particles of diameter 0.23 μm on the wavelength for different angles of incidence. As can be seen, the transmission maximum (λ_{max}) is shifted from 574 to 538 nm as the angle changes from 0 to 40°. In Fig. 17 *d* we present the dependence of transmission on the wavelength for 0.36-μm latex particles at the same crystal thickness. The relation between λ_{max}, the angle of incidence and distance d_{111} between the (111) planes of a colloid crystal is given by the Bragg equation

$$\lambda_{max} = 2d_{111}(n_a - \sin^2\theta)^{1/2},$$

where n_a is the refractive index (1.489 for the ensemble of polystyrene spheres characterised by a packing density of 0.74%). Figure 18 presents the experimental and calculated λ_{max} values for colloid crystal comprised of polystyrene spheres.

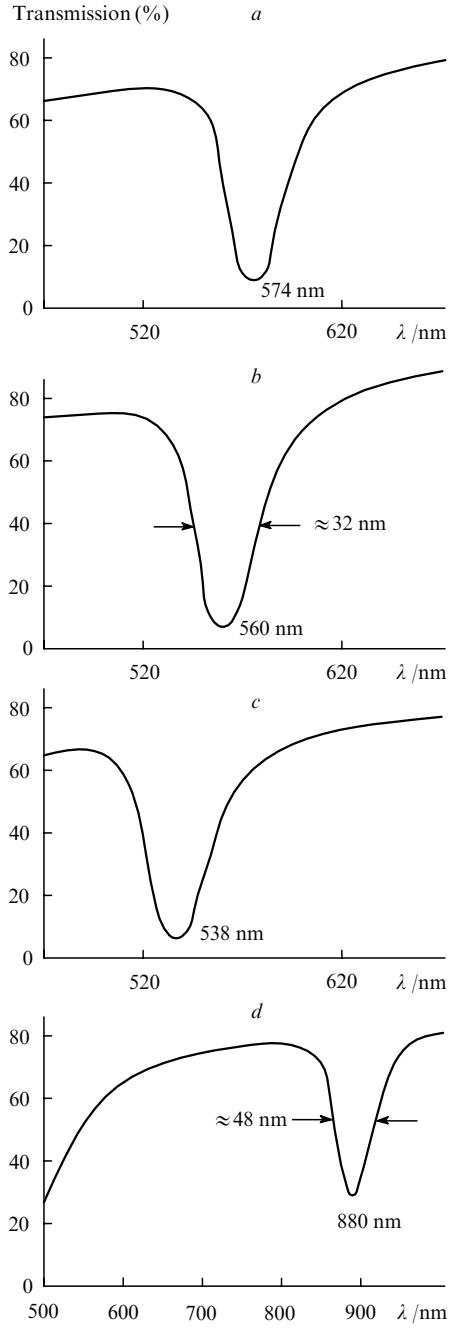


Figure 17. Transmission of a colloid crystal comprised of polystyrene particles of size 0.23 μm (*a*–*c*) and 0.36 μm (*d*) as a function of the wavelength.[455]
Angle of incidence /deg: 0 (*a*, *d*), 20 (*b*) and 40 (*c*).

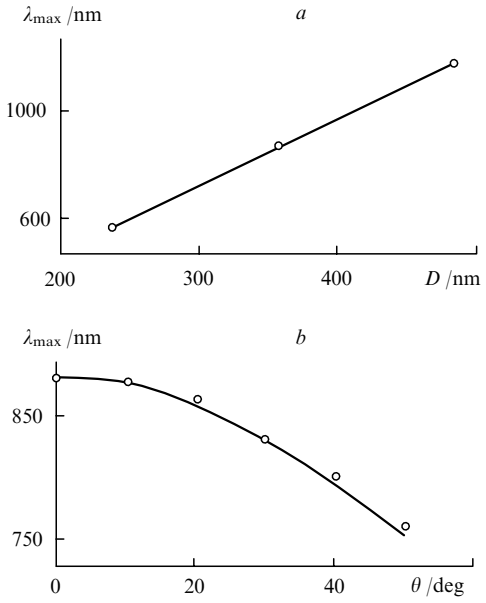


Figure 18. Absorption maximum wavelength plotted *vs.* particle size at zero angle of incidence (*a*) and *vs.* angle of incidence for 0.36 μm polystyrene particles (*b*).[455]
Experimental data (open circles) and results of calculations (solid lines).

It is possible to draw an analogy between the electron energy bands in semiconductors and in photonic crystals; however, in the latter case some features are observed. It should be noted that in photonic crystals it is possible to implement the lasing mechanism and superradiation associated with the boson nature of light, according to which a large number of photons can be in the same state. Recently, photonic crystals were fabricated,[456–458] which are characterised by localisation of electromagnetic waves in the spectral region extending from near IR to UV. Laser physics applications require that photonic crystals be tunable in the whole visible region.

A feature of photonic crystals is the change in the type of the interaction between the atoms and electromagnetic radiation. In particular, only radiation with particular wavelengths can propagate without losses through the band-type photonic crystals; therefore, atoms or molecules for which transitions between the energy levels correspond to the forbidden wavelengths, are not affected by the fluctuating vacuum field responsible for spontaneous quenching of excited states. As a result, a bound state atom–photon is created. A photon can travel a distance of several lattice constants from the atom by tunnelling before being trapped by another atom. As a consequence, relaxation of the excited

states of atoms in a photonic crystal obeys somewhat different laws compared to the case of free atoms and molecules.

Most often, photonic crystals are fabricated from silica spheres that are usually packed into the f.c.c. lattice.[459–461] By varying the size of the spheres it is possible to tune the band gap to the desired spectral region. Thermally induced tuning of the band gap is also possible.[462, 463] Fabrication of photonic crystals whose optical properties can be changed by applying the magnetic field was reported.[464, 465] By applying an external magnetic and electric field one can change the structure of the colloid crystals formed from particles of complex structure.[465] For instance, a martensite transition of the tetragonal b.c.c. lattice to the b.c.c. lattice followed by changes in the dielectric characteristics of the crystal was observed in crossed electric and magnetic fields. Recently, fabrication of inverted photonic crystals formed by the voids in the dielectric medium (usually, titania) was reported.[460, 461] Experiments showed that this structure is optimum for photonic crystals. To date, methods of fabrication of photonic crystals from various materials have been developed [466–472] and preparation of photonic crystals with the record characteristics seems not to be impossible. In this case, the interparticle distance is of great importance. Recently, methods of formation of nanoparticles coated with a thin silica shell were developed.[461, 473–476] This opens new possibilities of control of the optical properties of nanoparticles because permits variation of the core size and the thickness and composition of the shell. Spherical particles obtained following the above-mentioned routes are characterised by a narrow size distribution, being convenient building blocks for fabrication of photonic crystals. Ordered crystals obtained from such nanoparticles can be formed using various methods; however, the main procedure is based on the use of capillary forces. In particular, ordered structures from 50 nm gold nanoparticles covered with silica layers of different thickness were obtained.[415] Some examples illustrating the changes in the optical properties of photonic crystals fabricated from these particles covered with the SiO_2 shell of different thickness are shown in Fig. 19.

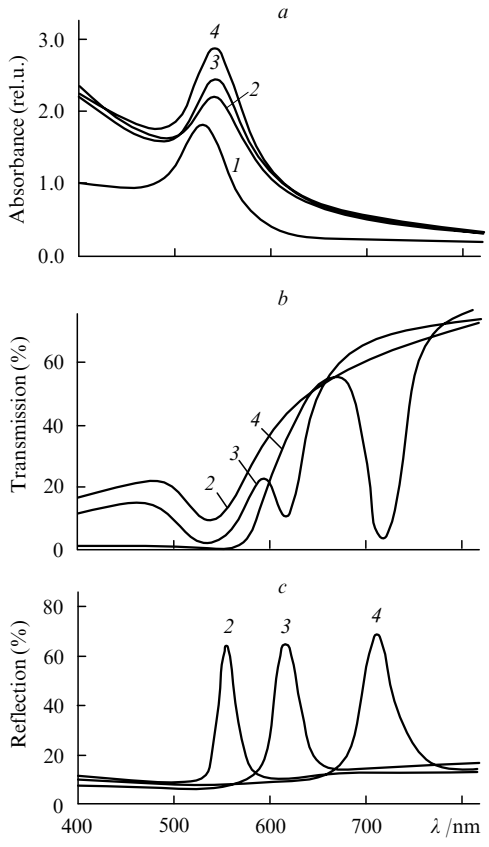


Figure 19. Optical characteristics of photonic crystals as functions of the thickness of the silica layer covering 50-nm gold nanoparticles.[415] Coverage thickness /nm: 0 (*1*), 70 (*2*), 80 (*3*) and 100 (*4*).

3. Magnetic properties

The monodomain structure of magnetic nanoparticles makes them of considerable interest, especially for fabrication of magnetic memory devices. The magnetic properties of nanoparticles differ from those of bulk magnets,[1, 6] because a decrease in the particle size is accompanied by an increase in the fraction of surface atoms. The electronic and magnetic structures of such atoms are affected by the smaller number of atoms in the particle compared to the bulk material; however, they are influenced by a large number of atoms of the dispersion medium (matrix). The surface effects can reduce the magnetic moment of particles;[477] however, for 'free' iron, cobalt and nickel particles the magnetic moment per atom increases [478] with the decrease in the particle size and tends to the limiting value characteristic of the single atom. Besides, the magnetic anisotropy of particles exceeds the corresponding bulk value.[479] The difference between these values is related to the increase in the magnetic orbital momentum of peripheral atoms.[480]

Magnetic nanoparticles are convenient objects for studying the quantum effects that manifest themselves on the mesoscopic length scale (between the quantum microscopic and classical macroscopic length scales).[481] However, real systems represent ensembles of particles, which are characterised by different size and shape. This hampers measurements of the quantum effects. The magnetic properties of such systems are determined by the properties of both the particles and the entire ensemble and these contributions are hard to be discriminated. Because of this, search for the systems suitable for wide-range variation of the average particle size, the particle size distribution and the spatial arrangement of the particles is topical. The properties of monolayers comprised of magnetic particles also depend on the procedure employed to form these objects.

A detailed study [482] on the magnetic properties of ensembles of nanoparticles involved the preparation of composites with different structural organisation of nanoparticles by layer-by-layer deposition [483] of magnetic cobalt particles on the Al_2O_3 matrix. Both ordered layers with controllable interparticle distance and random distributions of particles in the matrix (the particle size was 1 to 7 nm) were formed. Particles were formed by layer-by-layer deposition of cobalt and alumina. The results of electron microscopy study showed that the system contains isolated spherical nanoparticles whose size depends on the cobalt deposition time. This technique was used to form the films containing up to three hundred Co/Al_2O_3 bilayers. Measurements of the static and dynamic magnetic susceptibilities of these systems revealed the magnetic moment blockage effect, which is due to the magnetic anisotropy of particles. The reorientation time of the magnetic moment varies as follows

$$\tau = \tau_0 \exp\left(\frac{U_b}{kT}\right),$$

where $\tau_0 \approx 10^{-10}-10^{-13}$ s and U_b is the height of the energy barrier and is governed by the interaction between the magnetic moment of the particle and the phonon and magnon thermostats. The U_b value depends on the magnetic anisotropy constant K_{ef} and the particle volume V

$$U_b = K_{ef} V.$$

The magnetic anisotropy constant varies with the average particle size as

$$K_{ef} = K_\infty + \frac{6K_s}{\langle d \rangle},$$

where K_∞ is the magnetic anisotropy constant for the bulk material (5×10^4 J m^{-3}) and $K_s = 3.3 \times 10^{-1}$ mJ m^{-2}. An analogous increase in the magnetic anisotropy of nanoparticles was reported by many authors.[6, 479, 484]

The effect of the dipole–dipole interaction on the relaxation time of the magnetic moments of particles has been the subject of extensive literature. It was shown that the magnetic anisotropy constant increases as the number of the nearest neighbours increases.[485, 486] However, a model was proposed,[487] according to which the interaction between the magnetic moments causes a decrease in the parameter U_b. Experimental evaluation of these models faces some problems because the packing density of the particles can hardly be varied without changing the particle size. This can be done[482] by fabricating structures with different number of layers at the same cobalt sputtering tine. Experiments were carried out with the samples containing 1 and 30 monolayers of cobalt particles. The fact that both samples exhibited identical magnetisation curves confirmed coincidence of the particle sizes. The Curie–Weiss temperatures of the single-layered and thirty-layered films differed by nearly a factor of 2, which indicated a marked change in the average interparticle interaction. Measurements showed that the interaction between particles of the neighbouring layers (4.5 nm interlayer spacing) causes a substantial increase in the activation energy ($\sim$200 K for the systems under study). This value is nearly equal to the energy of the interaction between six nearest neighbours in the monolayer.

The magneto-optical properties of nanoparticles were studied.[225] Ordered ensembles of magnetite (Fe_3O_4) and cobalt ferrite ($CoFe_2O_4$) nanoparticles were first formed on the surface of the aqueous phase from the corresponding dispersions in organic solvents and then transferred on solid substrates. Particles stabilised by oleic acid were characterised by a broad size distribution; they were fractionated to obtain fractions with narrow size distributions in the range 2–10 nm and a scatter of 10% to 20%). It was established that the degree of local order of the structures under study depends on the particle size, namely, larger particles (6 nm) form ordered 'crystals', while small particles (2 nm) do not form ordered arrangements. The size of the ordered area can reach several micrometres. Figure 20 illustrates the effect of the strength of external magnetic field on the magnetic circular dichroism in the case of reflection of laser radiation by single-layered films. Measurements were carried out at different temperatures. The magnetisation curve of the two-dimensional ensemble of particles can be plotted using the results of measurements of the absorption difference between the waves with different circular polarisation as a function of the field strength. As can be seen, at room temperature the films behave as superparamagnetics. They exhibit no pronounced magnetisation hysteresis. As should be expected, the cobalt ferrite particles are first to possess hysteresis on lowering the temperature. The blocking temperature of cobalt ferrite is 200 K, while that of magnetite is 100 K. It should also be noted that cobalt ferrite is characterised by greater coercive force compared to magnetite. No significant changes in the magnetisation behaviour were observed after deposition of several layers. This indicates that in the systems under study the energy barrier associated with the crystal anisotropy is higher than the energy of the dipole–dipole interaction.

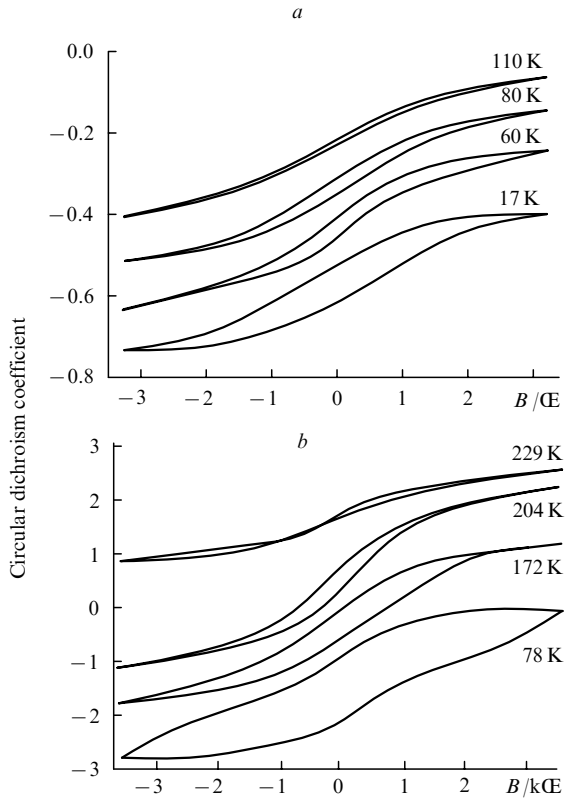


Figure 20. 'Circular dichroism–magnetic field strength (B)' dependences measured at different temperatures for a monolayer of magnetic particles;[225]
6 nm Fe_3O_4 particles (*a*) and 6 nm $CoFe_2O_4$ particles (*b*).

4. Thermal and mechanical properties

Colloid crystals are convenient for studying the phase transitions. Of particular interest are two-dimensional colloid crystals. It was established[488] that the melting transition in two-dimensional systems differs from the melting transition in three-dimensional crystals and occurs continuously involving dissociation of pair dislocations. More recently,[489, 490] it was shown that the newly formed phase is not an isotropic liquid and a second phase transition, which is due to the formation of disclinations, is necessary for the system to go from the so-called hexatic phase to the isotropic liquid. Such a two-step melting model is called the Kosterlitz–Thouless–Galperin–Nelson–Yang (KTGNY) theory. This theory predicts the temperatures at which the system becomes unstable and the topological defects (dislocations and disclinations) are formed. To test the theory, which was not necessarily confirmed in numerical experiments, the phase transition in a two-dimensional colloid crystal with well-defined magnetic interparticle interaction was studied.[491] Experiments with 4.7 μm iron oxide particles dispersed on the surface of water showed that melting of the crystal follows the KTGNY scenario. The shape of the pair distribution function was determined at different temperatures using a video camera. On melting of the two-dimensional crystal, the density correlation function first decreased following a power law with the exponent determined from the KTGNY theory and then decreased exponentially. Direct visual observations revealed the presence of a phase that was intermediate between the crystalline and liquid phases.

Two-step melting of two-dimensional ordered dusty plasma clusters was reported.[130] Numerical simulation showed that different cluster areas are disordered at different temperatures. However, this two-step mechanism can also be due to the finite size of the two-dimensional clusters under study.

The following should be pointed out. In spite of a large number of studies concerned with the formation of ordered monolayers comprised of nanoparticles, methods of structural characterisation of monolayers are still poorly developed. For instance, films formed at the gas–liquid interface are often characterised visually or by the packing density of the particles, which is determined from the compression isotherms. The only structural parameter used for the characterisation of monolayers is the regular lattice constant. Therefore, the general scheme[492] of analysis of the structure of nanoparticle monolayers is of great value. Two complementary methods were employed to derive this scheme. The properties of a monolayer were characterised using the pair distribution function while the presence of defects in the

monolayer was described by the Delaunay triangulation. A combination of the latter procedure and analysis of the Voronoi polyhedra can be applied to both two-dimensional and three-dimensional colloid structures.[493] The method was evaluated taking films comprised of silica particles formed on the surface of the liquid phase as an example. The particles were stabilised by alkylsilanes with different length of the hydrocarbon radical, which permitted variation of the force of the interparticle interaction. The properties of the films were also changed by varying the subphase composition and the degree of coverage of the particles with the alkylsilane adlayer. The energy of the particle–particle interaction on the surface of the subphase was calculated with inclusion of the van der Waals interaction and capillary forces. Figure 21 presents the dependence of the packing density of the particles in the monolayer on the surface of the liquid on the energy of the particle–particle interaction (at the minimum of the potential curve). In performing triangulation the triangles with vertices at the centres of spheres were plotted in such a way that no particles could pass through them. Figure 22 demonstrates some examples of the description of pores (defects) by different numbers of triangles (n_t). The pore size distribution was found to be lognormal. The pore size distribution for the monolayers of silica particles on the surfaces of various liquids is shown in Fig. 23.

These results were complemented with the data of a study on the structure and energy of defects in two-dimensional colloid crystal comprised of 0.36 μm polystyrene spheres.[494] Defects were formed using optical 'tweezers'. A colloid crystal with a lattice constant of 1.1 μm was formed by compression of the concentrated dispersion between two molten-quartz plates separated by a 2 μm gap. The motion of defects was studied using a video camera. General trends of the behaviour of dislocations were revealed. In particular, no single dislocations with the coordination number other than 6 (distorted coordination) were detected.

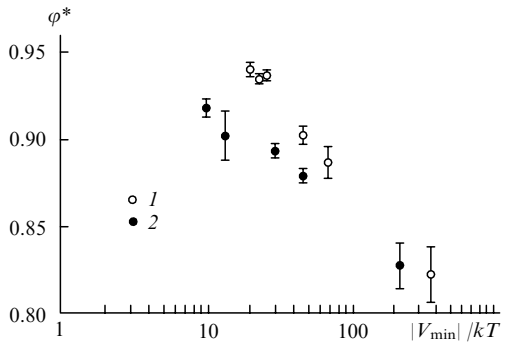


Figure 21. Packing degree of the monolayer of nanoparticles covered with octyltrichlorosilane (*1*) and octadecyltrichlorosilane (*2*) as function of the energy of the interparticle interaction at the potential well minimum.[492]

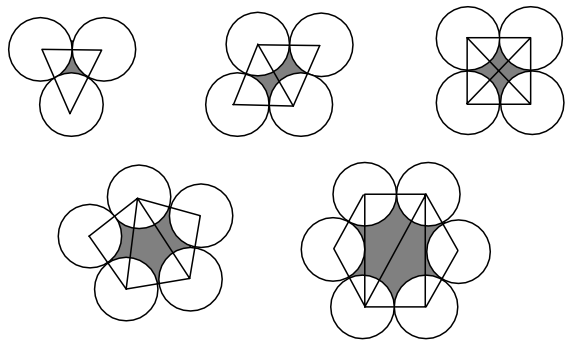


Figure 22. Triangulation schemes for various defects.[492]
For details, see text.

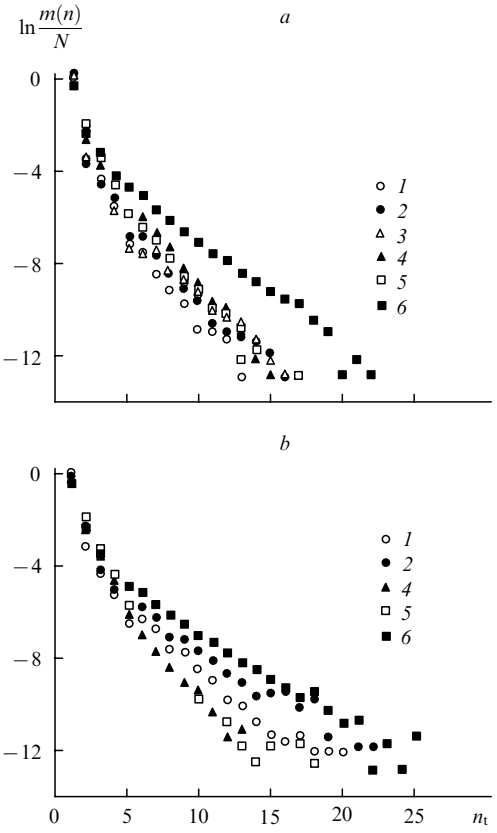


Figure 23. Pore size distribution in the monolayer of silica nanoparticles stabilised by octyltrichlorosilane (*a*) and octadecyltrichlorosilane (*b*) on the benzene (*1*), toluene (*2*), dichlorobenzene (*3*), dioxane (*4*), methoxyethanol (*5*) and water (*6*) surfaces.[492]

Only the pair, triplet, *etc*. dislocations with an average coordination number of 6 were observed. The sum of all vectors that emanate from the particles with a coordination number smaller than 6 and end at the neighbouring particles with a coordination number exceeding 6 equals nearly zero. This allows dislocations to be considered as multipoles with a zero summary Burgers vector.

The thermal and mechanical stability of the self-assembled ensembles of particles and their components play a significant role, because they can be at high temperature and pressure in the case of, *e.g*., catalytic applications. A particular role is played by the composition of the gaseous atmosphere. For instance, recrystallisation or even decomposition of platinum nanoparticles was observed at elevated temperature in an oxygen atmosphere in contrast to the hydrogen or noble-gas atmospheres,[495] whereas melting of the platinum particles of size from 5 to 20 nm on carbon substrate proceeds at 900 K.[496] The behaviour of single 20 nm platinum nanoparticles and their ensembles in oxygen atmosphere was studied.[497] An increase in the degree of crystallinity of the particles was observed at 700 K. The mechanism responsible for this process is still to be clarified, whereas the increase in the degree of crystallinity in the hydrogen atmosphere and *in vacuo* is due to diffusion of atoms in nanoparticles. According to atomic force microscopy data, the adhesive binding energy of the starting particles to the substrate was ≈ 0.8 mJ m^{-2} (the force measured was ≈ 10 nN). After treatment in hydrogen atmosphere at 700 K the adhesive binding energy became so high that it was impossible to measure its value. The observed changes in the degree of crystallinity and in the shape of the particles cannot be explained by their melting, because the particles of diameter 20 nm must melt at 2020 K even with inclusion of the dependence of the melting temperature on the particle size.

Recently, the properties of not only the metal 'core' of nanoparticles but also the single-layered organic shells have been the subject of investigations. The diversity of self-assembled ensembles of particles that can form on two-dimensional substrates [498] is also an intrinsic property of the molecular monolayers covering nanoparticles. These monolayers have a strong effect on the properties of the self-assembled ensembles of nanoparticles. A study on the ensembles of 4 nm silver and 3 nm gold nanoparticles stabilised by octadecanethiol, octanethiol, pentanethiol and butanethiol was reported.[499] The dried dispersions were mixtures of individual particles and colloid crystals. Analysis of the results of a differential scanning calorimetry study revealed two phase transitions corresponding to the melting of alkanethiol crystals (monolayers) and to the melting of the colloid crystal. The endothermic peak corresponding to the melting of the superlattice of gold particles is less pronounced than in the case of silver nanoparticles, thus indicating a lesser degree of crystallinity of the gold colloid crystal. The melting temperatures of the alkanethiol monolayers on the surface of silver nanoparticles also were found to be higher than on the surface of gold nanoparticles. This was explained by higher fraction of the organic phase in the case of gold particles.

The effect of thermal fluctuations in the ligand shell on the temperature dependence and on the topology of the order–disorder phase transition in the superlattice of nanoparticles was also studied [500] taking silver nanocrystals stabilised by alkanethiols (C_8, C_{12} and C_{16}) as examples. Measurements of the angular dependence of the X-ray scattering intensity at different temperatures showed that for all the samples under study the first diffraction peak disappeared in a rather narrow temperature range, thus indicating the topological disorder in the system. Near this temperature the peak markedly broadened due to enhancement of vibrations in the superlattice. This was similar to the situation observed for bulk crystals. However, above the melting temperature the superlattice behaved in another manner compared to conventional, 'atomic', crystals. All the samples under study were characterised by the appearance of a new peak at smaller values of the scattering vector q compared to those for the (111) diffraction peak. The new peak corresponds to the scattering region of size

$$\xi = \frac{2\pi}{q}.$$

As the temperature increases, the peak intensity increases and the peak is shifted towards small q values. This indicates the formation of a bicontinuous phase with spatially correlated regions whose sizes exceed both the thickness of the ligand shell and the size of nanocrystals. At a certain critical temperature T_c, the correlation region becomes infinitely large and the parameter ξ increases by a power law (Fig. 24):

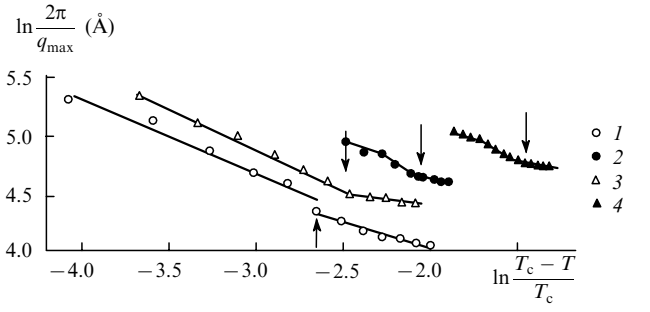


Figure 24. 'Characteristic size–temperature' plot for ensemble of sterically stabilised nanoparticles.[499]
The transition temperatures are shown by arrows. Particles were stabilised by alkanethiols containing a total of 8 (*1*), 12 (*2*, *3*) and 16 (*4*) carbon atoms in the alkyl chain. Chain length is 41 Å for (*2*) and 35 Å for (*3*).

$$\xi \propto \xi_0 \left(1 - \frac{T}{T_c}\right)^{-v}.$$

At a certain temperature T_x, the exponent v increases, becomes independent of the type of the ligand shell and corresponds to the critical index in the Ising model.

The supercrystal behaves similarly to the sponge phase of the surfactant, namely, its stabilisation is due to the long-range entropy forces related to fluctuations of the ligand 'membrane.' At high temperature (above the melting temperature of the superlattice), silver nanoparticles contacting one another bring closer together and form aggregates surrounded by the hydrocarbon chains attached to the surface of particles. The behaviour of such systems is governed by a complex combination of the van der Waals forces that act between the particles and hydrocarbon chains.

In conclusion, we will consider unusual self-assembled structures obtained upon binding of alkanethiol molecules functionalised by the COOH groups (*e.g.*, 11-mercaptoundecanoic or 1-mercaptohexadecanoic acids) and adsorbed on the surface of gold particles. Such structures are formed due to hydrogen bonds of the terminal carboxyl groups. They exhibit the ability to selectively transmit particular ions. The selectivity can be tuned by varying the pH value of the solution.[501] Changes in the morphology of ensembles of hydrogen bond stabilised nanoparticles upon variation of the pH value of the solution were studied.[502] To this end, gold nanoparticles stabilised by functionalised alkanethiols were obtained and alternating regions (of size nearly 2×2 μm) of monolayers of octadecanethiols containing the COOH and CH_3 terminal groups were formed by microcontact printing on a gold plate. The plate was dipped in a colloid solution containing gold nanoparticles. As a result, several layers of functionalised particles were deposited on the monolayer regions bearing the COOH groups, whereas no particle deposition occurred on the other regions. Atomic force microscopy studies revealed that variation of the pH value of the medium from 2 to 11 caused a twofold change in the height of the particle clusters (Fig. 25) due to the fact that the Debye length for the systems under study was several times longer than the interparticle distance and, hence, the charges of the particles were only partially screened. Such systems serve as the basis for fabrication of (i) membranes with tunable permeability towards different ions and (ii) recognition systems.

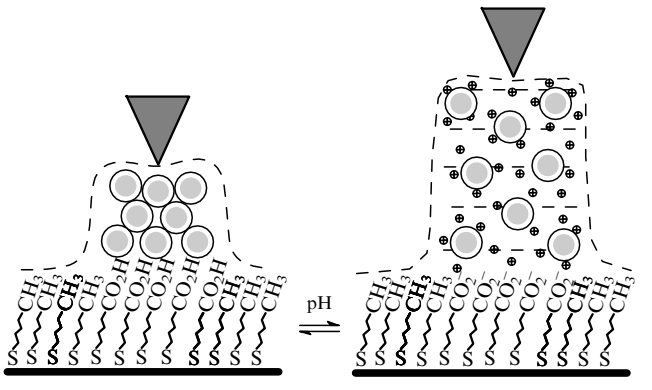


Figure 25. Changes in the size of a gold nanocluster depending on the pH of the solution.
For details, see text.

VI. Conclusion

Analysis of the available data (see above) shows that recently considerable advances in design of ordered ensembles of nano-

particles and in the studies of their properties have been achieved. The results obtained point to great prospects for the use of nanomaterials in the design of new-generation devices which can find various applications from medicine to microelectronics.

At the same time, many problems that arose in studies of ensembles of nanoparticles are still far from being solved. No efficient methods of fabrication of ensembles of monodisperse particles have been developed. Control of the interfacial behaviour of nanoparticles faces some problems (only preliminary results were obtained in this field). Realistic and reliable description of the physicochemical properties of ordered ensembles of nanoparticles with inclusion of co-operative effects is impossible, because most theories are still based on the single-particle approximation. Nevertheless, we hope that intensive research in the field will lead to new advances towards understanding of the physicochemical properties of ensembles of nanoparticles in the nearest future.

The author expresses his gratitude to V M Rudoy for help in the preparation of the review.

The review has been written with financial support from the Russian Foundation for Basic Research (Project No. 03-03-32513) and the Presidium of the Russian Academy of Sciences (Programme 'Fundamental Problems of Physics and Chemistry of Nanosystems and Nanomaterials').

References

1. Yu I Petrov *Klastery i Malye Chastitsy* (Clusters and Small Particles) (Moscow: Nauka, 1986)
2. S A Nepiiko *Fizicheskie Svoistva Malykh Metallicheskikh Chastits* (Physical Properties of Small Metallic Particles) (Kiev: Naukova Dumka, 1985)
3. A D Pomogailo, A S Rozenberg, I E Uflyand *Nanochastitsy Metallov v Polimerakh* (Metal Nanoparticles in Polymers) (Moscow: Khimiya, 2000)
4. V I Roldughin *Usp. Khim.* **69** 899 (2000) [*Russ. Chem. Rev.* **69** 821 (2000)]
5. B D Summ, N I Ivanova *Usp. Khim.* **69** 995 (2000) [*Russ. Chem. Rev.* **69** 911 (2000)]
6. I P Suzdalev, P I Suzdalev *Usp. Khim.* **70** 203 (2001) [*Russ. Chem. Rev.* **70** 177 (2001)]
7. G B Sergeev *Usp. Khim.* **70** 915 (2001) [*Russ. Chem. Rev.* **70** 809 (2001)]
8. R A Andrievskii *Usp. Khim.* **71** 967 (2002) [*Russ. Chem. Rev.* **71** 853 (2002)]
9. A I Gusev, A A Rempel' *Nanokristallicheskie Materialy* (Nanocrystalline Materials) (Fizmatlit: Moscow, 2001)
10. P Jensen *Rev. Mod. Phys.* **71** 1695 (1999)
11. S V Karpov, V V Slabko *Opticheskie i Fotofizicheskie Svoistva Fraktal'no-Strukturirovannykh Zolei Metallov* (Optical and Photophysical Properties of Fractal Structured Sols of Metals) (Novosibirsk: Siberian Branch of Russian Academy of Sciences, 2003)
12. A Globus, C W Bauschlicher, J Han, R L Jaffe, C Levit, D Srivastava *Nanotechnology* **9** 192 (1998)
13. A Martino, S A Yamanaka, J S Kawola, D A Loy *Chem. Mater.* **9** 423 (1997)
14. S Bharathi, N Fishelson, O Lev *Langmuir* **15** 1929 (1999)
15. T K Kundu, D Chakravorty *Appl. Organomet. Chem.* **13** 363 (1999)
16. N Sanz, A-C Gaillot, Y Usson, P I Baldeck, A Ibanez *J. Mater. Chem.* **10** 2723 (2000)
17. G De, G Mattei, C Sada, G Battaglin, A Quaranta *Chem. Mater.* **12** 2157 (2000)
18. A P Rao, G M Pajonk, A V Rao *J. Mater. Synth. Proc.* **9** 11 (2001)
19. M L Anderson, C A Morris, R M Strud, C I Merzbacher, D R Rolison *Langmuir* **15** 674 (1999)
20. D Schmeißer, O Böhme, A Yfantis, T Heller, D R Batchelor, I Lundstrom, A L Spetz *Phys. Rev. Lett.* **83** 380 (1999)
21. T Kawasaki, Y Takai, R Shimizu *Appl. Phys. Lett.* **79** 3509 (2001)
22. C P Collier, T Vossmeyer, J R Heath *Annu. Rev. Phys. Chem.* **49** 371 (1998)
23. C Wang, Y Li, X Bu, N Zheng, O Zivkovic, C-S Yang, P Feng *J. Am. Chem. Soc.* **123** 11506 (2001)
24. H Wu, N Bowden, G M Whitesides *Appl. Phys. Lett.* **75** 3222 (1999)
25. S R J Oliver, T D Clark, N Bowden, G M Whitesides *J. Am. Chem. Soc.* **123** 8119 (2001)
26. I F Efremov *Periodicheskie Kolloidnye Struktury* (Periodical Colloid Structures) (Leningrad: Khimiya, 1971)
27. Y Xia, B Gates, Y Yin, Y Lu *Adv. Mater.* **12** 693 (2000)
28. S Matsushita, T Miwa, A Fujishima *Langmuir* **13** 2582 (1997)
29. J L Fransaer, R M Penner *J. Phys. Chem.* **103** 7643 (1999)
30. M Alejandro-Arellano, T Ung, A Blanco, P Mulvaney, L M Liz-Marzan *Pure Appl. Chem.* **72** 257 (2000)
31. B V Deryagin, N V Churaev, V M Muller *Poverkhnostnye Sily* (Surface Forces) (Moscow: Nauka, 1985)
32. P de Gennes *Adv. Colloid Interface Sci.* **27** 189 (1987)
33. S Ramakrishnan, C F Zukoski *J. Chem. Phys.* **113** 1237 (2000)
34. B A Korgel, D Fitzmaurice *Phys. Rev. B* **59** 14191 (1999)
35. S Hachisu, K Takano *Adv. Colloid Interface Sci.* **16** 233 (1982)
36. R Williams, R S Crandall *Phys. Lett. A* **48** 225 (1974)
37. W Y Shih, I A Aksay, R Kikuchi *J. Chem. Phys.* **86** 5127 (1987)
38. C G de Kruif, P W Row, J W Jansen, A Vrij *J. Phys. C* **46** 295 (1985)
39. P N Pusey, W van Megen *Nature (London)* **320** 340 (1986)
40. A R Denton, H Lowen *Phys. Rev. Lett.*, **81** 469 (1998)
41. L Beloni *J. Chem. Phys.* **85** 519 (1986)
42. S Kahn, T L Morton, D Ronis *Phys. Rev. A* **35** 4295 (1987)
43. G F Wang, S K Lai *Phys. Rev. Lett.* **82** 3645 (1999)
44. S K Lai, W P Peng, G F Wang *Phys. Rev. E* **63** 041511 (2001)
45. J Groenewold, W K Kegel *J. Phys. Chem. B* **105** 11702 (2001)
46. W van Mengen, S M Underwood *Nature (London)* **362** 616 (1993)
47. R J Speedy *J. Chem. Phys.* **100** 6684 (1994)
48. M D Rintoul, S Torquato *Phys. Rev. Lett.* **77** 4198 (1996)
49. W K Kegel *Langmuir* **16** 939 (2000)
50. B J Alder, W G Hoover, D A Yung *J. Chem. Phys.* **49** 3688 (1968)
51. Y Monovoukas, A P Gast *J. Colloid Interface Sci.* **128** 533 (1989)
52. G A McConnell, A P Gast *Phys. Rev. E* **54** 5447 (1996)
53. H M Lindsay, P M Chaikin *J. Chem. Phys.* **76** 3774 (1982)
54. E Liniger, R Raj *J. Am. Chem. Soc.* **70** 843 (1987)
55. S Hachisu, S Yoshimura *Nature (London)* **283** 188 (1980)
56. S Yoshimura, S Hachisu *J. Phys. Colloq., C3* **46** 115 (1987)
57. W Y Shih, W-H Shih, I A Aksay *J. Chem. Phys.* **90** 4506 (1989)
58. L D Landau, E M Lifshits *Statisticheskaya Fizika* (Statistical Physics) (Moscow: Nauka, 1976)
59. S Ichimaru *Rev. Mod. Phys.* **54** 1017 (1982)
60. J H Chu, I Lin *Phys. Rev. Lett.* **72** 4009 (1994)
61. V E Fortov, A P Nefedov, O F Petrov, A A Samarian, A V Chernyshov, A M Lipaev *Pis'ma Zh. Eksp. Teor. Fiz.* **63** 176 (1996) [a]
62. V E Fortov, A P Nefedov, O F Petrov, A A Samaryan, A V Chernyshev *Zh. Eksp. Teor. Fiz.* **111** 467 (1997) [b]
63. V N Tsitovich *Usp. Fiz. Nauk* **167** 57 (1997) [*Physics-Uspekhi* **40** 53 (1997)]
64. S P Bakanov, B V Deryagin, V I Roldughin *Usp. Fiz. Nauk* **129** 256 (1979) [c]
65. V I Roldughin, V M Zhdanov *Adv. Colloid Interface Sci.* **98** 121 (2002)
66. V V Balabanov, L M Vasilyak, S P Vetchinin, A P Nefedov, D N Polyakov, V E Fortov *Zh. Eksp. Teor. Fiz.* **119** 99 (2001) [b]
67. V E Fortov, A P Nefedov, O F Petrov, A A Samaryan, Ya K Khodataev, A V Chernyshev *Zh. Eksp. Teor. Fiz.* **116** 1601 (1999) [b]
68. D N Gerasimov, O A Sinkevich *Teplofiz. Vys. Temp.* **37** 853 (1999)
69. G E Astrakharchik, A I Belousov, Yu E Lozovik *Zh. Eksp. Teor. Fiz.* **116** 1300 (1999) [b]
70. M Dijkstra, R van Roij, R Evans *Phys. Rev. Lett.* **81** 2268 (1998)
71. A Vrij *Pure Appl. Chem.* **48** 471 (1976)
72. G A Vliegenthart, H N W Lekkerkerker *J. Chem. Phys.* **111** 4153 (1999)
73. S M Ilett, A Orrock, W C K Poon, P Pusey *Phys. Rev. E* **51** 1344 (1995)

74. H N W Lekkerkerker, W C K Poon, P N Pusey, A Stroobants, P Warren *Europhys. Lett.* **20** 559 (1992)
75. N A M Verhaegh, D Ashnagi, H N W Lekkerkerker, M Gigho, L Cipelletti *Physica A* **242** 104 (1997)
76. Y Mao, M E Cates, H N W Lekkerkerker *Physica A* **222** 10 (1995)
77. G A Vliegenthart, A van Blaaderen, H N W Lekkerkerker *Faraday Discuss.* **112** 173 (1999)
78. E K Hobbie *Phys. Rev. Lett.* **81** 3996 (1998)
79. M Adams, S Dogic, S L Keller, S Fraden *Nature (London)* **393** 349 (1998)
80. K Yaman, C Jeppesen, C M Marques *Europhys. Lett.* **42** 221 (1998)
81. P Bolhuis, D Frenkel *J. Chem. Phys.* **101** 9869 (1994)
82. M Schmidt *Phys. Rev. E* **63** 050201 (2001)
83. L Onsager *Anal. N.Y. Acad. Sci.* **51** 627 (1949)
84. I Langmuir *J. Chem. Phys.* **6** 873 (1938)
85. M P B van Bruggen, J K G Dhont, H N W Lekkerkerker *Macromolecules* **32** 2256 (1999)
86. X M Dong, T Kimura, J F Revol, D G Gray *Langmuir* **12** 2076 (1996)
87. T Folda, H Hoffmann, H Chanzy, P Smith *Nature (London)* **333** 55 (1988)
88. A V Kaznacheev, A Yu Kovalevskii, I A Ronova, A S Sonin *Kolloid. Zh.* **62** 606 (2000) [d]
89. F M van der Kooij, H N W Lekkerkerker *J. Phys. Chem. B* **102** 7829 (1998)
90. F M van der Kooij, D van der Beek, H N W Lekkerkerker *J. Phys. Chem. B* **105** 1696 (2001)
91. M A Bates, D Frenkel *J. Chem. Phys.* **110** 6553 (1999)
92. J-C Loudet, P Barois, P Poulin *Nature (London)* **407** 611 (2000)
93. P Fabre, C Casagrande, M Veyssie, V Cabuil, R Massart *Phys. Rev. Lett.* **64** 539 (1990)
94. C Quilliet, V Ponsinet, V Cabuil *J. Phys. Chem.* **98** 3566 (1994)
95. C Menager, L Belloni, V Cabuil, M Dubois, T Gulik-Krzywicki, Th Zemb *Langmuir* **12** 3516 (1996)
96. W Wang, S Efrima, O Regev *J. Phys. Chem. B* **103** 5613 (1999)
97. C Smits, J S van Duijneveldt, J K G Dhont, H N W Lekkerkerker, W J Briels *Phase Transitions* **21** 157 (1990)
98. T Palberg, M Würth, J Schwarz, P Leiderer *Prog. Colloid Polym. Sci.* **98** 6 (1995)
99. M Würth, J Schwarz, F Culis, P Leiderer, T Palberg *Phys. Rev. E* **52** 6415 (1995)
100. M S Ripoll, C F Tejero, M Baus *Physica A* **234** 311 (1996)
101. E J Meijer, D Frenkel *J. Chem. Phys.* **94** 2269 (1991)
102. J M A Hofman, H J H Clercx, P P J M Schram *Phys. Rev. E* **62** 8212 (2000)
103. I V Melikhov, E N Kitova, A N Kamenskaya, E D Kozlovskaya, N B Mikheev, S A Kulyukhin *Kolloid. Zh.* **59** 780 (1997) [d]
104. G Schmid (Ed.) *Clusters and Colloids. From Theory to Applications* (Weinheim: VCH, 1994)
105. J H Fendler (Ed.) *Nanoparticles and Nanostructured Films/ Preparation Characterization and Applications* (Weinheim: Wiley-VCH, 1998)
106. P M Tessier, O D Velev, A T Kalambur, A M Lenhoff, J F Rabolt, E W Kaler *Adv. Mater.* **13** 396 (2001)
107. B Gates, Y Xia *Adv. Mater.* **12** 1329 (2000)
108. H Andersson, W van der Wijngaart, G Stemme *Electrophoresis* **22** 249 (2001)
109. H Weller *Angew. Chem., Int. Ed. Engl.* **35** 1079 (1996)
110. C B Murray, C R Kagan, M G Bawendi *Science* **270** 1335 (1995)
111. S Sun, C B Murray, D Weller, L Folks, A Moser *Science* **287** 1989 (2000)
112. R Micheletto, H Fukuda, M Ohtsu *Langmuir* **11** 3333 (1995)
113. N D Denkov, O D Velev, P A Kralchevsky, I B Ivanov, H Yoshimura, K Nagayama *Langmuir* **8** 3183 (1992)
114. S Rakers, L F Chi, H Fuchs *Langmuir* **13** 7121 (1997)
115. T Yonezava, S Onoue, N Kimizuka *Langmuir* **17** 2291 (2001)
116. S He, J Yao, P Jiang, D Shi, H Zhang, S Xie, S Pang, H Gao *Langmuir* **17** 1571 (2001)
117. J S Yin, Z L Wang *Phys. Rev. Lett.* **79** 2570 (1997)
118. L Motte, F Billoudet, E Lacaze, M P Pileni *Adv. Mater.* **8** 1018 (1996)
119. B A Korgel, D Fitzmaurice *Phys. Rev. Lett.* **80** 3531 (1998)
120. W Wang, S Efrima, O Regev *Langmuir* **14** 602 (1998)
121. N Dingenouts, M Ballauff *Langmuir* **15** 3283 (1999)
122. V Russier, C Petit, J Legrand, M P Pileni *Phys. Rev. B* **62** 3910 (2000)
123. A J Rondinone, A S C Samia, Z J Zhang *J. Phys. Chem. B* **104** 7919 (2000)
124. S H Sun, C B Murray *J. Appl. Phys.* **85** 4325 (1999)
125. J Legrand, C Petit, D Bazin, M P Pileni *Appl. Surf. Sci.* **164** 186 (2000)
126. P C Ohara, D V Leff, J R Heath, W M Gelbart *Phys. Rev. Lett.* **75** 3466 (1995)
127. R P Andres, J D Bielefeld, J I Henderson, D B James, V R Lolagunta, C P Kubiak, W J Mahoney, R G Osifchin *Science* **273** 1690 (1996)
128. P C Ohara, J R Heath, W M Gelbart *Angew. Chem., Int. Ed. Engl.* **36** 1077 (1997)
129. P C Ohara, W M Gelbart *Langmuir* **14** 3418 (1998)
130. P Moriarty, M D R Taylor, M Brust *Phys. Rev. Lett.* **89** 248 303 (2002)
131. M Green, S Norager, P Moriarty, M Motevalli, P O'Brien *J. Mater. Chem.* **10** 1939 (2000)
132. Z L Wang, S A Harfenist, I Vezmar, R L Whetten, J Bentley, N D Evans, K B Alexander *Adv. Mater.* **10** 808 (1998)
133. S A Harfenist, Z L Wang, M M Alvarez, I Vezmar, R L Wetten *J. Phys. Chem.* **100** 13 904 (1996)
134. L O Brown, J E Hutchison *J. Phys. Chem. B* **105** 8911 (2001)
135. A Courty, O Araspin, C Fermon, M P Pileni *Langmuir* **17** 1372 (2001)
136. P Hanarp, D S Sutherland, J Gold, B Kasemo *Colloids Surf., A* **214** 23 (2003)
137. G Schmid *J. Chem. Soc., Dalton Trans.* 1077 (1998)
138. S Chen *J. Phys. Chem. B* **104** 663 (2000)
139. V L Colvin, A N Goldstein, A P Alivisatos *J. Am. Chem. Soc.* **114** 5221 (1992)
140. H Haidara, K Mougin, J Schultz *Langmuir* **17** 1432 (2001)
141. G Bar, S Rubin, R W Cutts, T N Taylor, T A Zawodzinski *Langmuir* **12** 1172 (1996)
142. R H Therill, T A Postlethwaite, C H Chen, C D Poon, A Terzis, A Chen, J E Hutchison, M R Clark, G Wignall, J D Londono, R Superfine, M Falvo, C S Johnoson, E T Samulski, R W Murray *J. Am. Chem. Soc.* **117** 12537 (1995)
143. L H Dubois, R G Nuzzo *Annu. Rev. Phys. Chem.* **43** 437 (1992)
144. L Cusack, R Rizza, A Gorelov, D Fitzmaurice *Angew. Chem., Int. Ed. Engl.* **36** 848 (1997)
145. S Bharathi, M Nogami, O Lev *Langmuir* **17** 2602 (2001)
146. X M Lin, C M Sorensen, K J Klabunde *Chem. Mater.* **11** 198 (1999)
147. X M Lin, G M Wang, C M Sorensen, K J Klabunde *J. Phys. Chem. B* **103** 5488 (1999)
148. M Brust, D Bethel, D J Schiffrin, J K Kiely *Adv. Mater.* **7** 795 (1995)
149. T Prozorov, R Prozorov, A Gedanken *Adv. Mater.* **10** 1529 (1998)
150. D I Gittings, D Bethell, R J Nichols, D J Schiffrin *Adv. Mater.* **11** 737 (1999)
151. J P Novak, D L Feldheim *J. Am. Chem. Soc.* **122** 3979 (2000)
152. R P Andres, D J Bielefeld, J I Henderson, D B Janes, V R Kolagunta, C P Kubiak, W J Mahoney, R C Osifchin *Science* **273** 1690 (1999)
153. K S Mayya, V Patil, M Sastry *Bull. Chem. Soc. Jpn.* **73** 1757 (2000)
154. W Shenton, S A Devis, S Mann *Adv. Mater.* **11** 449 (1999)
155. C J Loweth, W B Caldwell, X Peng, A P Alivisatos, P G Schultz *Angew. Chem., Int. Ed.* **38** 1808 (1999)
156. A K Bodal, V M Rotello *Langmuir* **16** 9527 (2000)
157. Y Kim, R C Johnson, J T Hupp *Nano Lett.* **1** 165 (2001)
158. C Sanchez, G Soler-Illia, F Ribot, T Lalot, C R Mayer, V Cabuil *Chem. Mater.* **13** 3061 (2001)
159. C R Mayer, S Neveu, V Cabuil *Adv. Mater.* **14** 595 (2002)
160. J E Martin, J P Wilcoon, J Odinek, P Provencio *J. Phys. Chem. B* **104** 9475 (2000)

161. J Fink, J Kiely, D Bethel, D J Schiffrin *J. Chem. Mater.* **10** 922 (1998)
162. P Bartlett, R H Ottewill, P N Pusey *Phys. Rev. Lett.* **68** 3801 (1992)
163. M D Eldridge, P A Madden, D Frenkel *Nature (London)* **365** 35 (1993)
164. C J Kiely, J Fink, M Brust, D Bethel, D J Schiffrin *Nature (London)* **396** 444 (1998)
165. S V Anishchik, N N Medvedev *Phys. Rev. Lett.* **75** 4314 (1995)
166. M Antonietti, J Hartmann, M Neese, U Seifert *Langmuir* **16** 7634 (2000)
167. J J Gray, R T Bonnecaze *J. Chem. Phys.* **14** 1366 (2001)
168. J J Gray, D H Klein, R T Bonnecaze, B A Korgel *Phys. Rev. Lett.* **85** 4430 (2000)
169. J J Gray, D H Klein, B A Korgel, R T Bonnecaze *Langmuir* **17** 2317 (2001)
170. B J Alder, T E Wainwright *Phys. Rev.* **127** 359 (1962)
171. A Jaster *Phys. Rev. E* **59** 2594 (1999)
172. W Vermöhlen, N Ito *Phys. Rev. E* **51** 14 636 (1995)
173. M R Sadr-Lahijany, P Ray, H E Stanley *Phys. Rev. Lett.* **79** 3206 (1997)
174. J Talbot, P Schaaf *Phys. Rev. A* **40** 422 (1989)
175. J van de Lagemaat, K D Benkstein, A J Frank *J. Phys. Chem. B* **105** 12433 (2001)
176. M Hosino, H Nakano, H Kimura *J. Phys. Soc. Jpn.* **46** 1709 (1979)
177. P A Forsyth, S Marcelja, D J Mitchell, B W Ninham *Adv. Colloid Interface Sci.* **9** 37 (1978)
178. J Tang, S Fraden *Liq. Cryst.* **19** 459 (1995)
179. Z Dogic, S Fraden *Phys. Rev. Lett.* **78** 2417 (1997)
180. G F Grom, D J Lockwood, J P McCaffrey, H J Labbe, P M Fauchet, B White, J Diener, D Kovalev, F Koch, L Tsybeskov *Nature (London)* **407** 358 (2000)
181. X Peng, L Manna, Y Yang, J Wickham, E Scher, A Kadavanich, A P Alivisatos *Nature (London)* **404** 59 (2000)
182. B Nikoobakht, Z L Wang, M A El-Sayed *J. Phys. Chem. B* **104** 8635 (2000)
183. P A Kralchevsky, K Nagayama *Langmuir* **10** 23 (1994)
184. P A Kralchevsky, N D Denkov, V N Paunov, O D Velev, I B Ivanov, H Yoshimura, K Nagayama *J. Phys. C* **6** A395 (1994)
185. J Legrand, A Ngo, C Petit, M P Pileni *Adv. Mater.* **13** 58 (2001)
186. C Petit, A Taleb, M P Pileni *J. Phys. Chem. B* **103** 1805 (1999)
187. M Giersig, M Hilgendorff *J. Phys. D* **32** L111 (1999)
188. M Hilgendorff, B Tesche, M Giersig *Aust. J. Chem.* **54** 497 (2001)
189. M A Hayes, N A Polson, A A Garcia *Langmuir* **17** 2866 (2001)
190. J Legrand, C Petit, M P Pileni *J. Phys. Chem. B* **105** 5643 (2001)
191. K Loudiyi, B J Ackerson *Physica A* **184** 26 (1992)
192. H R Krishnamurthy *J. Indian Inst. Sci.* **76** 465 (1996)
193. K Lin, J C Crocker, V Prasad, A Schofield, D A Weitz, T C Lubensky, A Yodh *Phys. Rev. Lett.* **85** 1770 (2000)
194. A C Templeton, W P Wuelfing, R W Murray *Acc. Chem. Res.* **33** 27 (2000)
195. N D Denkov, O D Velev, P A Kralchevsky, I B Ivanov, H Yoshimura, K Nagayama *Nature (London)* **361** 26 (1993)
196. A S Dimitrov, K Nagayama *Langmuir* **13** 1303 (1993)
197. D J Norris, Y A Vlasov *Adv. Mater.* **13** 371 (2001)
198. C Damle, A Gole, M Sastry *J. Mater. Chem.* **10** 1389 (2000)
199. Y C Tian, J H Fendler *Chem. Mater.* **8** 969 (1996)
200. B O Dabbousi, C B Murray, M F Rubner, M G Bawendi *Chem. Mater.* **6** 216 (1994)
201. Gy Tolnai, F Csempesz, M Kabai-Faix, E Kalman, Zs Keresztes, A L Kovacs, J J Ramsden, Z Horvolgyi *Langmuir* **17** 2683 (2001)
202. J R Heath, C M Knobler, D V Leff *J. Phys. Chem. B* **101** 189 (1997)
203. K Abe, T Hanada, T Yamaguchi, H Takiguchi, H Nagasawa, M Nakamoto, K Yase *Mol. Cryst. Liq. Cryst.* **322** 173 (1998)
204. X Zhou, J Li, C Liu *J.Sci. China, Ser. B* **45** 358 (2002)
205. B Kim, S L Tripp, A Wei *J. Am. Chem. Soc.* **123** 7955 (2001)
206. L Maya, G Muralidharan, T G Thundat, E A Kenik *Langmuir* **16** 9151 (2000)
207. Z L Wang *Aust. J. Chem.* **54** 153 (2001)
208. K Muramatsu, M Takahashi, K Tajima, K Kobayashi *J. Colloid Interface Sci.* **242** 127 (2001)
209. Y Jin, S Dong *Angew. Chem., Int. Ed.* **41** 1040 (2002)
210. K V Sarathy, J P Thomas, J P Kulkarni, C N R Rao *J. Phys. Chem. B* **103** 399 (1999)
211. A Kumar, A B Mandale, M Sastry *Langmuir* **16** 6921 (2000)
212. M Brust, N Stuhr-Hansen, K Nugaard, J B Christensen, L K Nielsen, T Bjurnholm *Nano Lett.* **1** 189 (2001)
213. C P Collier, R J Saykally, J J Shiang, S E Henrichs, J R Heath *Science* **277** 1978 (1997)
214. T Hassenkam, K Nurgaard, L Iversen, C J Kelly, M Brust, T Bjurnholm *Adv. Mater.* **14** 1126 (2002)
215. S -W Chung, G Markovich, J R Heath *J. Phys. Chem. B* **102** 6685 (1998)
216. F C Meldrum, N A Kotov, J H Fendler *Mater. Sci. Eng., C* **3** 149 (1995)
217. W Wang, X Chen, S Efrima *J. Phys. Chem. B* **103** 7238 (1999)
218. S H Im, Y T Lim, D J Suh, O O Park *Adv. Mater.* **14** 1367 (2002)
219. K Nakahama, H Kawaguchi, K Fujimoto *Langmuir* **16** 7882 (2000)
220. S Chen *Adv. Mater.* **12** 186 (2000)
221. S Chen *Langmuir* **17** 2878 (2001)
222. W Li, R Xu, L Wang, H Cui, S Xi *Mol. Cryst. Liq. Cryst.* **337** 185 (1999)
223. F C Meldrum, N A Kotov, J H Fendler *J. Phys. Chem.* **98** 4506 (1994)
224. S Lefebuer, C Menager, V Cabuil, M Assenheimer, F Gallet, C Flament *J. Phys. Chem. B* **102** 2733 (1998)
225. T Fried, G Shemer, G Markovich *Adv. Mater.* **13** 1158 (2001)
226. S Chang, C Shin, C Chen, C Lai, C R C Wang *Langmuir* **15** 701 (1999)
227. H Maeda, Y Maeda *Langmuir* **12** 1446 (1996)
228. B A Korgel, D Fitzmaurice *Adv. Mater.* **10** 661 (1998)
229. F Kim, S Kwan, J Akana, P Yang *J. Am. Chem. Soc.* **123** 4360 (2001)
230. D Yogev, S Efrima *J. Phys. Chem.* **92** 5754 (1988)
231. H Schwartz, Y Harel, S Efrima *Langmuir* **17** 3884 (2001)
232. K S Mayya, M Sastry *Langmuir* **15** 1902 (1999)
233. D Wyrwa, N Beyer, N Schmid *Nano Lett.* **2** 419 (2002)
234. A Kumar, S Mandal, S P Mathew, P R Selvakannan, A B Mandale, R V Chaudhair, M Sastry *Langmuir* **18** 6478 (2002)
235. S D Sathaye, K R Patil, D V Paranjape, A Mitra, S V Awate, A B Mandale *Langmuir* **16** 3487 (2000)
236. R Aveyard, J H Clint, D Nees, N Quirke *Langmuir* **16** 8820 (2000)
237. R Aveyard, J H Clint, D Nees, V N Paunov *Langmuir* **16** 1696 (2000)
238. R K Iler *J. Colloid Interface Sci.* **21** 569 (1966)
239. N A Kotov, I Dekany, H J Fendler. *J. Phys. Chem.* **99** 13065 (1995)
240. E Hao, T Lian *Langmuir* **16** 7879 (2000)
241. T Ung, L M Liz-Marzan, P Mulvaney. *J. Phys. Chem. B* **105** 3441 (2001)
242. A A Mamedov, A Belov, M Giersig, N N Mamedova, N A Kotov *J. Am. Chem. Soc.* **123** 7738 (2001)
243. A K Newman, J M Liu *J. Appl. Phys.* **82** 4637 (1997)
244. M R Geller *Phys. Rev. Lett.* **78** 110 (1997)
245. R R Bhat, D A Fischer, J Genzer *Langmuir* **18** 5640 (2002)
246. C A Mirkin, R L Letsibger, R C Mucic, J J Storhoff *Nature (London)* **382** 607 (1996)
247. J J Storhoff, C A Mirkin *Chem. Rev.* **99** 1849 (1998)
248. A P Alivisatos, K P Johnsson, X Peng, T E Wilson, C J Loweth, M P Bruchez, P G Schultz *Nature (London)* **382** 609 (1996)
249. E T Kisak, M T Kennedy, D Trommeshauser, J A Zasadzinski *Langmuir* **16** 2825 (2000)
250. S Mann, W Shenton, M Li, S Connolly, D Fitzmaurice *Adv. Mater.* **12** 147 (2000)
251. S Connolly, S Cobbe, D Fitzmaurice *J. Phys. Chem. B* **105** 2222 (2001)
252. S Connolly, D Fitzmaurice *Adv. Mater.* **11** 1202 (1999)
253. D Fitzmaurice, S N Rao, J A Prece, J F Stoddart, S Wenger, N Zaccheroni *Angew. Chem., Int. Ed.* **38** 1147 (1999)

254. D Ryan, S N Rao, H Rensmo, D Fitzmaurice, J A Preece, S Wenger, J F Stoddart, N Zaccheroni *J. Am. Chem. Soc.* **122** 6252 (2000)
255. S Brown *Nano Lett.* **1** 391 (2001)
256. J Zhang, A Alsayed, K H Lin, S Sanyal, W-J Pao, V S K Balagurusamy, P A Heiney, A G Yodh *Appl. Phys. Lett.* **81** 3176 (2002)
257. R M Bright, M D Musick, M J Natan *Langmuir* **14** 5695 (1998)
258. G Schmid, M Baumle, N Beyer *Angew. Chem., Int. Ed.* **39** 181 (2000)
259. S M Marinakos, L C Brousseau, A Jones, D L Feldheim *Chem. Mater.* **10** 1214 (1998)
260. J Schmitt, G Decher, W J Dressik, S L Brandow, R E Geer, R Shaahidhar, J M Calvert *Adv. Mater.* **9** 61 (1997)
261. P Alivisatos *Pure Appl. Chem.* **72** 3 (2000)
262. A D Lazardies, G C Schatz *J. Phys. Chem. B* **104** 460 (2000)
263. M L Sauthier, R L Carroll, C B Gormn, S Franzen *Langmuir* **18** 1825 (2002)
264. J J Storhoff, R Elghanian, R C Mucic, C A Mirkin, R L Letsinger *J. Am. Chem. Soc.* **120** 1959 (1998)
265. O D Velev, E W Kaler *Langmuir* **15** 3693 (1999)
266. N G Khlebtsov, V A Bogatyrev, L A Dykman, Ya M Krasnov, A G Melnikov *Izv. Vyssh. Uchebn. Zaved. AND* **10** 172 (2002)
267. A V Bogatyrev, L A Dykman, Ya M Krasnov, V K Plotnikov, N G Khlebtsov *Kolloid. Zh.* **64** 671 (2002) [d]
268. T A Taton, R C Mucic, C A Mirkin, R Letsinger *J. Am. Chem. Soc.* **122** 6305 (2000)
269. B Koltover, J O Ridler, C R Safinya *Phys. Rev. Lett.* **82** 1991 (1999)
270. S Nomura, N Kajimura, K Matoba, T Miyata, R Ortenberg, M Mevarech, H Kamikubo, M Kataoka, Y Harada *Langmuir* **15** 214 (1999)
271. S A Davis, M Dreulmann, K H Rhodes, B Zhang, S Mann *Chem. Mater.* **13** 3218 (2001)
272. S Mann *J. Mater. Chem.* **5** 935 (1995)
273. S Mann *J. Chem. Soc., Dalton Trans.* 3953 (1997)
274. M Antonietti, C Gilltner *Angew. Chem., Int. Ed.* **36** 910 (1997)
275. N Combs, D Khushalani, S Oliver, G A Ozin, G S Shen, I Sokolov, H Yang *J. Chem. Soc. Dalton Trans.* 3941 (1997)
276. E Dujardin, S Mann *Adv. Mater.* **14** 775 (2002)
277. O D Velev, P M Tesier, A M Lenhoff, E W Kaler *Nature (London)* **401** 548 (1999)
278. G L Egan, J S Yu, C H Kim, S J Lee, R E Schaak, T E Mallouk *Adv. Mater.* **12** 1040 (2000)
279. H Yan, C F Blanford, J C Lytle, C B Carter, W H Smyrl, A Stein *Chem. Mater.* **13** 4314 (2001)
280. P Jiang, J Cizeron, J F Bertone, V L Colvin *J. Am. Chem. Soc.* **121** 7957 (1999)
281. H Yan, C F Blandford, B T Holland, M Parent, W H Smyrl, A Stein *Adv. Mater.* **11** 1003 (1999)
282. B T Holland, L Abrams, A Stein *J. Am. Chem. Soc.* **121** 4308 (1999)
283. H Miguez, F Meseguer, C Lopez, M Holdago, G Andreasen, A Mifsud, V Fornes *Langmuir* **16** 4405 (2000)
284. B T Holland, C F Blandford, A Stein *Science* **281** 538 (1998)
285. Z L Xiao, C Y Han, U Welp, H H Wang, V K Vlasko-Vlasov, W K Kwok, D J Muller, J M Hiller, R E Cook, G A Willing, G W Grabtree *Appl. Phys. Lett.* **81** 2869 (2002)
286. L Xu, W Zhou, M E Kozlov, I I Khayrullin, I Udod, A A Zakhidov, R H Baughman, J B Wiley *J. Am. Chem. Soc.* **123** 763 (2001)
287. D F Sievenpiper, M E Sickmiller, E Yablonovitch *Phys. Rev. Lett.* **76** 2480 (1996)
288. C Lellig, W Härtl, J Wagner, R Hempelmann *Angew. Chem., Int. Ed.* **41** 102 (2002)
289. P V Braun, P Wiltzius *Nature (London)* **402** 603 (1999)
290. A Y Vlasov, N Yao, D J Norris *Adv. Mater.* **11** 165 (1999)
291. C R Martin *Science* **266** 1961 (1994)
292. C R Martin *Chem. Mater.* **8** 1739 (1996)
293. A Huczko *Appl. Phys. A* **70** 365 (2000)
294. M Chen, Y Xie, H Chen, Z Qiao, Y Zhu, Y Qian *J. Colloid Interface Sci.* **229** 217 (2000)
295. G L Che, B B Lakshmi, C R Martin, E R Fisher, R S Ruoff *Chem. Mater.* **10** 260 (1998)
296. T Kyotani, L-F Tsai, A Tomita *Chem. Commun.* 701 (1997)
297. G L Che, B B Lakshmi, C R Martin, E R Fisher *Langmuir* **15** 750 (1999)
298. B K Pradhan, T Toba, T Kyotani, A Tomita *Chem. Mater.* **10** 2510 (1998)
299. M Freemantle *Chem. Eng. News* **74** 62 (1996)
300. H Masuda, F Hasegawa, S Ono *J. Electrochem. Soc.* **144** L127 (1997)
301. O Jessensky, F Müller, U Gösele *Appl. Phys. Lett.* **72** 1173 (1998)
302. D S Xu, Y J Hu, D P Chen, G L Guo, L L Gui, Y Q Tang *Chem. Phys. Lett.* **325** 340 (2000)
303. D S Xu, Y J Hu, D P Chen, G L Guo, L L Gui, Y Q Tang *Adv. Mater.* **12** 520 (2000)
304. Y Li, D S Xu, Q M Zhang, D P Chen, F Z Huang, Y J Xu, G L Guo, Z N Gu *Chem. Mater.* **11** 3433 (1999)
305. X Y Zhang, L D Zhang, W Chen, G W Meng, M J Zheng, L X Zhao *Chem. Mater.* **13** 2511 (2001)
306. M J Zheng, L D Zhang, G H Li, X Y Zhang, X F Wang *Appl. Phys. Lett.* **79** 839 (2001)
307. H Masuda, M Yotsuya, M Ishida *Jpn J. Appl. Phys.* **37** L1090 (1998)
308. M S Sander, A L Prieto, R Gronsky, T Sands, A M Stacy *Adv. Mater.* **14** 665 (2002)
309. Y-J Han, J M Kim, G D Stucky *Chem. Mater.* **12** 2068 (2000)
310. L-Z Wang, J-L Shi, W- H Zhang, M-L Ruan, J Yu, D-S Yan *Chem. Mater.* **11** 3015 (1999)
311. L Bronstein, D Chernyshov, P Valetsky, N Tkachenko, H Lemmetyinen, J Hartmann, S Förster *Langmuir* **15** 83 (1999)
312. R S Kane, R E Cohen, R Silbey *Langmuir* **15** 39 (1999)
313. L I Trakhtenberg, G N Gerasimov, E I Grigor'ev *Zh. Fiz. Khim.* **73** 264 (1999) [e]
314. D I Svergun, E V Shtykova, A T Dembo, L M Bronstein, O A Platonova, A N Yakunin, P M Valetsky, A R Khokhlov *J. Chem. Phys.* **109** 11109 (1998)
315. F Baumann, B Deubzer, M Geck, J Dauth, S Sheiko, M Schmidt *Adv. Mater.* **9** 955 (1997)
316. C Roos, M Schmidt, J Ebenhoch, F Baumann, B Deubzer, J Weis *Adv. Mater.* **11** 761 (1999)
317. S H Choi, K L Wang, M S Leung, G W Stupian, N Presser, S W Chung, G Markovich, S H Kim, J R Heath *J. Vac. Sci. Technol., A* **17** 1425 (1999)
318. A Kumar, G M Whitesides *Appl. Phys. Lett.* **63** 2002 (1993)
319. T Sato, D G Hasko, H Ahmed *J. Vac. Sci. Technol., B* **15** 45 (1997)
320. J Zheng, Z Zhu, H Chen, Z Liu *Langmuir* **16** 4409 (2000)
321. M Winzer, M Kleiber, N Dix, R Wiesendanger *Appl. Phys. A: Mater. Sci. Process.* **63** 617 (1996)
322. F Burmeister, C Schäfle, B Keilhofer, C Bechinger, J Boneberg, P Leiderer *Adv. Mater.* **10** 495 (1998)
323. T L Morkved, P Wiltzius, H M Jaeger, D G Grier, T A Witten *Appl. Phys. Lett.* **64** 422 (1994)
324. R W Zehner, W A Lopes, T L Morkved, H Jaeger, L Sita *Langmuir* **14** 241 (1998)
325. P C Hidber, W Helbig, E Kim, G M Whitesides *Langmuir* **12** 1375 (1996)
326. S Palacin, P C Hidber, J Bourgoin, C Miramond, C Fermon, G M Whitesides *Chem. Mater.* **8** 1316 (1996)
327. M A McCord *J. Vac. Sci. Technol., B* **15** 2125 (1997)
328. J P Silverman *J. Vac. Sci. Technol., B* **15** 2117 (1997)
329. J Melngailis, A A Mondelli, I L Berri, R Mohondro *J .Vac. Sci. Technol., B* **16** 927 (1998)
330. T M Bloomstein, M W Horn, M Rothschild, R R Kunz, S T Palmacci, R B Goodman *J. Vac. Sci. Technol., B* **15** 2112 (1997)
331. S C Kitson, W L Barnes, J R Sambles *IEEE Photonics Technol. Lett.* **8** 1662 (1996)
332. K Bromann, C Felix, H Brune, W Harbich, R Monot, J Buttet, K Kern *Science* **274** 956 (1996)
333. G Springholz, V Holy, M Pinczolits, G Bauer *Science* **282** 734 (1998)
334. H W Deckman, J H Dunsmuir, S Garoff, J A McHenry, D J Peiffer *J. Vac. Sci. Technol., B* **6** 333 (1988)
335. J C Hulteen, R P Van Duyne *J. Vac. Sci. Technol., A* **13** 2117 (1995)

336. J C Hulteen, D A Treichel, M T Smith, M L Duval, T R Jensen, R P Van Duyne *J. Phys. Chem. B* **103** 3854 (1999)
337. J C Hulteen, R P Van Duyne *J. Vac. Sci. Technol., A* **13** 1553 (1995)
338. F Burmeister W Badowsky, T Braun, S Wieprich, J Boneberg, P Leidere *Appl. Surf. Sci.* **144 – 145** 461 (1999)
339. T J Jensen, M L Duval, K L Kelly, A A Lazarides, G C Schatz, R P Van Duyne *J. Phys. Chem. B* **103** 9846 (1999)
340. X M Lin, R Parthasarathy, H M Jaeger *Appl. Phys. Lett.* **78** 1915 (2001)
341. M H V Werts, M Lambert, J-P Bourgon, M Brust *Nano Lett.* **2** 43 (2002)
342. J Y Chen, J F Klemic, M Elimelech *Nano Lett.* **2** 393 (2002)
343. H Sugimura, N Takgiri *J. Am. Chem. Soc.* **119** 9226 (1997)
344. R Resch, C Baur, A Bugacov, B E Koel, A Madhukar, A A G Requicha, P Will *Langmuir* **14** 6613 (1998)
345. S Meltzer, R Resch, B E Koel, M E Thompson, A Madhukar, A A G Requicha, P Will *Langmuir* **17** 1713 (2001)
346. R D Piner, J Zhu, F Xu, S H Hong, C A Mirkin *Science* **283** 661 (1999)
347. S H Hong, C A Mirkin *Science* **288** 1808 (2000)
348. Y Li, B B Maynor, J Liu *J. Am. Chem. Soc.* **123** 2105 (2001)
349. B W Maynor, Y Li J Liu *Langmuir* **17** 2575 (2001)
350. F Caruso, R A Caruso, H Möhwald *Science* **282** 1111 (1998)
351. F Caruso *Chem. Eur. J.* **6** 413 (2000)
352. C W Chen, T Serizawa, M Akashi *Chem. Mater.* **11** 1381 (1999)
353. Y Kobayashi, V Salgueirino-Maceira, L M Liz-Marzan *Chem. Mater.* **13** 1630 (2001)
354. C W Chen, M Q Chen, T Serizawa, M Akashi *Chem. Mater.* **10** 122 (1998)
355. A Dokuchaev, J T James, S C Koene, S Pathak, G K S Prakash, M E Tompson *Chem. Mater.* **11** 2389 (1999)
356. N Arul Dhas, A Zaban, A Gedanken *Chem. Mater.* **11** 806 (1999)
357. Z Zong, Y Mastay, Y Koltypin, Y Zhao, A Gedanken *Chem. Mater.* **11** 2350 (1999)
358. S Ramesh, Y Kohen, R Prosorov, K V P M Shafi, D Aurbach, A Gedanken *J. Phys. Chem. B* **102** 10234 (1998)
359. S L Westcott, S J Oldenburg, T Randall Lee, N J Halas *Langmuir* **14** 5396 (1999)
360. A B R Mayer, W Grebner, W Wannenmacher *J. Phys. Chem. B* **104** 7278 (2000)
361. C Caruso *Adv. Mater.* **13** 11 (2001)
362. G Decher, J D Hong *Ber. Bunsen-Ges. Phys. Chem.* **95** 1430 (1995)
363. G Decher *Science* **277** 1232 (1997)
364. F Caruso, M Spasova, V Salgueirino-Maceira, L M Liz-Marzan *Adv. Mater.* **13** 1090 (2001)
365. Z Bao, L Chen, M Weldon, E Chandross, O Cherniavskaya, Y Dai, J B-H Tok *Chem. Mater.* **14** 24 (2002)
366. K C Grabar, P C Smith, M D Musick, J A Davis, D G Water, M A Jackson, A P Guthrie, M J Nata *J. Am. Chem. Soc.* **118** 1148 (1996)
367. T Sato, D Brown, B F G Johnson *Chem. Commun.* 1007 (1997)
368. S Liu, T Zhu, R Hu, Z Liu *Phys. Chem. Chem. Phys.* **4** 6059 (2002)
369. Y Yin, Y Xia *Adv. Mater.* **13** 267 (2001)
370. J Aizenberg, P V Braun, P Wiltzius *Phys. Rev. Lett.* **27** 2997 (2000)
371. A Kumar, H A Beibuyck, G M Whiteside *Langmuir* **13** 5349 (1994)
372. A J Parker, P A Childs, R E Palmer, M Brust *Appl. Phys. Lett.* **74** 2833 (1999)
373. K M Chen, X Jiang, L C Kimerling, P T Hammond *Langmuir* **16** 7825 (2000)
374. G Decher, M Eckle, J Schmitt, B Struth *Curr. Opin. Colloid Interface Sci.* **3** 32 (1998)
375. P T Hammond *Curr. Opin. Colloid Interface Sci.* **4** 430 (2000)
376. J A He, L Li, J Kumar, S K Tripathy *J. Phys. Chem. B* **102** 7067 (1998)
377. A Wu, D Yoo J-K Lee, M F Rubner *J. Am. Chem. Soc.* **121** 4883 (1999)
378. J H Cheung, A F Fou, M F Rubner *Thin Solid Films* **244** 985 (1994)
379. Y M Lvov, G N Kamau, D L Zhou, J F Rusling *J. Colloid Interface Sci.* **212** 570 (1999)
380. A Mamedov, J W Ostrander, F Aliev, N A Kotov *Langmuir* **16** 3941 (2000)
381. I Lee, H Zheng, M F Rubner, P T Hammond *Adv. Mater.* **14** 572 (2002)
382. D Qin, Y Xia, B Xu, H Yang, H Zhu, G M Whitesides *Adv. Mater.* **11** 1433 (1999)
383. A D Kent, T M Show, S von Molnar, D D Awschalom *Science* **262** 1249 (1992)
384. K L Lee, M Hatzakis *J. Vac. Sci. Technol., B* **7** 1941 (1989)
385. Z Zhong, B Gates, Y Xia, D Qin *Langmuir* **16** 10369 (2000)
386. A Kumar, H Biebuyck, G M Whitesides *Langmuir* **8** 2672 (1994)
387. A J Parker, P A Childs, R E Palmer, M Brust *Nanotechnology* **12** 6 (2001)
388. T O Hutchinson, Y-P Liu, C Kiely, M Brust *Adv. Mater.* **13** 1800 (2001)
389. S Chen, R S Ingram, M J Hostetler, J J Pietron, R W Murray, T G Schaaff, J T Khoury, M M Alvarez, R L Whetten *Science* **280** 2098 (1998)
390. S Chen *J. Am. Chem. Soc.* **122** 7420 (2000)
391. J F Sampaio, K C Beverly, J R Heath *J. Phys. Chem. B* **105** 8797 (2001)
392. S Henrichs, C P Collier, R J Saykally, Y R Shen, J R Heath *J. Am. Chem. Soc.* **122** 4077 (2000)
393. G Markovich, C P Collier, J R Heath *Phys. Rev. Lett.* **80** 3807 (1998)
394. N Fishelson, I Shkrob, O Lev, J Gun, A D Modestov *Langmuir* **17** 403 (2001)
395. M Brust, D Bethel, C J Kiely, D J Schiffrin *Langmuir* **14** 5425 (1998)
396. V V Vysotskii, V I Roldughin *Kolloid. Zh.* **60**729 (1998) [d]
397. V V Vysotskii, V I Roldughin *Kolloid. Zh.* **61** 190 (1999) [d]
398. V I Roldughin, V V Vysotskii *Prog. Org. Coat.* **39** 81 (2000)
399. J J Shiang, J R Heath, C P Collier, R J Saykally *J. Phys. Chem. B* **102** 3425 (1998)
400. F Remacle *J. Phys. Chem. A* **104** 4739 (2000)
401. Y Imry *Introduction to Mesoscopic Physics* (2nd Ed.) (Oxford: Oxford University Press, 2002)
402. J M Ziman *Principles of the Theory of Solids* (2nd Ed.) (Cambride: Cambride University Press, 1972)
403. S-H Kim, G Medeiros-Ribeiro, D A A Ohlberg, R S Williams, J R Heath *J. Phys. Chem. B* **103** 10341 (1999)
404. K Inukai, Y Hotta, S Tomura, M Takahashi, A Yamagishi *Langmuir* **16** 7679 (2000)
405. C T Blank, C B Murray, R L Sandstrom, S Sun *Science* **290** 1131 (2000)
406. U Kreibig, M Vollmer *Optical Properties of Metal Clusters* (Berlin: Springer, 1995)
407. S Link, M A El-Sayed *J. Phys. Chem. B* **103** 8410 (1999)
408. M P Pileni *Pure Appl. Chem.* **72** 53 (2000)
409. S Torquato, F Lado *Phys. Rev. B* **33** 6428 (1986)
410. I Farbman, O Levi, S Efrima *J. Chem. Phys.* **96** 6477 (1992)
411. R Berndt, J K Gimzewski, P Johansson *Phys. Rev. Lett.* **67** 3769 (1991)
412. C Girardin *J. Phys. III* **6** 661 (1996)
413. T Baum, D Bethell, M Brust, D J Schiffrin *Langmuir* **15** 866 (1999)
414. M I Stockman, S V Faleev, D J Bergman *Phys. Rev. Lett.* **87** 167401 (2001)
415. Y Lu, Y Yin, Z-Y Li, Y Xia *Nano Lett.* **2** 785 (2002)
416. M Quinten, A Leitner, J R Krenn, F R Aussenegg *Opt. Lett.* **23** 1331 (1998)
417. J R Krenn, A Dereux, J C Weeber, E Bourliott, Y Lacrout, J P Goudonnet, G Schider, W Gotschy, A Leitner, F R Aussenegg, C Giarad *Phys. Rev. Lett.* **82** 2590 (1999)
418. M D Malinsky, K L Kelly, G C Schatz, R P Van Duyne *J. Phys. Chem. B* **105** 2343 (2001)
419. M Yamada, T Tadera, K Kubo, H Nishihara *Langmuir* **17** 2363 (2001)
420. E S Kooij, H Wormeester, E A M Brouwer, E von Vroonhover, A von Silfhout, B Poelsema *Langmuir* **18** 4410 (2002)
421. E Hutter, J H Fendler, D Roy *J. Phys. Chem. B* **105** 11 159 (2001)

422. H Yanagi, N Matsuoka, M Kondo, M Nagawa, Y Taniguchi *Chem. Mater.* **13** 4800 (2001)
423. H Yanagi, N Matsuoka, M Kondo, M Nagawa, Y Taniguchi *Langmuir* **17** 5491 (2001)
424. M Sirota, E Minkin, E Lifshitz, V Hensel, M Lahav *J. Phys. Chem. B* **105** 6792 (2001)
425. J R Sheats, H Antoniadis, M Hueschen, W Leonard, J Miller, R Moon, R Roitman, A Stocking *Science* **273** 884 (1996)
426. N Tessler *Adv. Mater.* **11** 363 (1999)
427. J H Shön, Ch Kloc, A Dodabalapur, B Batlogg *Science* **289** 599 (2000)
428. P Schuck *Annu. Rev. Biophys. Biomol. Struct.* **26** 541 (1997)
429. L A Lyon D J Pena, M J Natan *J. Phys. Chem. B* **103** 5826 (1999)
430. R K Chang, T E Furtak (Eds) *Surface-Enhanced Raman Scattering* (New York: Plenum, 1981)
431. M Moskovits *Rev. Mod. Phys.* **57** 783 (1985)
432. R G Freeman, M B Hommer, K C Grabar, M A Jackson, M J Natan *J. Phys. Chem.* **100** 718 (1996)
433. J Hu, B Zhao, W Xu, Y Fan, B Li, Y Ozaki *Langmuir* **18** 6839 (2002)
434. S Nie, S R Emory *Science* **275** 1102 (1997)
435. H Xu, E J Bjerneld, M Käll, L Börjesson *Phys. Rev. Lett.* **83** 4357 (1999)
436. T L Haslett, L Tay, M Moskovits *J. Chem. Phys.* **113** 1641 (2000)
437. D J Maxwell, S R Emory, S Nie *Chem. Mater.* **13** 1082 (2001)
438. J H Holtz, S A Asher *Nature (London)* **389** 829 (1997)
439. J M Weissman, H B Sunkara, A S Tse, S A Asher *Science* **274** 959 (1996)
440. R J Spry, D J Kosan *Appl. Spectrosc.* **40** 782 (1986)
441. J D Joannopoulos, R D Meade, J N Winn *Photonic Crystals: Molding the Flow of Light* (Prinston: Prinston University Press, 1995)
442. I I Trahan, G H Watson *Phys. Rev. Lett.* **76** 315 (1996)
443. A R Parker, R C McPhedran, D R Mckenzie, L C Botten, N A P Nicorovici *Nature (London)* **409** 36 (2001)
444. K M Ho, C T Chan, C M Soukoulis *Phys. Rev. Lett.* **65** 3152 (1990)
445. A Moroz *Phys. Rev. Lett.* **83** 5274 (1999)
446. S John *Phys. Rev. Lett.* **58** 2486 (1987)
447. E Yablonovitch *Phys. Rev. Lett.* **58** 2059 (1987)
448. E Yablonovitch *Nature (London)* **401** 539 (1999)
449. A Blanco, E Chomski, S Grabtchak, M Ibisate, S John, S W Leonard, C Lopez, F Meseguer, H Miguez, J P Mondia, G A Ozin, O Toader, H M van Driel *Nature (London)* **405** 437 (2000)
450. Y Shen, C S Friend, Y Jiang, D Jakubczyk, J Swiatkiewicz, P Prasad *J. Phys. Chem. B* **104** 7577 (2000)
451. Y Yamamoto, R E Slusher *Phys. Today* **46** 66 (1993)
452. U Grüning, V Lehmann, S Ottow, K Busch *Appl. Phys. Lett.* **68** 747 (1996)
453. S Kawakami *Electron. Lett.* **33** 1260 (1997)
454. T Baba, T Matsuzaki *Jpn. J. Appl. Phys.* **35** 1348 (1996)
455. S H Park, Y Xia *Langmuir* **15** 266 (1999)
456. Y N Xia, B Gate, S H Park *J. Lightwave Technol.* **17** 1956 (1999)
457. Z-Z Gu, S Kubo, W Qian, Y Einaga, A Fujishima, O Sato *Langmuir* **17** 6751 (2001)
458. A A Zakhidov, R H Baughman, Z Iqbal, C X Cui, I Khayrullin, S O Dantas, I Marti, V G Ralchenko *Science* **282** 897 (1998)
459. Y Fink, A M Urbas, M G Bawendi, J D Joannopoulas, E L Thomas *J. Lightwave Technol.* **17** 1963 (1999)
460. J E G J Wijhoven, L V Vos *Science* **281** 802 (1998)
461. G Subramania, K Constant, R Biswas, M M Sigalas, K M Ho *Appl. Phys. Lett.* **74** 3933 (1999)
462. G Pan, R Kesavamoorthy, S A Asher *J. Am. Chem. Soc.* **120** 6525 (1998)
463. J Ballato, A Jame *J. Am. Ceram. Soc.* **82** 2273 (1999)
464. Y Lu, Y Yin, B T Mayers, Y Xia *Nano Lett.* **2** 183 (2002)
465. P Sheng, W Wen, N Wang, H Ma, Z Lin, W Y Zhang, X Y Lei, Z L Wang, D G Zheng, W Y Tam *Pure Appl. Chem.* **72** 309 (2000)
466. J Song, H Sun, Y Xu, Y Fu, S Matsuo, H Misawa, G Du *Opt. Quantum Electron.* **32** 1295 (2000)
467. Y D Yin, Y Lu, Y N Xia *J. Am. Chem. Soc.* **123** 771 (2001)
468. Y D Yin, Y Lu, B Gates, Y N Xia *J. Am. Chem. Soc.* **123** 8718 (2001)
469. R C Hayward, D A Saville, I A Aksay *Nature (London)* **404** 56 (2000)
470. O D Velev, A M Lenhoff, E W Kaler *Science* **287** 2240 (2000)
471. B A Ozin, S M Yang *Adv. Funct. Mater.* **11** 95 (2001)
472. Z-Z Gu, A Fujishima, O Sato *Angew. Chem., Int. Ed.* **41** 2068 (2002)
473. L M Liz-Marzan, P Mulvaney *New J. Chem.* **22** 1285 (1998)
474. G Wang, A Harrison *J. Colloid Interface Sci.* **217** 203 (1999)
475. L M Liz-Marzan, M Giersig, P Mulvaney *Chem. Commun.* 731 (1996)
476. V V Hardikar, E Matijevic *J. Colloid Interface Sci.* **221** 133 (2000)
477. R H Kodama, A E Berkovitz, E J McNiff, S Foner. *Phys. Rev. Lett.* **77** 394 (1996)
478. M L Billas, A Chatelain, W A de Heer *Science* **265** 1682 (1994)
479. J P Chen, C M Sorensen, K J Klabunde, G C Hadjipanayis *Phys. Rev. B* **51** 11527 (1995)
480. K W Edmons, C Binns, S H Baker, S C Thornton, C Norri, J B Goedkoop, F U Hillbrecht *Phys. Rev. B* **59** R701 (1999)
481. Y E Volokitin, Doctoral Thesis, University Leiden, Leiden, 1997
482. F Luis, J M Torres, L M Garcia, J Bartolome, J Stankiewicz, F Petroff, F Fettar, J-L Maurice, A Vaures *Phys. Rev. B* **65** 094 409 (2002)
483. D Babonneau, F Petroff, J-L Maurice, F Fettar, A Vaures *Appl. Phys. Lett.* **76** 2892 (2000)
484. M Respaud, J M Broto, H Rakoto, A R Fert, L Thomas, B Barbara, M Verelst, E Snoeck, P Lecante, A Mosset, J Osuna, T Ould Ely, C Amiens, B Chaudret *Phys. Rev. B* **57** 2925 (1998)
485. S Shtrikman, E P Wholfarth *Phys. Lett. A* **85** 467 (1981)
486. J L Dorman, L Bessais, D Fiorani *J. Phys. C* **21** 2015 (1988)
487. S Mørup, E Tronc *Phys. Rev. Lett.* **72** 3278 (1994)
488. J M Kosterlitz, D J Thouless *J. Phys. C* **6** 1181 (1973)
489. A P Young *Phys. Rev. B* **19** 1855 (1979)
490. D R Nelson, B I Halperin *Phys. Rev. B* **19** 2457 (1979)
491. K Zahn, R Lenke, G Maret *Phys. Rev. Lett.* **82** 2721 (1999)
492. P H F Hansen, S Rödner, L Bergtröm *Langmuir* **17** 4867 (2001)
493. S Sastry, D S Corti, P G Debenedetti, F H Stillinger *Phys. Rev. E* **56** 5524 (1997)
494. A Pertsinidis, X C Ling *Phys. Rev. Lett.* **87** 098 303 (2001)
495. S Johansson, K Wong, V P Zhdanov, B Kasemo *J. Vac. Sci. Technol., A* **17** 297 (1999)
496. Z L Wang, J L Petroski, T C Green, M A El-Sayed *J. Phys. Chem. B* **102** 6145 (1998)
497. A S Eppler, G Rupprechter, E A Anderson, G A Samorjai *J. Phys. Chem.* **104** 7286 (2000)
498. A Ulman *Chem. Rev.* **96** 1533 (1996)
499. N Sandhyarani, M R Resmi, R Unnikrishnan, R Vidyasagar, S Ma, M P Antony, G P Selvam, V Visalakshi, N Chandrakumar, K Pandian, Y T Tao, T Pradeep *Chem. Mater.* **12** 104 (2000)
500. B A Korgel *Phys. Rev. Lett.* **86** 127 (2001)
501. W X Zheng, M M Maye, F L Leibowitz, C J Zhong *Anal. Chem.* **72** 2190 (2000)
502. M M Maye, J Luo, L Han, C-J Zhong *Nano Lett.* **1** 575 (2001)

[a] — *J. Exp. Theor. Phys. Lett. (Engl. Transl.)*
[b] — *J. Exp. Theor. Phys. (Engl. Transl.)*
[c] — *Physics-Uspekhi (Engl. Transl.)*
[d] — *Colloid. J. (Engl. Transl.)*
[e] — *Russ. J. Phys. Chem. (Engl. Transl.)*